

**OFFICE OF CIVILIAN RADIOACTIVE WASTE MANAGEMENT  
CALCULATION COVER SHEET**

1. QA: QA

Page:1

Of: 24

2. Calculation Title  
Rock Fall on Drip Shield

MOI.20010713.0043

3. Document Identifier (including Revision Number)  
CAL-EDS-ME-000001 REV 01

4. Total Attachments  
3

5. Attachment Numbers - Number of pages in each  
I-17, II-43, III (compact disc, see Section 8)

	Print Name	Signature	Date
6. Originator	Zekai Ceylan	<i>Zekai Ceylan</i>	7/2/01
7. Checker	Timothy A. Schmitt	<i>Tim Schmitt</i>	7/2/01
8. Lead	Scott M. Bennett	<i>Scott M. Bennett</i>	07/2/01

9. Remarks

**Revision History**

10. Revision No.	11. Description of Revision
REV 00	Initial issue
REV 01	Issued approved. Calculation was revised to include the effects of temperature-dependent material properties and maximum corrosion. Design changes were made. Markings were omitted because of the full revision.

**CONTENTS**

	<b>Page</b>
1. PURPOSE.....	3
2. METHOD .....	3
3. ASSUMPTIONS.....	3
4. USE OF COMPUTER SOFTWARE AND MODELS .....	5
4.1 SOFTWARE.....	5
4.2 MODELS.....	6
5. CALCULATION.....	6
5.1 MATERIAL PROPERTIES .....	6
5.1.1 Calculations for Available Elevated-Temperature Material Properties.....	8
5.1.2 Calculations for True Measures of Ductility.....	9
5.1.3 Calculations for Tangent Moduli.....	10
5.2 ROCK VELOCITY AND MAXIMUM ANGLE OF INCLINATION.....	11
5.2.1 Calculations for Impact Velocity.....	11
5.2.2 Calculations for Maximum Angle of Rock Inclination .....	14
5.3 GEOMETRIC DIMENSIONS OF DRIP SHIELD .....	14
5.4 REDUCTION OF THICKNESS DUE TO CORROSION.....	15
5.5 FINITE ELEMENT REPRESENTATION .....	15
6. RESULTS .....	17
7. REFERENCES .....	20
8. ATTACHMENTS.....	22

## 1. PURPOSE

The objective of this activity is to determine the structural performance of the drip shield under a rock fall design basis event. The scope of this activity is limited to determining maximum displacement and stresses in the drip shield when subjected to rock fall events for the following rock masses: 6 Metric Tons (MT), 15 MT, 19 MT, 30 MT, 36 MT, and 52 MT. The residual stresses caused by the rock fall are also reported in the results section of this calculation. The information provided by the sketches that are attached to this calculation is modified as stated in Section 5.3 and is that of the potential design for the type of drip shield considered in this calculation. This activity is associated with the drip shield design and performed in accordance with *Technical Work Plan for: Waste Package Design Description for SR* (Ref. 1). AP-3.12Q, *Calculations* (Ref. 2), is used to develop and document the calculation.

## 2. METHOD

The finite element solution is obtained using the commercially available ANSYS version (V) 5.4 and LS-DYNA V950.C finite element codes. The results of this calculation are reported in terms of the maximum displacement and stresses. The control of the electronic management of data is accomplished in accordance with the methods specified in Reference 1.

## 3. ASSUMPTIONS

In the course of developing this document, assumptions were made regarding the drip shield structural calculations. These are identified below.

- 3.1 No failure condition is conservatively assumed for the rock. The rock block would realistically be expected to break under an impact load, absorbing some energy, thereby leaving less impact load over the drip shield. However, the finite element representation (FER) does not include any failure strain or stress value for the rock. The rationale for this assumption is to obtain bounding stress results for the drip shield subjected to the rock fall design basis event. This assumption is used in Section 5.5.
- 3.2 Temperature-dependent Poisson's ratio and elongation are not available for Ti-7, Ti-24, and Alloy 22. Similarly, the modulus of elasticity as a function of temperature is not available for Ti-24. Therefore, the room temperature Poisson's ratio, elongation, and modulus of elasticity (for Ti-24) are assumed for these materials. The impact of using such material properties at room temperature is anticipated to be small. The rationale for this assumption is twofold: for the subject materials, these properties do not change significantly at the temperature of interest in this calculation; secondly, the material properties in question do not have a dominant impact on the calculation results. This assumption is used in Section 5.1.

- 3.3 The temperature-dependent material properties are not available for Topopah Spring Welded-Lithophysal Poor (TSw2) rock. The corresponding room temperature material properties are assumed for this material. The impact of using room temperature material properties is anticipated to be small. The rationale for this assumption is that the material properties relevant for representing the rock as an elastic solid (namely, modulus of elasticity, and Poisson's ratio) do not change significantly at the temperatures experienced in the emplacement drift. This assumption is used in Section 5.1.
- 3.4 Some of the rate-dependent material properties are not available for materials used at any strain rate. The material properties obtained under the static loading conditions are assumed for all materials. The impact of using material properties obtained under static loading conditions is anticipated to be small. The rationale for this assumption is that the mechanical properties of subject materials do not significantly change at the peak strain rates that occur during the rock fall (maximum plastic strain rate being approximately  $6 \text{ s}^{-1}$  as indicated in Figure II-11). A possible exception is TSw2 rock, but since the rock is represented as the elastic solid, the same justification is valid for the relevant rock properties as well. This assumption is used in Section 5.1.
- 3.5 Poisson's ratio of Alloy 22 is not available in literature. Poisson's ratio of Alloy 625 (SB-443 N06625) is assumed for Alloy 22. The impact of this assumption is anticipated to be negligible. The rationale for this assumption is that the chemical compositions of Alloy 22 and Alloy 625 are similar (see Ref. 3 [Sect. II, SB-575, Table 1] and Ref. 4, p. 143, respectively). This assumption is used in Section 5.1.
- 3.6 The uniform strains of Ti-7 and Ti-24 are not available in literature. Therefore, it is assumed that the uniform strain is equal to the elongation. The rationale for this assumption is that the difference between the uniform strain and elongation is small for many ductile materials and the difference does not have a significant effect on the calculation results. This assumption is used in Section 5.1.2.
- 3.7 The temperature-dependent tensile strength of Ti-24 is not available in the literature. Therefore, the lower end of the tensile strength range for titanium alloys at 216 °C (Ref. 5, p. 626) is assumed for Ti-24. The rationale for this assumption is that Ti-24 is a titanium alloy and the lower end of the range provides a bounding value of tensile strength for this calculation. This assumption is used in Section 5.1.
- 3.8 The corrosion rate of Ti-24 is not available in the literature. Therefore, the corrosion rate of Ti-7 is assumed for Ti-24. The rationale for this assumption is that the difference in corrosion behavior between different grades of the same material is insignificant since the chemical compositions are similar. This assumption is used in Sections 5.1 and 5.4.

- 3.9 The temperature-dependent yield strength of Ti-24 is not available in the literature. Therefore, the room temperature yield strength is decreased linearly in accordance with the change in tensile strength from room temperature to 216 °C. The rationale for this assumption is that any decrease in the yield strength of materials indicates comparably the same amount of decrease in the tensile strength. This assumption is used in Section 5.1.1.
- 3.10 The uniform strain of Alloy 22 is not available in literature. Therefore, it is conservatively assumed that the uniform strain is 90% of the elongation. The rationale for this assumption is the character of stress-strain curve for Alloy 22 (Ref. 6). This assumption is used in Section 5.1.2.
- 3.11 The gantry rail is assumed to constrain the lateral displacement of the drip shield side-walls during the post-closure period (see Figures II-4 and II-5). The gantry rail is made of steel sets, which are not anticipated to remain intact during the post-closure period; however, the rationale for this assumption is that the current design evaluations consider modifications to the emplacement pallet design. One of these modifications is that the lateral displacement of the side-walls is constrained as if the rails were in place. Additional plates welded to the bottom of the emplacement pallet, on which the drip shield rests, is a potential design feature currently being considered. This assumption is used in Section 5.5.

#### 4. USE OF COMPUTER SOFTWARE AND MODELS

##### 4.1 SOFTWARE

One of the finite element analysis (FEA) computer codes used for this calculation is ANSYS V5.4, which is obtained from Software Configuration Management in accordance with appropriate procedures, and is identified by Computer Software Configuration Item number (CSCI) 30040-5.4 (Ref. 7). ANSYS V5.4 is a commercially available FEA code and is appropriate for structural calculations of drip shields as performed in this calculation. The calculations using ANSYS V5.4 software were executed on the Hewlett-Packard (HP) 9000 series UNIX workstations identified with the YMP (Yucca Mountain Project) property tag numbers 117161 and 117162, located in Las Vegas, Nevada. ANSYS evaluation performed for this calculation is fully within the range of the validation performed for ANSYS V5.4 code. Access to the code is granted by the Software Configuration Management in accordance with the appropriate procedures.

The output files (identified by .out file extensions) for ANSYS V5.4 are provided in Attachment III; the corresponding input files are listed at the beginning of each output file.

The second FEA computer code, used for this calculation, is the Livermore Software Technology Corporation LS-DYNA V950.C, which is obtained from Software Configuration Management in accordance with appropriate procedures, and is identified by Software Tracking Number (STN) 10300-950-00 (Ref. 8). LS-DYNA V950.C is a commercially available FEA code and is appropriate

for structural calculations of drip shields as performed in this calculation. The calculations were executed on HP 9000 series UNIX workstations identified with the YMP property tag numbers 117161 and 117162, located in Las Vegas, Nevada. The LS-DYNA V950.C evaluation performed for this calculation is fully within the range of the validation performed for LS-DYNA V950.C code. Access to the code is granted by the Software Configuration Management in accordance with the appropriate procedures.

The input files (identified by .k and .inc file extensions) and output files (d3hsp) for LS-DYNA V950.C are provided in Attachment III.

## 4.2 MODELS

None used.

## 5. CALCULATION

### 5.1 MATERIAL PROPERTIES

Material properties used in this calculation are listed in this section. Some of the temperature-dependent and rate-dependent material properties are not available for Ti-7, Ti-24, Alloy 22, and TSw2 rock. Therefore, room temperature modulus of elasticity, Poisson's ratio, and elongation obtained under the static loading conditions are used for the subject materials (Assumptions 3.2, 3.3, and 3.4).

Ti-7 (Titanium Grade 7) (SB-265 R52400, drip shield plate material, see Attachment I):

- Modulus of elasticity = 96.5 GPa ( $14 * 10^6$  psi at 400 °F) (Ref. 3, Section II-D, Table TM-5)  
Modulus of elasticity = 91.7 GPa ( $13.3 * 10^6$  psi at 500 °F) (Ref. 3, Section II-D, Table TM-5)
- Density = 4512 kg/m<sup>3</sup> (0.163 lb/in<sup>3</sup>) (Ref. 3, Section II-D, Table NF-2)
- Poisson's ratio = 0.34 at 20 °C (Ref. 5, p. 621) (Assumption 3.2)
- Yield strength = 128 MPa (18.6 ksi at 400 °F) (Ref. 9, Section II-D, Table Y-1)  
Yield strength = 112 MPa (16.3 ksi at 450 °F) (Ref. 9, Section II-D, Table Y-1)
- Tensile strength = 213 MPa (30.9 ksi at 400 °F) (Ref. 3, Section II-D, Table U)  
Tensile strength = 183 MPa (26.6 ksi at 500 °F) (Ref. 3, Section II-D, Table U)

- Elongation = 0.2 at 20 °C (Ref. 3, Section II-B, SB-265, Table 3) (Assumption 3.2)
- Corrosion rate =  $1.5 \cdot 10^{-4}$  mm/year (Ref. 10 is used to corroborate information provided in Ref. 21, Figure 3-71)

Ti-24 (Titanium Grade 24) (SB-265 R56405; in regard to this UNS designation, note that Ti-24 has the same mechanical properties with Ti-5 since the compositions are almost identical, see Ref. 3, Section II-B, SB-265, Tables 3 and 1) (drip shield stiffener [bulkhead] material, see Attachment I) (first three material properties of Ti-24 given below are specified using the nominal composition, 6Al-4V, in Ref. 5):

- Modulus of elasticity = 113.8 GPa at 20 °C (Ref. 5, p. 621) (Assumption 3.2)
- Density = 4430 kg/m<sup>3</sup> (Ref. 5, p. 620)
- Poisson's ratio = 0.342 at 20 °C (Ref. 5, p. 621) (Assumption 3.2)
- Yield strength = 828 MPa at 20 °C (Ref. 3, Section II-B, SB-265, Table 3)
- Tensile strength = 895 MPa at 20 °C (Ref. 3, Section II-B, SB-265, Table 3)
- Tensile strength = 620 MPa at 216 °C (Ref. 5, p. 626) (Assumption 3.7)
- Elongation = 0.1 at 20 °C (Ref. 3, Section II-B, SB-265, Table 3) (Assumption 3.2)
- Corrosion rate =  $1.5 \cdot 10^{-4}$  mm/year (Assumption 3.8)

Alloy 22 (SB-575 N06022, drip shield base material, see Attachment I):

- Modulus of elasticity = 196 GPa at 204 °C (Ref. 11, p. 14)
- Modulus of elasticity = 190 GPa at 316 °C (Ref. 11, p. 14)
- Density = 8690 kg/m<sup>3</sup> (0.314 lb/in<sup>3</sup>) (Ref. 3, Section II-B, SB-575, Section 7.1)
- Poisson's ratio = 0.278 at 20 °C (Ref. 4, p. 143) (Assumption 3.5)
- Yield strength = 236 MPa (34.3 ksi at 400 °F) (Ref. 3, Section II-D, Table Y-1)
- Yield strength = 229 MPa (33.2 ksi at 450 °F) (Ref. 3, Section II-D, Table Y-1)

- Tensile strength = 657 MPa (95.3 ksi at 400 °F) (Ref. 3, Section II-D, Table U)  
Tensile strength = 641 MPa (92.9 ksi at 500 °F) (Ref. 3, Section II-D, Table U)
- Elongation = 0.45 at 20 °C (Ref. 3, Section II-B, SB-575, Table 3) (Assumption 3.2)

Rock block (Topopah Spring Welded-Lithophysal Poor [TSw2]):

- Modulus of elasticity = 33.03 GPa at 20 °C (Ref. 12, Table 3) (Assumption 3.3)
- Density = 2370 kg/m<sup>3</sup> (Ref. 13, Table 2)
- Poisson's ratio = 0.21 at 20 °C (Ref. 12, Table 4) (Assumption 3.3)

Emplacement drift diameter = 5.5 m (Ref. 14, p. 14)

Drift invert = 0.806 m (Ref. 15, Figure 5)

### 5.1.1 Calculations for Available Elevated-Temperature Material Properties

The maximum drip shield temperature in repository emplacement drift is  $T_{\max} = 216^{\circ}\text{C}$  (Ref. 16, Table 6-7). The material properties at this temperature are obtained by linear interpolation of corresponding material properties presented in Section 5.1, by using the formula:

$$p = p(T) = p_l + \left( \frac{T - T_l}{T_u - T_l} \right) \cdot (p_u - p_l)$$

Subscripts  $u$  and  $l$  denote the bounding values of generic material property  $p$  at the corresponding bounding temperatures.

For Ti-7, available material properties at  $421^{\circ}\text{F}$  ( $216^{\circ}\text{C}$ ) are:

$$\text{Yield strength} = 18.6 + \left[ \frac{(421 - 400)}{(450 - 400)} \right] \cdot (16.3 - 18.6) = 17.6 \text{ ksi (121 MPa)}$$

$$\text{Tensile strength} = 30.9 + \left[ \frac{(421 - 400)}{(500 - 400)} \right] \cdot (26.6 - 30.9) = 30.0 \text{ ksi (207 MPa)}$$

$$\text{Modulus of elasticity} = 14.0 + \left[ \frac{(421 - 400)}{(500 - 400)} \right] \cdot (13.3 - 14.0) = 13.85 \cdot 10^6 \text{ psi (95.5 GPa)}$$

Similarly, for Ti-24:

$$\text{Yield strength} = 828 \cdot \left[ \frac{620}{895} \right] = 574 \text{ MPa (Assumption 3.9)}$$

Finally, for Alloy 22:

$$\text{Yield strength} = 34.3 + [(421 - 400)/(450 - 400)] \cdot (33.2 - 34.3) = 33.8 \text{ ksi (233 MPa)}$$

$$\text{Tensile strength} = 95.3 + [(421 - 400)/(500 - 400)] \cdot (92.9 - 95.3) = 94.8 \text{ ksi (654 MPa)}$$

$$\text{Modulus of elasticity} = 196 + [(216 - 204)/(316 - 204)] \cdot (190 - 196) = 195 \text{ GPa}$$

### 5.1.2 Calculations for True Measures of Ductility

The material properties in Section 5.1 refer to engineering stress and strain definitions:  $s = P/A_0$  and  $e = L/L_0 - 1$  (see Ref. 17), where  $P$  stands for the force applied during a static tensile test,  $L$  is the length of the deformed specimen, and  $L_0$  and  $A_0$  are the original length and cross-sectional area of the specimen, respectively. The engineering stress-strain curve does not give a true indication of the deformation characteristics of a material during plastic deformation since it is based entirely on the original dimensions of the specimen. In addition, ductile metal that is pulled in tension becomes unstable and necks down during the course of the test. Hence, LS-DYNA V950.C FEA code requires input in terms of true stress and strain definitions:  $\sigma = P/A$  and  $\epsilon = \ln(L/L_0)$  (see Ref. 17).

The relationships between the true stress and strain definitions and the engineering stress and strain definitions,  $\sigma = s \cdot (1 + e)$  and  $\epsilon = \ln(1 + e)$ , can be readily derived based on constancy of volume ( $A_0 \cdot L_0 = A \cdot L$ ) and strain homogeneity during plastic deformation (see Ref. 17). These expressions are applicable only in the hardening region of the stress-strain curve that is limited by the onset of necking.

The following parameters are used in subsequent calculations:

$$s_y \approx \sigma_y = \text{yield strength}$$

$$s_u = \text{engineering tensile strength}$$

$$\sigma_u = \text{true tensile strength}$$

$$e_y \approx \epsilon_y = \text{strain corresponding to yield strength}$$

$$e_u = \text{engineering strain corresponding to tensile strength (engineering uniform strain)}$$

$$\epsilon_u = \text{true strain corresponding to tensile strength (true uniform strain)}$$

For titanium grades 7 and 24, in absence of data on the uniform strain in available literature, the uniform strain is assumed to be the same as the material elongation (strain corresponding to rupture of the tensile specimen) (Assumption 3.6).

In the case of Ti-7, the true measures of ductility are

$$\varepsilon_u = \ln(1 + e_u) = \ln(1 + 0.2) = 0.18$$

$$\sigma_u = s_u \cdot (1 + e_u) = 207 \cdot (1 + 0.2) = 248 \text{ MPa}$$

Therefore, the true strength of Ti-7 at 216 °C is 248 MPa.

Similarly, for Ti-24:

$$\varepsilon_u = \ln(1 + e_u) = \ln(1 + 0.1) = 0.095$$

$$\sigma_u = s_u \cdot (1 + e_u) = 620 \cdot (1 + 0.1) = 682 \text{ MPa}$$

Therefore, the true tensile strength of Ti-24 at 216 °C is 682 MPa.

The literature indicates that the stress-strain curve for Alloy 22 does not manifest three-stage deformation character (Assumption 3.10). Therefore, an elongation reduced by 10% (to take into account the specimen-failure part of the stress-strain curve) is assumed for uniform strain.

For Alloy 22 ( $e_u = 0.9 \cdot \text{elongation} = 0.405$ ), the true measures of ductility are

$$\varepsilon_u = \ln(1 + e_u) = \ln(1 + 0.405) = 0.34$$

$$\sigma_u = s_u \cdot (1 + e_u) = 654 \cdot (1 + 0.405) = 919 \text{ MPa}$$

Hence, the true tensile strength of Alloy 22 at 216 °C is 919 MPa.

### 5.1.3 Calculations for Tangent Moduli

The results of this simulation are required to include elastic and plastic deformations for Ti-7, Ti-24, and Alloy 22. When materials are driven into the plastic range, the slope of stress-strain curve continuously changes. A ductile failure is preceded by a protracted regime of hardening and substantial accumulation of inelastic strains. Thus, a simplification for stress-strain curve is needed to incorporate plasticity into the FEA. A standard approximation commonly used in engineering is to use a straight line that connects the yield point and the tensile strength point of the material. The parameters used in the subsequent calculations in addition to those defined in Section 5.1.2 are modulus of elasticity ( $E$ ) and tangent (hardening) modulus ( $E_1$ ). The tangent modulus represents the slope of the stress-strain curve in the plastic region.

For Ti-7, the tangent modulus is:

$$E_1 = (\sigma_u - \sigma_y) / (\epsilon_u - \sigma_y / E) = (0.248 - 0.121) / (0.18 - 0.121 / 95.5) = 0.71 \text{ GPa} \text{ (see Sections 5.1.1 and 5.1.2)}$$

Similarly, for Ti-24:

$$E_1 = (\sigma_u - \sigma_y) / (\epsilon_u - \sigma_y / E) = (0.682 - 0.574) / (0.095 - 0.574 / 113.8) = 1.2 \text{ GPa} \text{ (see Sections 5.1, 5.1.1, and 5.1.2)}$$

Finally, for Alloy 22:

$$E_1 = (\sigma_u - \sigma_y) / (\epsilon_u - \sigma_y / E) = (0.919 - 0.233) / (0.34 - 0.233 / 195) = 2.02 \text{ GPa} \text{ (see Sections 5.1.1 and 5.1.2)}$$

## 5.2 ROCK VELOCITY AND MAXIMUM ANGLE OF INCLINATION

### 5.2.1 Calculations for Impact Velocity

To reduce the computer execution time while preserving all features of the problem relevant to the structural calculation, the rock is set in a position just before impact and given an appropriate initial velocity. The initial velocity is defined by the peak ground velocity (PGV) due to seismic activity ( $V_{pg} = 0.939 \text{ m/s}$  for  $10^{-5}$  annual exceedence probability [Ref. 18]) and the maximum distance between the drip shield and the emplacement drift ceiling ( $H_{max}$ ).

The distance between the drip shield and the emplacement drift ceiling is calculated below by using the following parameters:

$$D = 5.5 \text{ m} = \text{emplacement drift diameter (Section 5.1)}$$

$$a = 0.806 \text{ m} = \text{drift invert (Section 5.1)}$$

$$hg = 2.8264 \text{ m} = \text{drip shield maximum height (Section 5.3)}$$

The distance between the drip shield and the emplacement drift ceiling is

$$H_{max} = D - a - hg = 5.5 - 0.806 - 2.8264 = 1.8676 \text{ m}$$

From the equation of motion of a falling object ( $g = 9.81 \text{ m/s}^2$  is gravitational acceleration):

$$\ddot{y} = \pm g$$

and the initial conditions ( $t = 0$ ):

$$\dot{y}(0) = V_{pg} \text{ and } y(0) = 0$$

the position of the body can obtained in the form

$$y = \pm g \cdot t^2 / 2 + V_{pg} \cdot t \quad (1)$$

The corresponding velocity

$$\dot{y} = \pm g \cdot t + V_{pg} \quad (2)$$

is readily obtained by differentiation with respect to time of the Eq. (1). The positive sign corresponds to the case when gravity acceleration acts in the positive direction of the coordinate axis, and vice versa. These two expressions represent the solution of the problem of a falling object.

In order to derive the maximum impact velocity, it is necessary to postulate the most conservative sequence of events amenable to the closed-form solution. Due to the high-frequency nature of the seismic event (causing the rock fall), the number of scenarios is virtually unlimited. Nonetheless, the most conservative set of boundary conditions is the following:

- i) The initial distance between the loose rock and the drip shield is equal to the initial distance between the emplacement drift ceiling and the drip shield ( $H_{\max}$ ).
- ii) The initial velocity of both the loose rock and the drip shield is the maximum possible velocity, i.e. the PGV ( $V_{pg}$ ), in the direction of gravity (downward).
- iii) The final velocity of the drip shield, just before the impact, is the PGV, in the direction opposite to gravity (upward).

The first two conditions can be achieved if the ground during the earthquake originally moves upward with the PGV, and then reverses the motion with the reversal acceleration equal to the acceleration due to gravity. At the moment when the ground, moving downward, reaches the PGV the rock gets loose. This sequence of events also ensures that the contact between the drip shield and the emplacement drift floor is maintained incessantly; events including contact separations are beyond the scope of present calculation. The velocity of the drip shield is, under these circumstances, controlled by the ground motion and the most conservative scenario is that it is moving downward with the PGV ( $V = V_{pg} = \text{Const.}$ ). On the other hand, the loose rock is accelerating due to gravity. Thus, the rock is catching up with the drip shield, and finally they get into contact. It is supposed that just before the impact the ground momentarily reaches the PGV in the direction opposite to the

gravity. This simplified approach maximizes the duration of the rock fall and consequently maximizes the velocity of the rock and the impact velocity.

Consequently, the distance traveled by the rock before the impact

$$S_{rock} = g \cdot t_f^2 / 2 + V_{pg} \cdot t_f \quad (3)$$

is obtained by substituting the impact time ( $t \equiv t_f$ ) into the Eq. (1). Since the drip shield is moving with constant velocity ( $V = V_{pg} = Const.$ ), the distance it travels before the impact is simply

$$S_{ds} = V_{pg} \cdot t_f$$

The final time by which the rock catches up with the drip shield

$$t_f = \sqrt{\frac{2 \cdot H_{max}}{g}} \quad (4)$$

can be derived straightforwardly from the condition  $S_{rock} = H_{max} + S_{ds}$ .

It should be noted that the finite reversal acceleration and the subsequent time necessary for the reversal are not incorporated into the calculations; it is conservatively considered that the reversal of ground velocity from  $V_{pg}$  to  $-V_{pg}$  is instantaneous.

The maximum velocity of the rock relative to the drip shield is obtained in the case when the drip shield, just prior to the impact, moves in the direction opposite to rock with velocity  $V_{ds} = -V_{pg}$ :

$$V = V_f - V_{ds} = 2 \cdot V_{pg} + \sqrt{2 \cdot g \cdot H_{max}}$$

Therefore, for previously calculated  $H_{max} = 1.8676 \text{ m}$  and  $V_{pg} = 0.939 \text{ m/s}$  (Ref. 18), the impact velocity is:

$$V = 2 \cdot V_{pg} + \sqrt{2 \cdot g \cdot H_{max}} = 2 \cdot 0.939 + \sqrt{2 \cdot 9.81 \cdot 1.8676} = 7.93 \text{ m/s}$$

An impact velocity of 8.0 m/s will be conservatively used in calculations.

### 5.2.2 Calculations for Maximum Angle of Rock Inclination

The rock length ( $L_R$ ) and the maximum distance between the emplacement drift ceiling and the drip shield define the maximum angle of rock inclination with respect to horizontal plane at the moment of impact:

$$\alpha = \arcsin(H_{\max}/L_R)$$

The maximum distance between the emplacement drift ceiling and the drip shield is calculated in Section 5.2.1. The rock lengths and apex heights are available in Reference 19, Attachment IX, Table IX-2 for selected rock sizes. The maximum angles of rock inclination with respect to the horizontal plane are calculated using the relation given above.  $H_{\max}$  was obtained from a drip shield overall height that was raised by 0.3 m in comparison to the original design (see Sections 5.2.1 and 5.3). However, the original drip shield height is conservatively used in the following calculations of angles of rock inclination, as the increased distance between the emplacement drift ceiling and the drip shield results in larger rock inclination angles and subsequent larger stresses on the drip shield. The maximum angles of rock inclination and apex heights corresponding to various rock sizes are given in Table 1.

As an example calculation, the 6-MT rock angle of inclination is provided below:

$$\alpha = \arcsin((1.8676 + 0.3)/5.38) = 24^\circ$$

The rock length of the 5-MT rock is conservatively used for the 6-MT rock since the dimensions of a 6-MT rock was not reported in Reference 19.

Table 1. Maximum Angle of Rock Inclination

Mass (MT)	Length (m)	Apex (m)	Angle (degrees)
6	5.38	1.28	24
15	13.65	1.31	9
19	15.96	1.31	8
30	24.79	1.30	5
36	28.94	1.29	4
52	40.49	1.27	3

### 5.3 GEOMETRIC DIMENSIONS OF DRIP SHIELD

This calculation is performed for a drip shield design that is modified from the sketches provided in Attachment I. These modifications are described below:

- Stiffener plates (Ti-24) of 20 mm in thickness and 50 mm in width are welded to the bottom, on both sides of the bulkheads as shown in Figures II-1, II-2, and II-3. These stiffeners extend from one drip shield side wall to the other.

- Longitudinal stiffener beams (Ti-24) of 38 mm in thickness are welded to the top plate on the drip shield symmetry plane. The width of these longitudinal stiffeners are equal to the distance between the bulkhead stiffener plates and the top plate. Figures II-2 and II-3 show one section of these longitudinal stiffeners.
- Two sets of longitudinal stiffeners (Ti-24), 225 mm apart from the ones on the symmetry plane are also welded to the top plate. The dimensions are the same as the dimensions of the longitudinal stiffeners located on the symmetry plane, as described above. Figures II-2 and II-3 show one half-symmetry finite element representation; therefore, the longitudinal stiffeners at the center and only one of the off-centered ones can be seen in these figures.
- Overall height of the drip shield is raised by 300 mm, which results in an overall height of 2.8264 m (overall height is shown as 2.5264 on p. I-4). This is accomplished by extending the upper end of the vertical support beams, side-wall plate, external support plate, and by simply raising all structural components constituting the top portion of the drip shield. This modification results in substantial amount of added material to the drip shield design. This taller design is illustrated in Figures II-1 through II-10.

#### 5.4 REDUCTION OF THICKNESS DUE TO CORROSION

Corrosion rate for Ti-7 is  $1.5 \cdot 10^{-4}$  mm/year (Section 5.1). Therefore, expected cumulative decrease of thickness on both sides of the drip shield plates over 10,000 years of post-closure period would be two times this value, times 10,000 years, which is 3.0 mm. Hence, the simulation of rock fall on the corroded drip shield is performed with thicknesses of all titanium plates conservatively reduced for 3.0 mm. In absence of data on the corrosion rate of Ti-24, the corrosion rate of Ti-7 is used for that of Ti-24 (Assumption 3.8).

The corrosion rate of Alloy 22 for the base plate is not included in the finite element simulations due to the fact that the effect of the base plate corrosion rate on the rock fall performance of the drip shield is inconsequential.

#### 5.5 FINITE ELEMENT REPRESENTATION

Two different rock fall events are considered: horizontal rock fall and pointed-edge rock fall. Two different rock sizes, 6 MT and 52 MT, are used in horizontal rock fall simulations. The 6 MT is the design basis rock size; 52 MT is the largest rock size reported in Reference 19. These two rock sizes are used as the base cases for the horizontal rock fall calculations.

For the pointed-edge rock fall event, stress concentration effects due to localized deformations over the drip shield top plate necessitated evaluations using a range of rock sizes obtained from Reference 19: 6 MT, 15 MT, 19 MT, 30 MT, 36 MT, and 52 MT.

Although all of the simulations are performed using actual rock size and dimensions, some simplifications are made to the drip shield representation for computational purposes. The finite element representations of different rock sizes include different section lengths of drip shields. For rock sizes of 6 MT, 15 MT, and 19 MT, for both horizontal and pointed-edge rock falls, a drip shield length of 5.3 m is conservatively used. For rock sizes of 30 MT, 36 MT, and 52 MT of the pointed-edge rock fall, a drip shield length of 17 m is used. For the horizontal fall of 52 MT size rock, a drip shield length of 34.2 m is used. In all these simulations, the section of the drip shield is sufficiently long since all the stress and deformation results are captured throughout the dynamic impact between the two objects. The benefit of using this approach is to reduce the computer execution time while preserving all features of the problem relevant to the structural calculation.

The finite element representation includes certain simplifications in the drip shield design. The FER was first developed to represent the interlocking drip shield design (see pp. I-1 and I-2). Therefore, the drip shield FER is developed such that the mid-section between the connector assemblies is continuously extended along the axis of the drip shield; the components of the connector assembly are conservatively excluded from the FER (see Figures II-1 through II-10).

In relation to the stand-alone drip shield design (pp. I-3 through I-16), this FER is used to obtain one set of preliminary, estimated stress and deformation results. One difference between the FER and the stand-alone design is the separation of drip shields from end-to-end by certain size of spacing. Although the large size rocks are anticipated to impart kinetic energy over more than one stand-alone drip shield, the structural response between a number of stand-alone drip shields and a continuous one is anticipated to be different. Since no structural credit is taken for the drip shield enclosure panels by using only the top plates and the stiffeners in this FER, the results are deemed to represent an estimate of what should be expected from the structural performance of the stand-alone drip shields. Nevertheless, further confirmation of this assessment is required in future evaluations.

Three-dimensional, half-symmetry FERs of the drip shield and the rock are developed in ANSYS V5.4 for the above mentioned rock sizes. FERs are developed by using the dimensions provided in Attachment I and Section 5.3. These three FERs are then used in LS-DYNA V950.C to perform a transient dynamic analysis of rock fall. No failure condition is conservatively assumed for the rock blocks (Assumption 3.1). The rock shapes are based on the rock geometry and dimensions obtained from the Subsurface Facility Department (Ref. 19).

The boundary conditions are such that the drip shield is constrained only in vertical direction. However, contact elements are defined between the drip shield side walls and the gantry rails (see Assumption 3.11). The rails are simulated using rigid shell elements (see Figure II-5) that are fixed in all directions.

Since one half-symmetry FER is developed, symmetry boundary conditions are used at the nodes located on the plane of symmetry.

For all rock fall simulations, the simulation termination times are such to allow the rock to bounce off the drip shield after the impact; subsequently, the maximum stresses and deformations are recorded and tabulated.

All finite element simulations include the most conservative case, the corroded drip shield; the thickness of the titanium structural components is appropriately reduced based on the calculation of the depth of corroded layer presented in Section 5.4.

The mesh of the FER was appropriately generated and refined in the contact region according to standard engineering practice (see Figure II-10). Thus, the accuracy and representativeness of the results of this calculation were deemed acceptable.

## 6. RESULTS

This document may be affected by technical product input information that requires confirmation. Any changes to the document that may occur as a result of completing the confirmation activities will be reflected in subsequent revisions. The status of the technical product input information quality may be confirmed by review of the Document Input Reference System database.

LS-DYNA V950.C stress results include high-frequency response. In the case of stress histories used for determination of residual stresses, these results are filtered using a Butterworth low-pass filter with cut-off frequency of 20 Hz. The purpose of the filtering is to obtain steady-state residual stresses by removing the high-frequency response. Since the stress results after the filtering produced steady-state values anticipated by visual inspection of unfiltered (raw) stress histories (see, for example, Figures II-14, II-18 and II-22), this type of filtering was deemed acceptable.

The stress results obtained from LS-DYNA V950.C are reported in terms of maximum stress intensity. The maximum stresses are found by careful examination of each time step recorded by LS-DYNA V950.C, which outputs the element with the highest magnitude of certain stress component, at each recorded step, for each defined part.

The results of the finite element solutions are summarized in Tables 2 and 3. These tables provide the results for eight different finite element solutions of rock fall on drip shield. The solutions are grouped in accordance with the type of the rock fall event and the mass of the rock. In Table 2, the drip shield structural response is given in two categories. First, the drip shield immediate response to impact is given in terms of the maximum deflection and maximum stress intensity. The maximum allowable stress magnitude of Ti-7 before failure is also provided for comparison with the stress intensity. Second, the drip shield response to stress corrosion cracking is reported in terms of the maximum residual stress intensity in the drip shield top plate. The threshold stress for crack initiation is also given to compare against the maximum residual stress intensity.

Table 3 summarizes the results in terms of the maximum stress intensity in the bulkheads. The function of the bulkheads is to provide structural support for the drip shield plates. This component is made of Ti-24 and its allowable stress is also provided for comparison in Table 3.

In the case of a horizontal rock fall on drip shield, a fairly uniform residual stress pattern is observed on the drip shield top plate in the region of contact between the rock and the drip shield. The reason for such a stress pattern is that the dynamic load is taken both by the stiffeners and the drip shield top plate sections close to those stiffeners. The residual stress quantity used in determining susceptibility of the material to stress corrosion cracking was the stress intensity (difference between the first and the third principal stresses) on the top surface of the drip shield top plate. The stress intensity congregates the maximum effect of all three principal stress components into a single quantity; therefore, it is used to compare against the material stress allowables.

The most essential rock fall cases are the ones that include the design basis rock size, 6 MT horizontal and pointed-edge rock falls. Nevertheless, the drip shield immediate response to rock fall shows that there is no failure in the drip shield top plate for any of the rock sizes considered (see Tables 2 and 3). However, based on the threshold stress value for stress corrosion crack initiation, which is 10% of the material yield strength (see Ref. 20, Section 6.5.2), several assessments are made on the potential for initiation of stress corrosion cracking due to the residual stresses caused by the rock fall. For the horizontal rock fall event, the results indicate that the maximum residual stress intensity in the drip shield top plate is 170 MPa. The average value of the stress intensity over the top plate in the region of contact is approximately half of the maximum value. Therefore, the drip shield top plate area that contacts the rock block is anticipated to be susceptible to stress corrosion cracking subsequent to rock fall. However, an important feature of the drip shield design, as explained in Section 5.3, is that the top plate is supported not only by the bulkheads approximately 1 m apart from each other but also with three longitudinal stiffeners, one at the center, and two 225 mm apart from the center. Since the maximum stresses occur at the top section of the drip shield top plate and the stiffeners are anticipated to remain intact due to their high strength and thicknesses, the maximum potential plate failure section size per 1 m length of the drip shield top plate due to stress corrosion cracking is anticipated to be less than 1 m x 0.2 m. This type of failure is of course, possible only in the highly unlikely event that multiple cracks form a rectangular section through the thickness in the top plate. In case of a pointed-edge rock fall, the area of contact, and consequently, the surface area of the top plate susceptible to stress corrosion cracking, is smaller than the previous case.

Since the drip shield overall height is raised by 300 mm and the previously available gap between the drip shield and the waste package was 80 mm (see p. I-17), the minimum gap is now increased to 380 mm. Therefore, it is evident from the maximum gap closure values in Table 2 that the drip shield design precludes contact between the drip shield and the waste package for all rock fall events and waste package sizes.

Table 2. Summary of Results for the Drip Shield Structural Performance under Rock Fall (Top plate, Ti-7)

Rock Fall Event	Rock Mass (MT)	Vertical Peak Ground Velocity Corresponding to Annual Probability of Exceedence (APE)	DS Immediate Response to Impact			DS Response to SCC due to Residual Stresses	
			Maximum Gap Closure Between DS and Waste Package (m)	Maximum Stress Intensity in DS Top Plate (MPa)	Maximum Allowable True Stress (MPa)	Maximum Residual Stress Intensity in DS Top Plate (MPa)	Threshold Stress for Crack Initiation (10% of yield strength) (MPa)
Horizontal Rock Fall	6	0.939 m/s (10 <sup>-5</sup> APE) (Ref. 18)	0.116 (Figure II-12)	188 (Figure II-13)	248 (Section 5.1.2)	110 (Figure II-14)	12 (Section 5.1.1)
	52		0.224 (Figure II-16)	208 (Figure II-17)		170 (Figure II-18)	
Pointed-edge Rock Fall	6		0.073* (Figure II-20)	208 (Figure II-21)		180 (Figure II-22)	
	15		0.143* (Figure II-24)	216 (Figure II-25)		170 (Figure II-26)	
	19		0.170* (Figure II-28)	220 (Figure II-29)		180 (Figure II-30)	
	30		0.209 (Figure II-32)	229 (Figure II-33)		220 (Figure II-34)	
	36		0.231 (Figure II-36)	230 (Figure II-37)		225 (Figure II-38)	
	52		0.283 (Figure II-40)	232 (Figure II-41)		210 (Figure II-42)	

\*Maximum displacement is located in the longitudinal stiffener on symmetry axis; therefore, 0.02 m subtracted from the actual displacement due to the additional gap provided by the thickness of the stiffener plate at the bottom of the bulkhead.

Table 3. Summary of Results for the Drip Shield Structural Performance under Rock Fall (Bulkheads, Ti-24)

Rock Fall Event	Rock Mass (MT)	Vertical Peak Ground Velocity Corresponding to Annual Probability of Exceedence (APE)	DS Immediate Response to Impact	
			Maximum Stress Intensity in DS Bulkheads (MPa)	Maximum Allowable True Stress (MPa)
Horizontal Rock Fall	6	0.939 m/s (10 <sup>-5</sup> APE) (Ref. 18)	618 (Figure II-15)	682 (Section 5.1.2)
	52		653 (Figure II-19)	
Pointed-edge Rock Fall	6		645 (Figure II-23)	
	15		647 (Figure II-27)	
	19		653 (Figure II-31)	
	30		655 (Figure II-35)	
	36		657 (Figure II-39)	
	52		665 (Figure II-43)	

## 7. REFERENCES

1. BSC (Bechtel SAIC Company) 2001. *Technical Work Plan for: Waste Package Design Description for SR*. TWP-EBS-MD-000003 REV 01. Las Vegas, Nevada: Bechtel SAIC Company. URN-0879
2. AP-3.12Q, Rev. 0, ICN 4. *Calculations*. Washington, D.C.: U.S. Department of Energy, Office of Civilian Radioactive Waste Management. ACC: MOL.20010404.0008.
3. ASME (American Society of Mechanical Engineers) 1998. *1998 ASME Boiler and Pressure Vessel Code*. 1998 Edition with 1999 and 2000 Addenda. New York, New York: American Society of Mechanical Engineers. TIC: 247429.
4. ASM (American Society for Metals) 1980. *Properties and Selection: Stainless Steels, Tool Materials and Special-Purpose Metals*. Volume 3 of *Metals Handbook*. 9th Edition. Benjamin, D., ed. Metals Park, Ohio: American Society for Metals. TIC: 209801.
5. ASM International 1990. *Properties and Selection: Nonferrous Alloys and Special-Purpose Materials*. Volume 2 of *ASM Metals Handbook*. Materials Park, Ohio: American Society for Metals. TIC: 241059.
6. CRWMS M&O 2000. *Stress-Strain-Curve Character for Alloy 22 and 316 Stainless Steel*. Input Transmittal 00384.T. Las Vegas, Nevada: CRWMS M&O. ACC: MOL.20001013.0053.
7. CRWMS M&O 1998. *ANSYS*. V5.4. HP-UX 10.20. 30040 5.4.
8. CRWMS M&O 2000. *Software Code: LS-DYNA*. V950. HP 9000. 10300-950-00.
9. ASME (American Society of Mechanical Engineers) 1995. *1995 ASME Boiler and Pressure Vessel Code*. New York, New York: American Society of Mechanical Engineers. TIC: 245287.
10. BSC (Bechtel SAIC Company) 2001. *Drip Shield General Corrosion Rate for Drip Shield Thinning with Time for Rock Fall Damage to Drip Shield*. Input Transmittal 00425.T. Las Vegas, Nevada: Bechtel SAIC Company. ACC: MOL.20010220.0061.
11. Haynes International 1997. *Hastelloy C-22 Alloy*. Kokomo, Indiana: Haynes International. TIC: 238121.
12. MO0003RIB00079.000. Rock Mechanical Properties. Submittal date: 03/30/2000.
13. MO9808RIB00041.000. Reference Information Base Data Item: Rock Geomechanical Properties. Submittal date: 08/05/1998.

14. CRWMS M&O 2000. *Emplacement Drift System Description Document*. SDD-EDS-SE-000001 REV 01. Las Vegas, Nevada: CRWMS M&O. ACC: MOL.20000803.0348.
15. CRWMS M&O 2000. *Invert Configuration and Drip Shield Interface*. TDR-EDS-ST-000001 REV 00. Las Vegas, Nevada: CRWMS M&O. ACC: MOL.20000505.0232.
16. CRWMS M&O 2000. *Drift Scale Thermal Analysis*. CAL-WIS-TH-000002 REV 00. Las Vegas, Nevada: CRWMS M&O. ACC: MOL.20000420.0401.
17. Dieter, G.E. 1976. *Mechanical Metallurgy*. 2nd Edition. Materials Science and Engineering Series. New York, New York: McGraw-Hill Book Company. TIC: 247879.
18. MO0008SEPPGVRL.020. Preliminary Seismic Design Peak Ground Velocity for the Repository Level (Point B) for 10-5 Annual Exceedence Probability. Submittal date: 08/24/2000. Submit to RPC URN-0878
19. CRWMS M&O 2000. *Drift Degradation Analysis*. ANL-EBS-MD-000027 REV 01. Las Vegas, Nevada: CRWMS M&O. ACC: MOL.20001206.0006.
20. CRWMS M&O 2000. *Stress Corrosion Cracking of the Drip Shield, the Waste Package Outer Barrier, and the Stainless Steel Structural Material*. ANL-EBS-MD-000005 REV 00 ICN 01. Las Vegas, Nevada: CRWMS M&O. ACC: MOL.20001102.0340.
21. CRWMS M&O 2000. *Waste Package Degradation Process Model Report*. TDR-WIS-MD-000002 REV 00 ICN 02. Las Vegas, Nevada: CRWMS M&O. ACC: MOL.20001228.0229.

## 8. ATTACHMENTS

Attachment I (17 pages): Design sketches

Attachment II (43 pages): Figures obtained from LS-DYNA V950.C

Attachment III (compact disc): ANSYS V5.4 and LS-DYNA V950.C electronic files

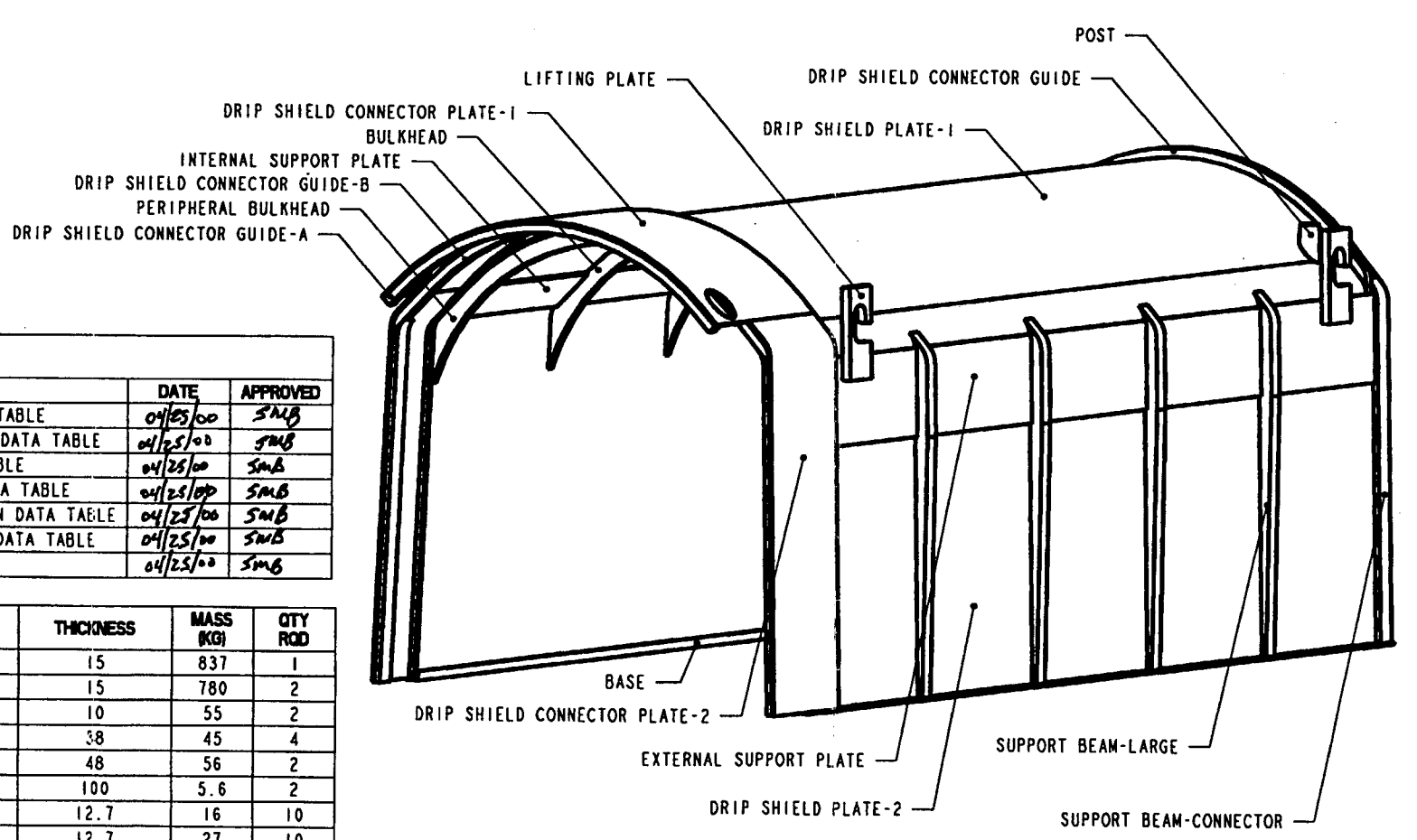
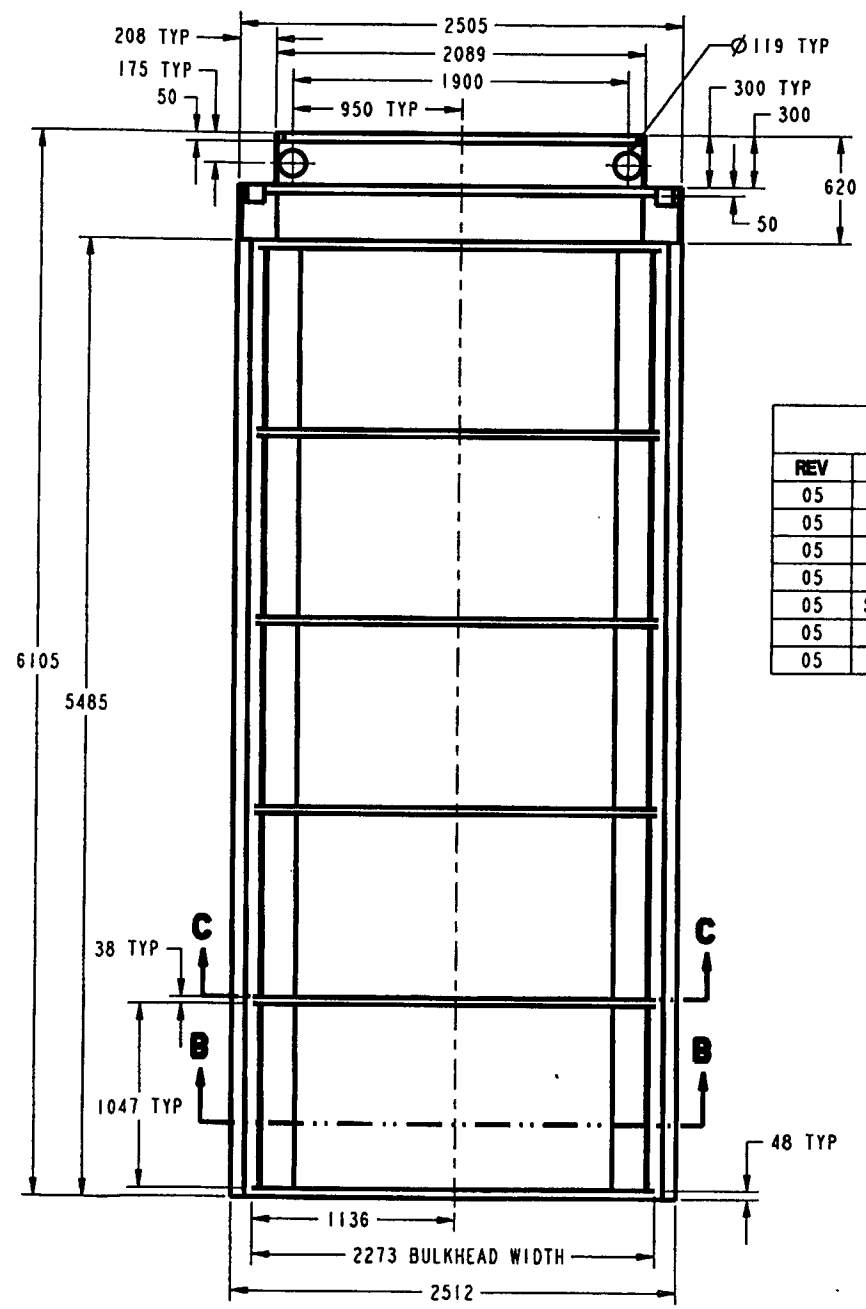
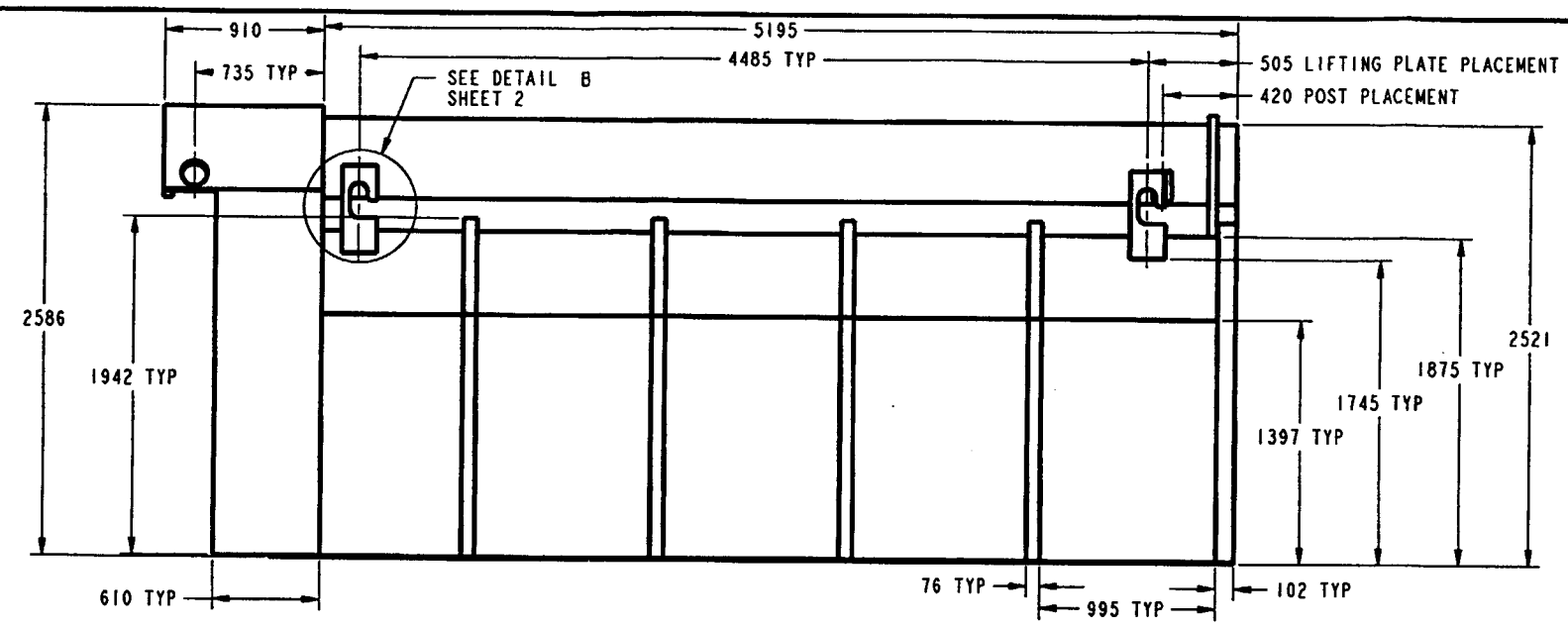
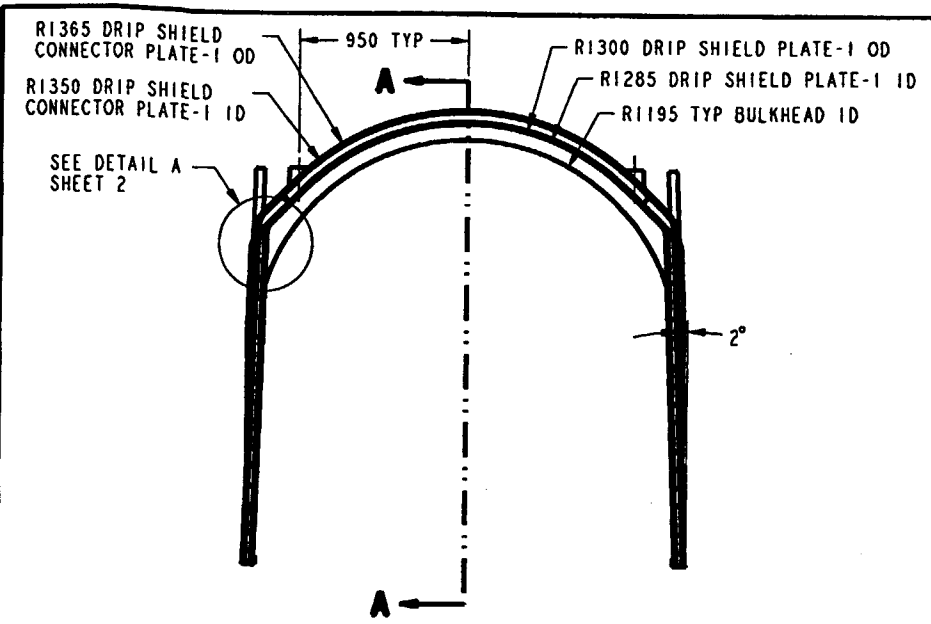
Table 4 includes the name, size, date, and time for each electronic file in Attachment III. File sizes may slightly vary depending on the operating system.

Table 4. File Names, Sizes, Dates, and Times in Attachment III

Directory	File Name	Size	Date	Time
h6mt	bc1.inc	11 KB	06/20/01	6:19 pm
	bc2.inc	1 KB	06/20/01	6:19 pm
	bc3.inc	15 KB	06/20/01	6:19 pm
	bc4.inc	1 KB	06/20/01	6:19 pm
	d3hsp	9496 KB	06/20/01	6:19 pm
	elem1.inc	1093 KB	06/20/01	6:19 pm
	elem2.inc	991 KB	06/20/01	6:19 pm
	h6mt.k	2 KB	06/20/01	6:19 pm
	h6mt.old.out	157 KB	06/20/01	6:19 pm
	node.inc	1688 KB	06/20/01	6:19 pm
h52mt	bc1.inc	39 KB	06/20/01	6:12 pm
	bc2.inc	2 KB	06/20/01	6:12 pm
	bc3.inc	53 KB	06/20/01	6:12 pm
	bc4.inc	1 KB	06/20/01	6:11 pm
	d3hsp	33369 KB	06/20/01	6:11 pm
	elem1.inc	4452 KB	06/20/01	6:11 pm
	elem2.inc	3965 KB	06/20/01	6:11 pm
	h52mt.k	2 KB	06/20/01	6:11 pm
	h52mt.old.out	516 KB	06/20/01	6:11 pm
	node.inc	6869 KB	06/20/01	6:11 pm
c6mt	bc1.inc	11 KB	06/20/01	6:05 pm
	bc2.inc	1 KB	06/20/01	6:05 pm
	bc3.inc	15 KB	06/20/01	6:05 pm
	bc4.inc	1 KB	06/20/01	6:05 pm
	d3hsp	9489 KB	06/20/01	6:07 pm
	elem1.inc	991 KB	06/20/01	6:07 pm
	elem2.inc	1093 KB	06/20/01	6:07 pm
	c6mt.k	2 KB	06/20/01	6:06 pm
	c6mt.old.out	157 KB	06/20/01	6:07 pm
	node.inc	1688 KB	06/20/01	6:07 pm

c15mt	bc1.inc	11 KB	06/20/01	6:20 pm
	bc2.inc	1 KB	06/20/01	6:20 pm
	bc3.inc	16 KB	06/20/01	6:20 pm
	bc4.inc	1 KB	06/20/01	6:20 pm
	c15mt.k	2 KB	06/20/01	6:20 pm
	c15mt.old.out	157 KB	06/20/01	6:20 pm
	d3hsp	10214 KB	06/20/01	6:20 pm
	elem1.inc	1304 KB	06/20/01	6:20 pm
	elem2.inc	991 KB	06/20/01	6:20 pm
	node.inc	1855 KB	06/20/01	6:20 pm
c19mt	bc1.inc	11 KB	06/20/01	6:21 pm
	bc2.inc	1 KB	06/20/01	6:21 pm
	bc3.inc	16 KB	06/20/01	6:21 pm
	bc4.inc	1 KB	06/20/01	6:21 pm
	c19mt.k	2 KB	06/20/01	6:21 pm
	c19mt.old.out	157 KB	06/20/01	6:21 pm
	d3hsp	10214 KB	06/20/01	6:21 pm
	elem1.inc	1304 KB	06/20/01	6:21 pm
	elem2.inc	991 KB	06/20/01	6:21 pm
	node.inc	1855 KB	06/20/01	6:21 pm
c30mt	bc1.inc	34 KB	06/20/01	6:14 pm
	bc2.inc	1 KB	06/20/01	6:14 pm
	bc3.inc	43 KB	06/20/01	6:14 pm
	bc4.inc	1 KB	06/20/01	6:14 pm
	c30mt.k	2 KB	06/20/01	6:14 pm
	c30mt.old.out	328 KB	06/20/01	6:14 pm
	d3hsp	26684 KB	06/20/01	6:14 pm
	elem1.inc	3465 KB	06/20/01	6:13 pm
	elem2.inc	3165 KB	06/20/01	6:13 pm
	node.inc	5341 KB	06/20/01	6:13 pm
c36mt	bc1.inc	34 KB	06/20/01	6:15 pm
	bc2.inc	1 KB	06/20/01	6:15 pm
	bc3.inc	43 KB	06/20/01	6:15 pm
	bc4.inc	1 KB	06/20/01	6:15 pm
	c36mt.k	2 KB	06/20/01	6:15 pm
	c36mt.old.out	328 KB	06/20/01	6:15 pm
	d3hsp	26684 KB	06/20/01	6:15 pm
	elem1.inc	3465 KB	06/20/01	6:15 pm
	elem2.inc	3165 KB	06/20/01	6:15 pm
	node.inc	5341 KB	06/20/01	6:15 pm
c52mt	bc1.inc	34 KB	06/20/01	6:17 pm
	bc2.inc	1 KB	06/20/01	6:17 pm
	bc3.inc	43 KB	06/20/01	6:17 pm
	bc4.inc	1 KB	06/20/01	6:17 pm
	c52mt.k	2 KB	06/20/01	6:16 pm
	c52mt.old.out	328 KB	06/20/01	6:17 pm
	d3hsp	26689 KB	06/20/01	6:16 pm
	elem1.inc	3465 KB	06/20/01	6:16 pm
	elem2.inc	3165 KB	06/20/01	6:16 pm
	node.inc	5341 KB	06/20/01	6:16 pm

Note that some of the computer simulations were terminated after the necessary number of load steps had been obtained for a steady-state solution. This has no effect on the results since the steady-state solutions in terms of displacements, strains, and stresses were essentially obtained during the time of computer simulations.



REVISION HISTORY			
REV	DESCRIPTION	DATE	APPROVED
05	BULKHEAD MATERIAL UNS NUMBER CHANGED ON DATA TABLE	04/25/00	SMB
05	PERIPHERAL BULKHEAD MATERIAL UNS NUMBER CHANGED ON DATA TABLE	04/25/00	SMB
05	POST MATERIAL UNS NUMBER CHANGED ON DATA TABLE	04/25/00	SMB
05	LIFTING PLATE MATERIAL UNS NUMBER CHANGED ON DATA TABLE	04/25/00	SMB
05	SUPPORT BEAM-CONNECTOR MATERIAL UNS NUMBER CHANGED ON DATA TABLE	04/25/00	SMB
05	SUPPORT BEAM-LARGE MATERIAL UNS NUMBER CHANGED ON DATA TABLE	04/25/00	SMB
05	REVISION HISTORY TABLE ADDED	04/25/00	SMB

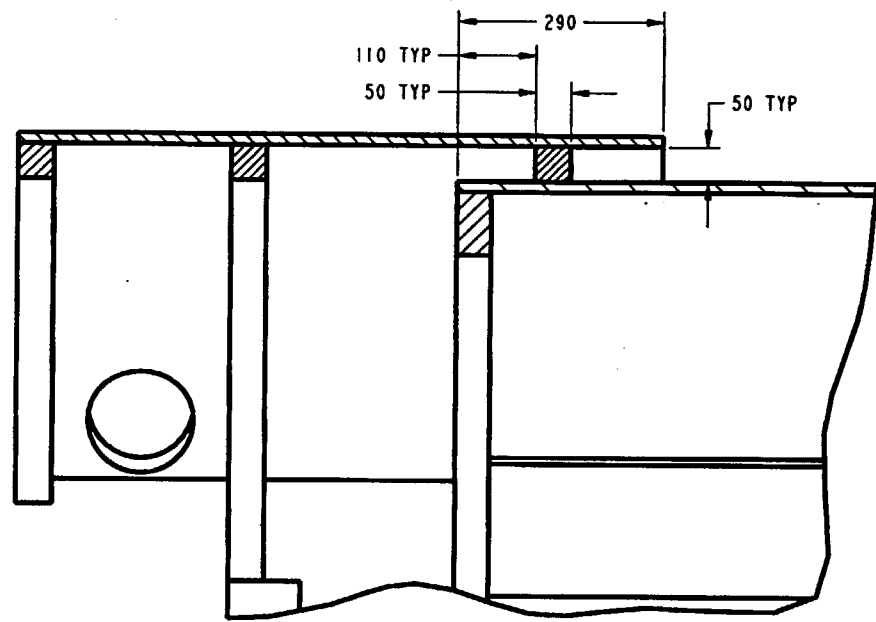
COMPONENT NAME	MATERIAL	THICKNESS	MASS (KG)	QTY	ROD
DRIP SHIELD PLATE-1	SB-265 R52400	15	837	1	
DRIP SHIELD PLATE-2	SB-265 R52400	15	780	2	
BASE	SB-575 N06022	10	55	2	
BULKHEAD	SB-265 R56405	38	45	4	
PERIPHERAL BULKHEAD	SB-265 R56405	48	56	2	
POST	SB-265 R56405	100	5.6	2	
INTERNAL SUPPORT PLATE	SB-265 R52400	12.7	16	10	
EXTERNAL SUPPORT PLATE	SB-265 R52400	12.7	27	10	
LIFTING PLATE	SB-265 R56405	50	17	4	
SUPPORT BEAM-CONNECTOR	SB-265 R56405	102	27	6	
SUPPORT BEAM-LARGE	SB-265 R56405	76	37	8	
DRIP SHIELD CONNECTOR GUIDE	SB-265 R52400	50	30	2	
DRIP SHIELD CONNECTOR PLATE-1	SB-265 R52400	15	142	1	
DRIP SHIELD CONNECTOR PLATE-2	SB-265 R52400	15	89	2	
DRIP SHIELD CONNECTOR GUIDE-A	SB-265 R52400	50	26	1	
DRIP SHIELD CONNECTOR GUIDE-B	SB-265 R52400	50	31	1	
DRIP SHIELD ASSEMBLY	-	-	4203	1	

"FOR INFORMATION ONLY"

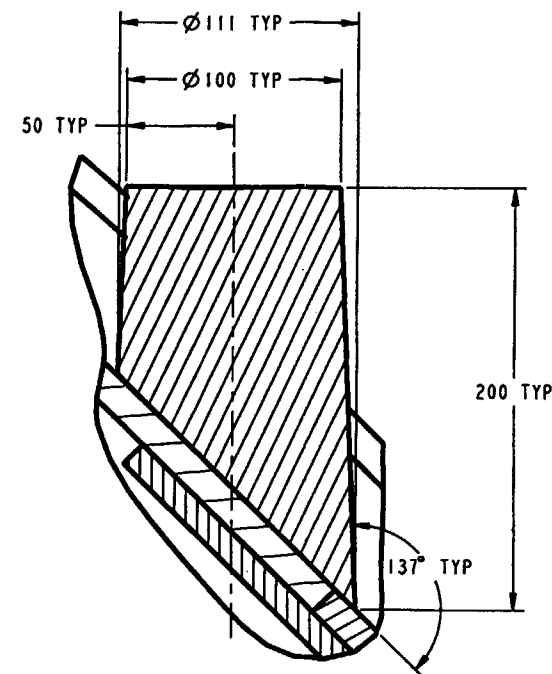
### SR DRIP SHIELD

SKETCH NUMBER: SK-0148 REV 05 SHEET 1 OF 2  
 SKETCHED BY: BRYAN HARKINS  
 DATE: 04/21/00  
 FILE: /home/harkins/proe/drip\_shield/sk-0148\_rev05.dwg

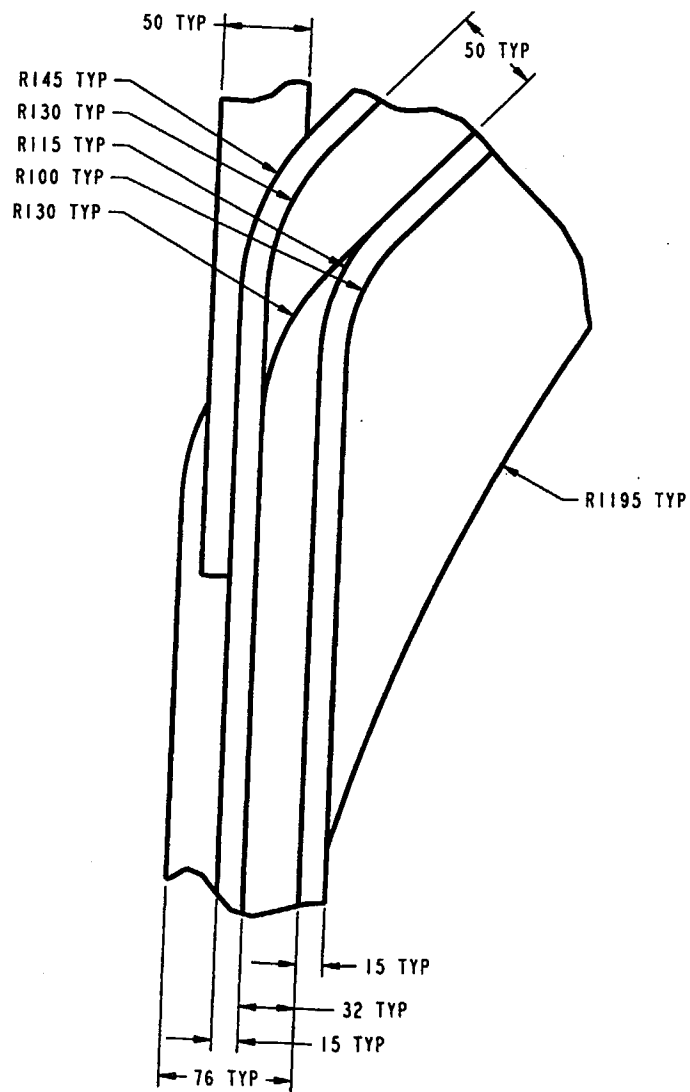
UNITS: mm  
 DO NOT SCALE FROM SKETCH



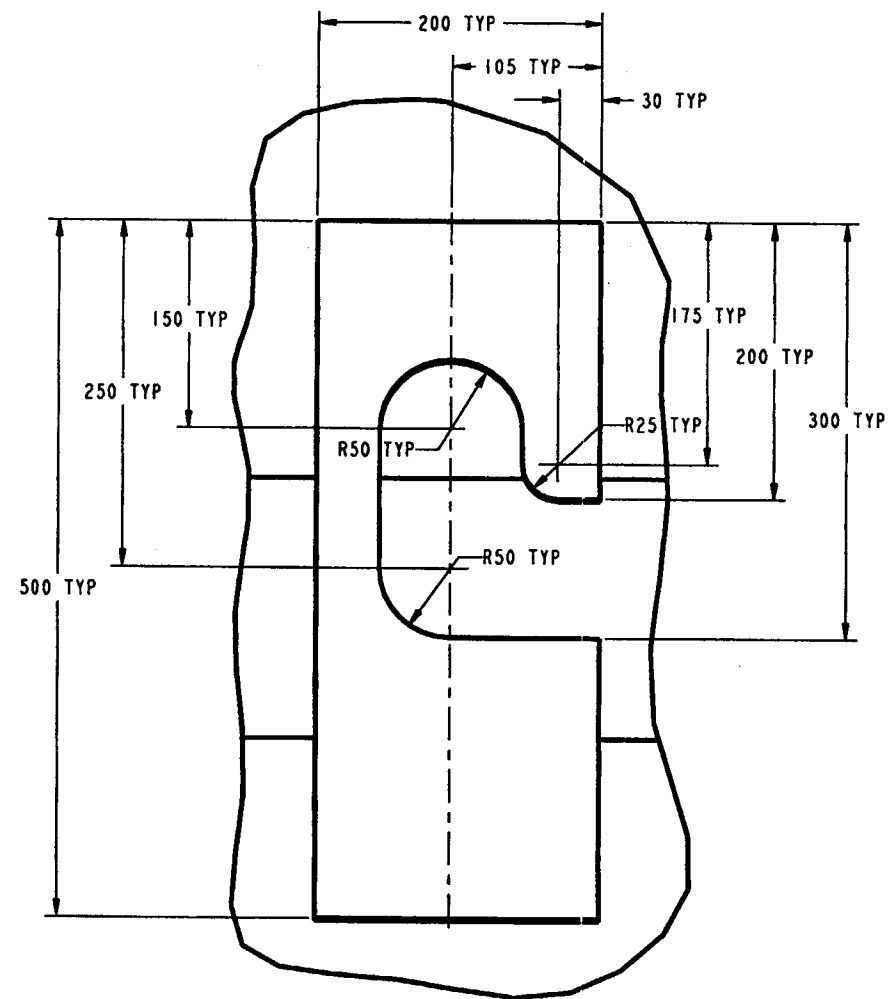
SECTION A-A



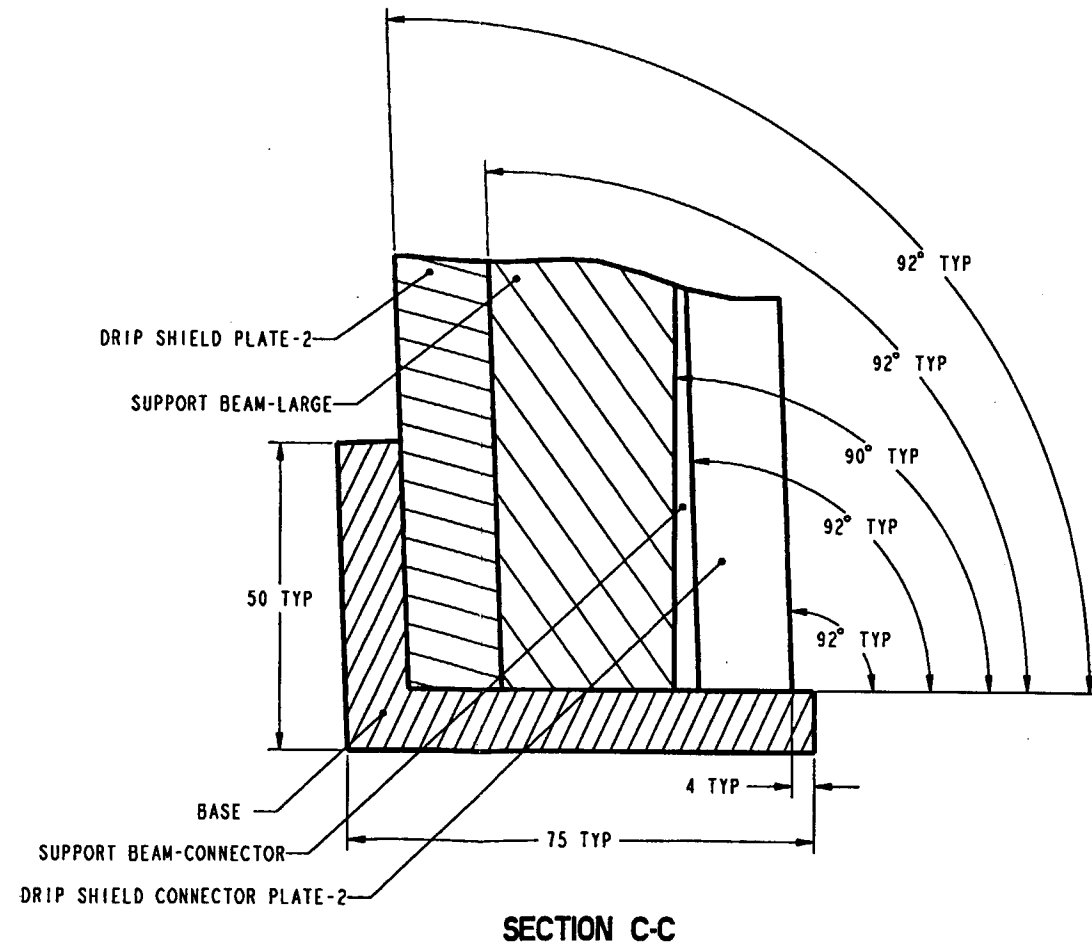
SECTION B-B



DETAIL A



DETAIL B



SECTION C-C

8 7 6 5 4 3 1

SM-20-MS  
120-MS  
1 OF 14  
NOI1A32

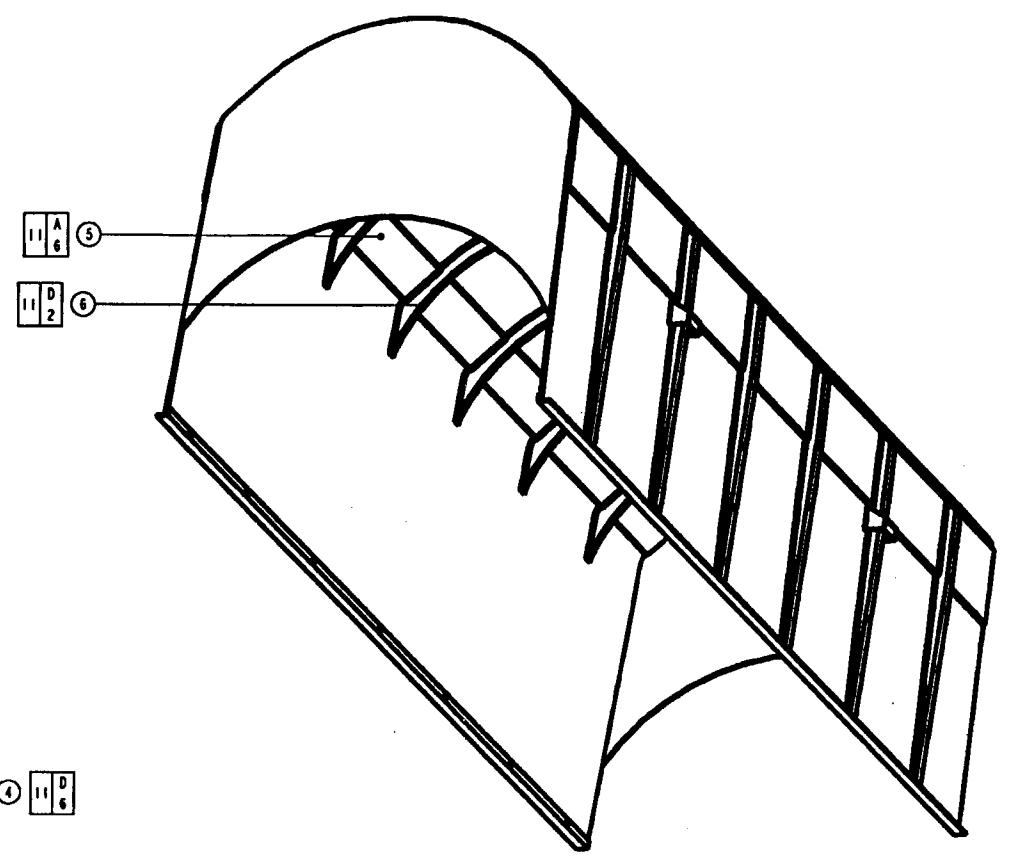
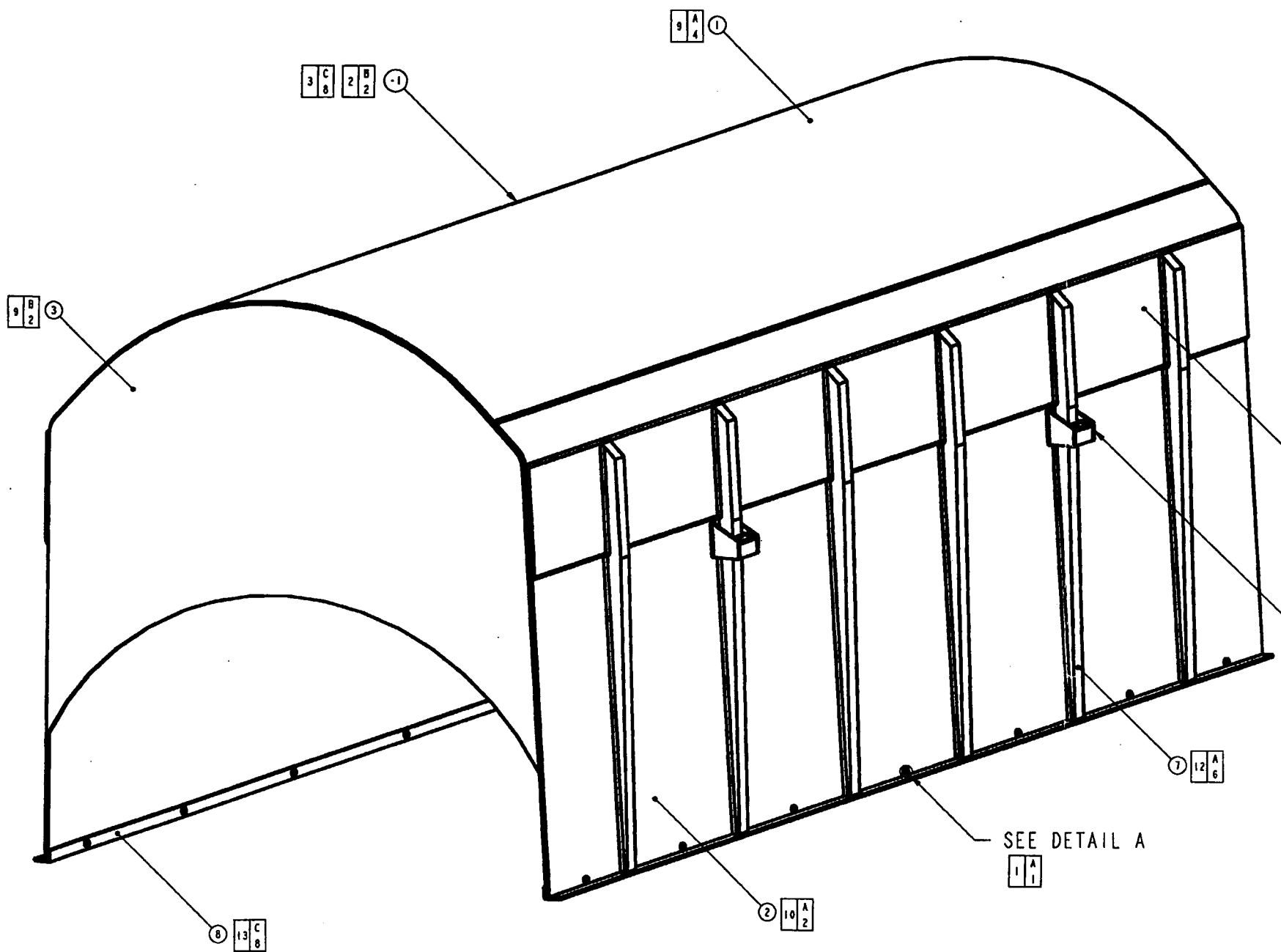
ALL SHEETS ARE THE SAME REVISION STATUS

REVISION HISTORY		DATE	APPROVED
ZONE	REV	DESCRIPTION	
-	-	ISSUED APPROVED	

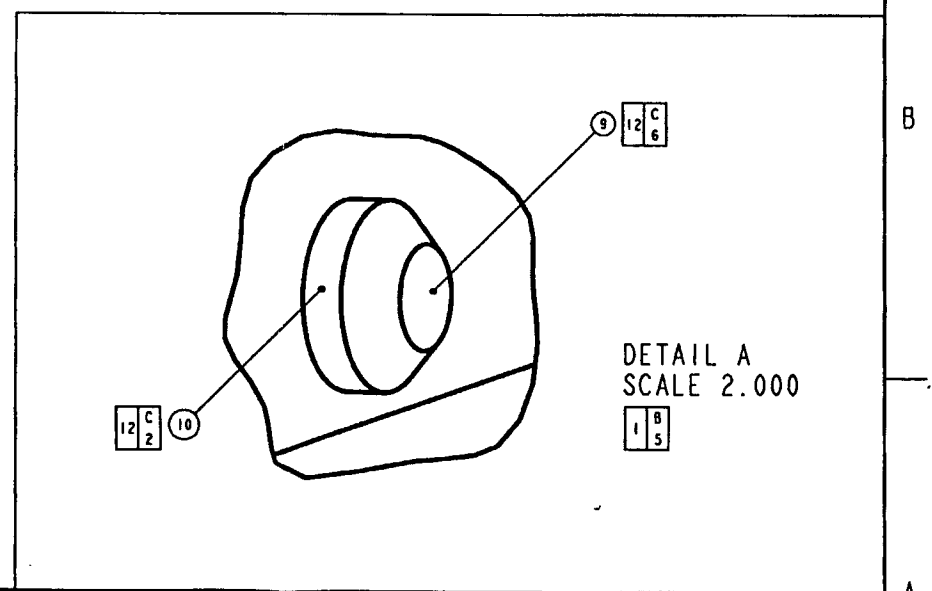
- NOTES:
1. DIMENSIONS SHOWN IN BRACKETS ARE IN INCHES
  2. WELD 10 SQUARE BUTT WELDS ARE PLACED ON THE EXPOSED SURFACES ABOVE THE OPEN CREVICE CREATED BETWEEN THE MATING SURFACES OF THE VERTICAL SUPPORT BEAMS AND THE EXTERNAL SUPPORT PLATES. THIS WELD IS INTENDED TO INSURE THAT THE CREVICE CREATED BETWEEN THESE COMPONENTS IS NOT CORRODED BY WATER.
  3. FOR COMPONENT LIST SEE SHEET 14
  4. FOR WELD LIST SEE SHEET 14

D  
C  
B  
A

D  
C  
B  
A

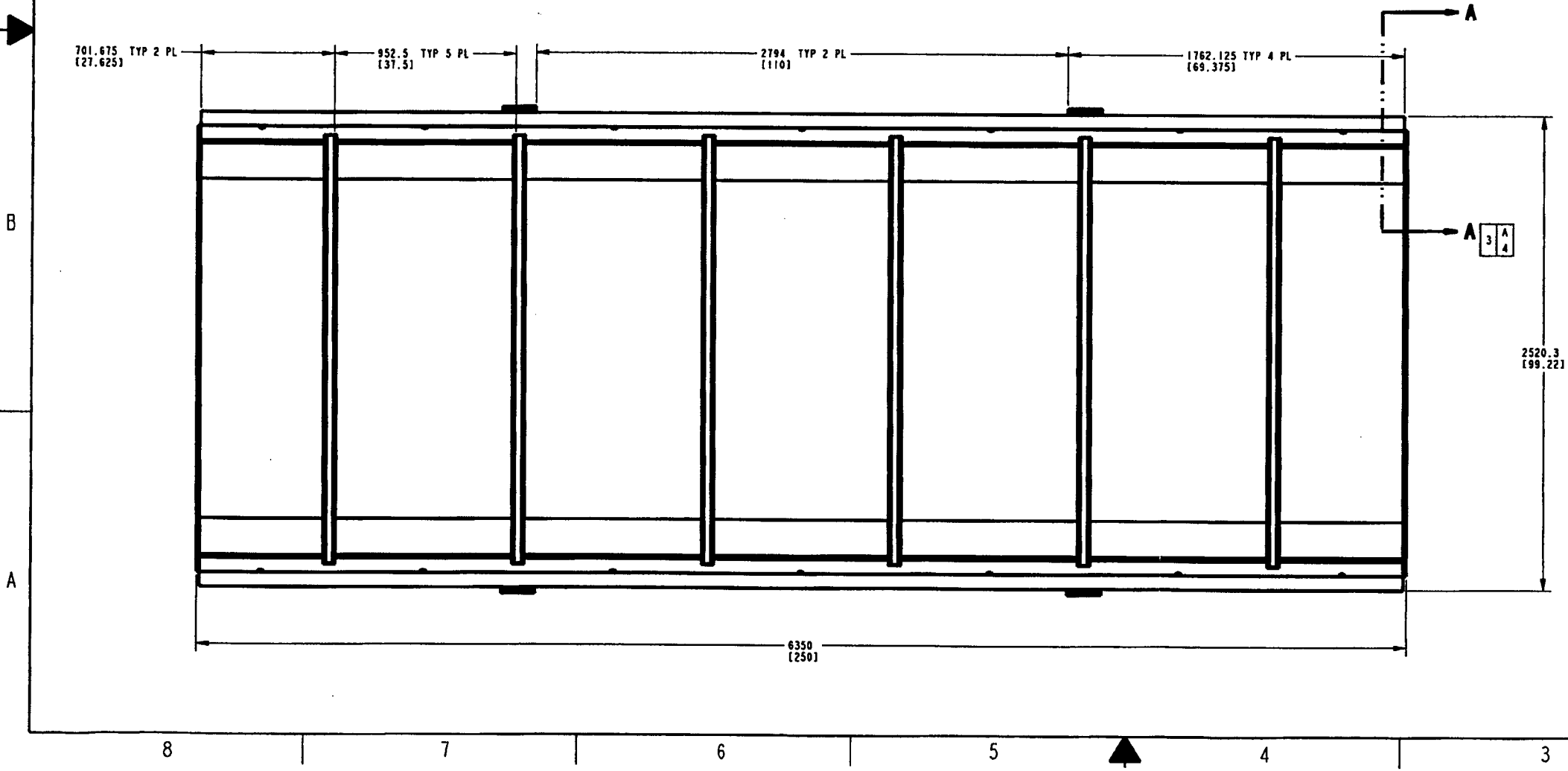
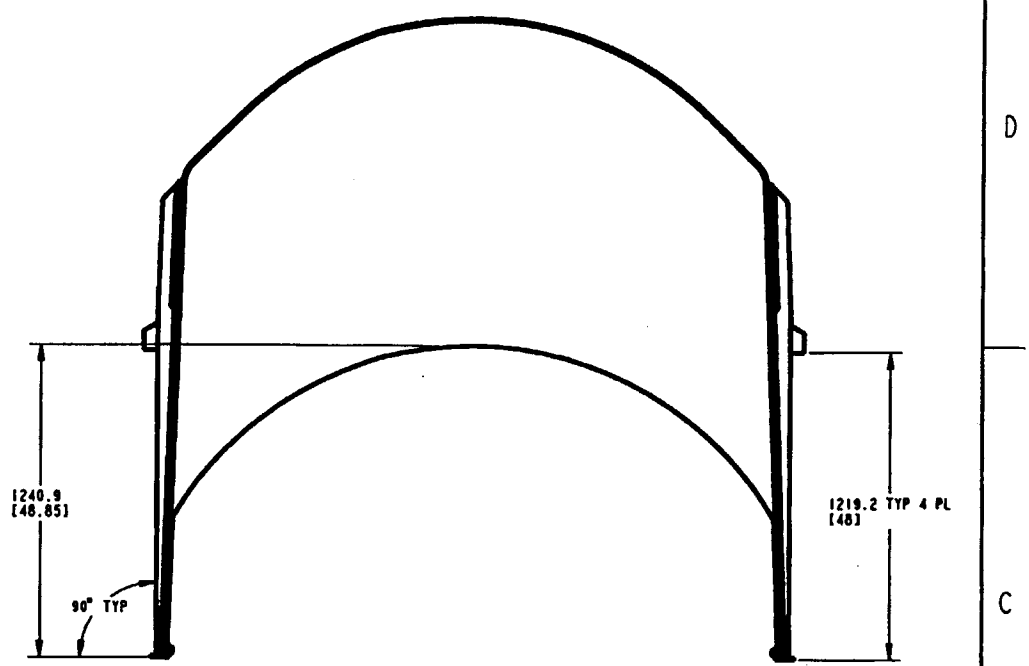
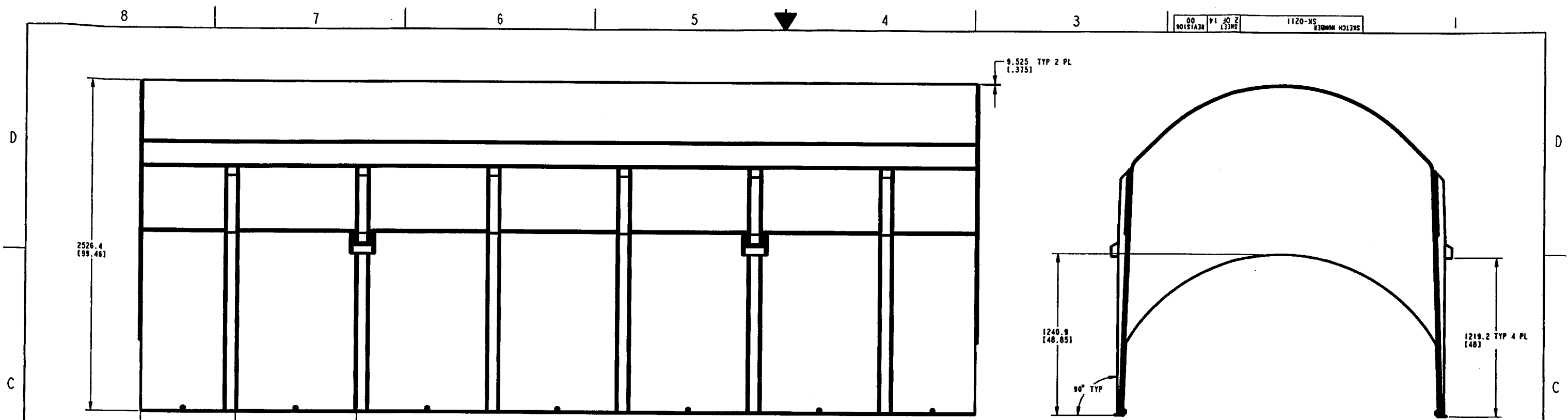


SEE DETAIL A  
11/1



<p>"FOR INFORMATION ONLY"</p> <p>THIRD ANGLE PROJECTION</p> <p>DIMENSIONS ARE IN MILLIMETERS AND DEGREES UNLESS OTHERWISE NOTED</p> <p>DO NOT SCALE FROM SKETCH</p>	<p>APPROVALS</p> <p>SKETCHED BY BRYAN HARKINS</p> <p>CHECKED BY EUGENE CONNELL</p> <p>STRUCTURAL LEAD SCOTT BENNETT</p> <p>MANUFACTURING MGR JERRY COGAR</p> <p>DESIGN GROUP MGR MICHAEL ANDERSON</p>	<p>INITIAL/DATE</p> <p>BH 05/29/01</p> <p>Jocelyn Gooden 5/29/01</p> <p>SMB 05/30/01</p> <p>Joc 5/29/01</p> <p>SL 5/30/01</p>	<p>WASTE PACKAGE PROJECT</p> <p><b>Bechtel SAIC Company, LLC</b></p> <p>TITLE</p> <p>STAND ALONE DRIP SHIELD-LONG</p> <p>SKETCH NUMBER SK-0211</p> <p>SCALE 0.075</p>	<p>REVISION</p> <p>00</p> <p>SHEET 1 OF 14</p>
---	---	---	---	--

8 7 6 5 4 3 2 1

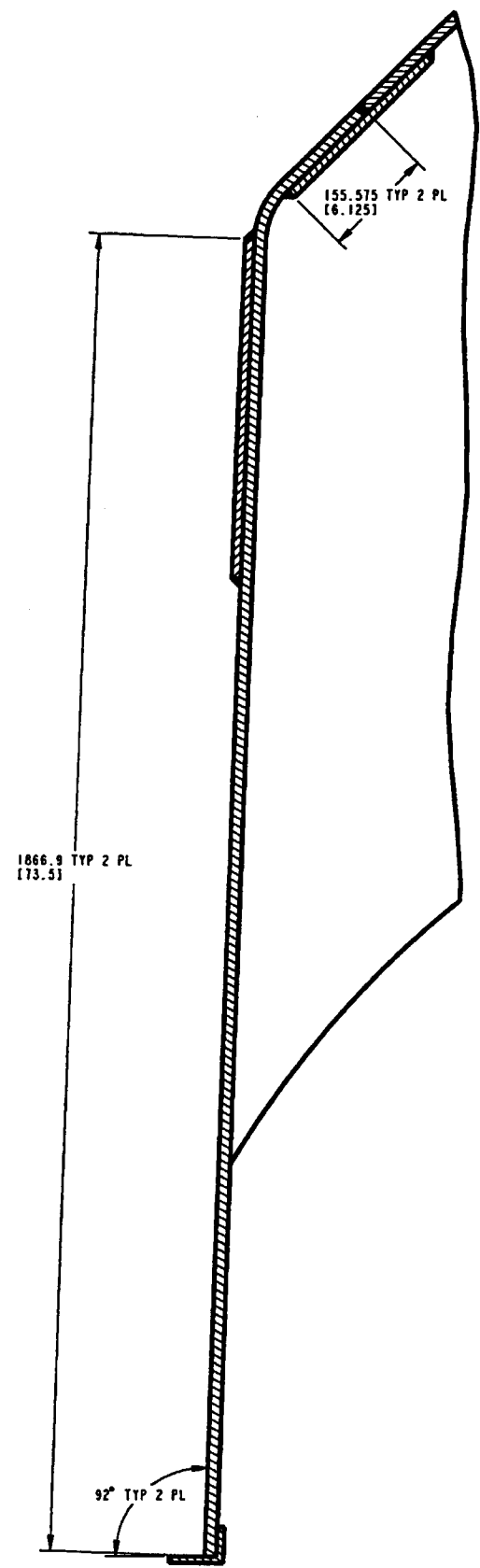


ASSEMBLY - I  
 STAND ALONE DRIP SHIELD-LONG  
 SCALE 0.075  
 1 0 1

WASTE PACKAGE PROJECT	
<b>Bechtel SAIC Company, LLC</b>	
SKETCH NUMBER	REVISION
SK-0211	00
SCALE 0.075	SHEET 2 OF 14

ASSEMBLY -1  
 STAND ALONE DRIP SHIELD-LONG  
 SCALE 0.225

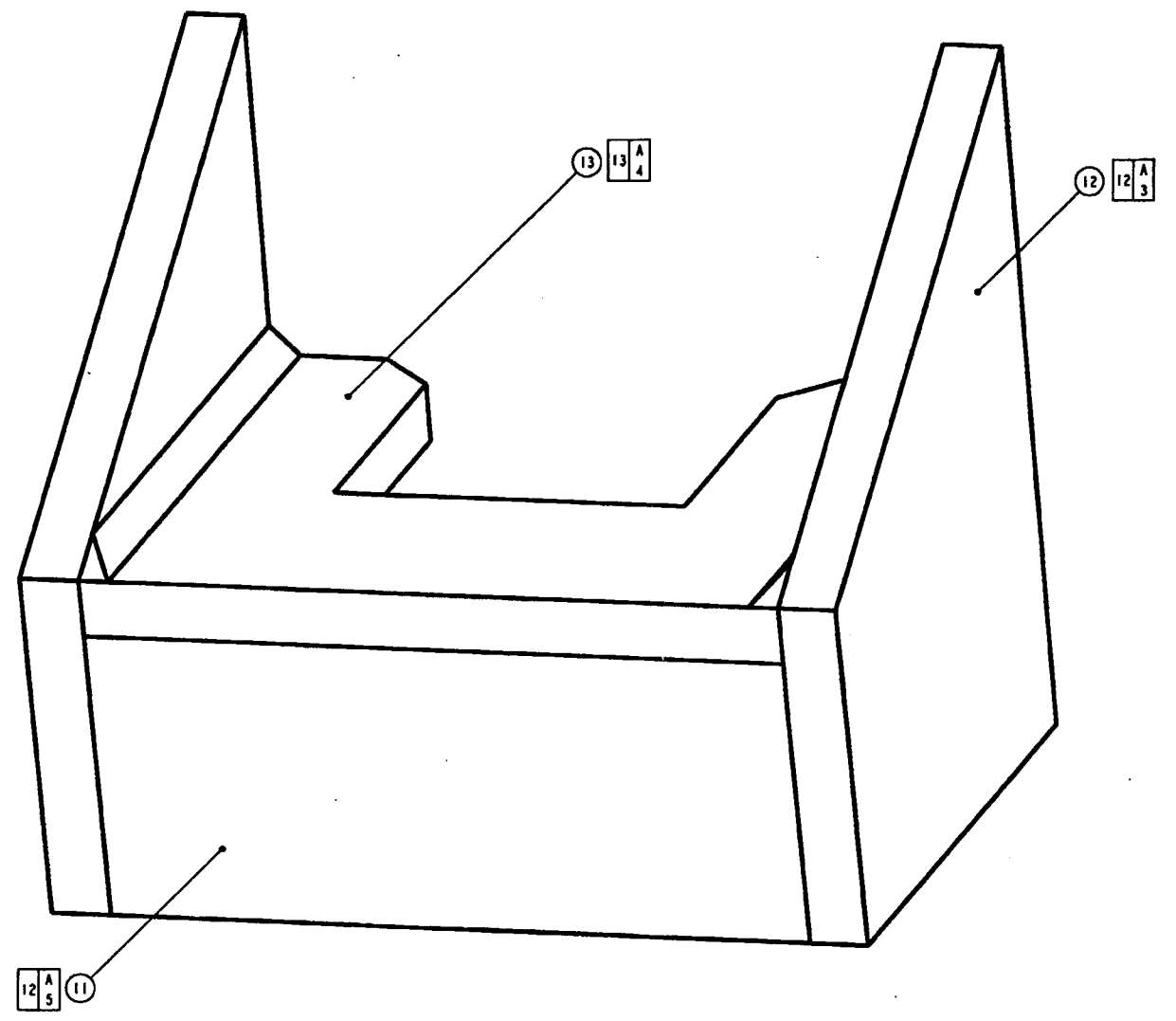
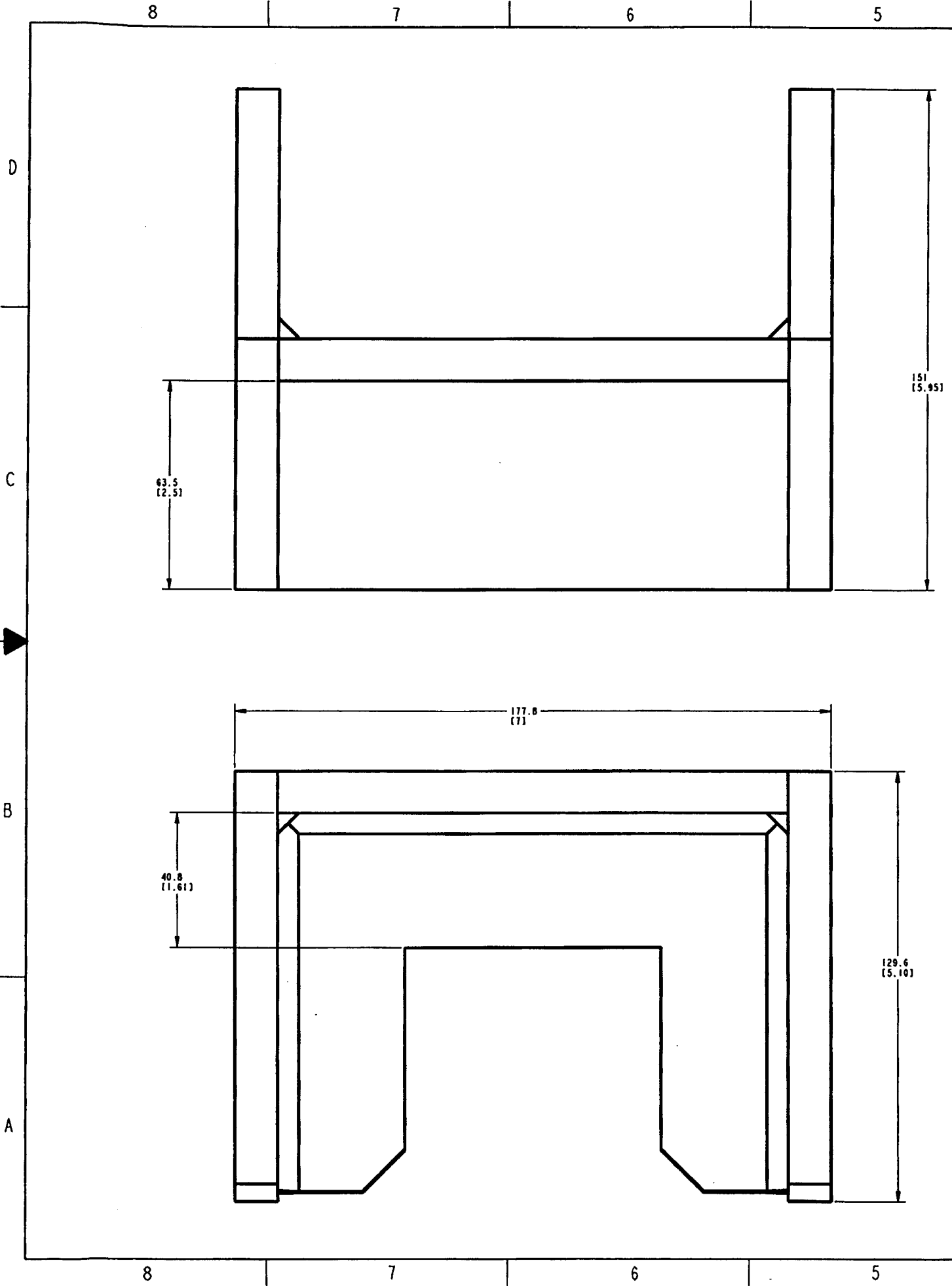
1 0  
 1 7



SECTION A-A  
 SCALE 0.225

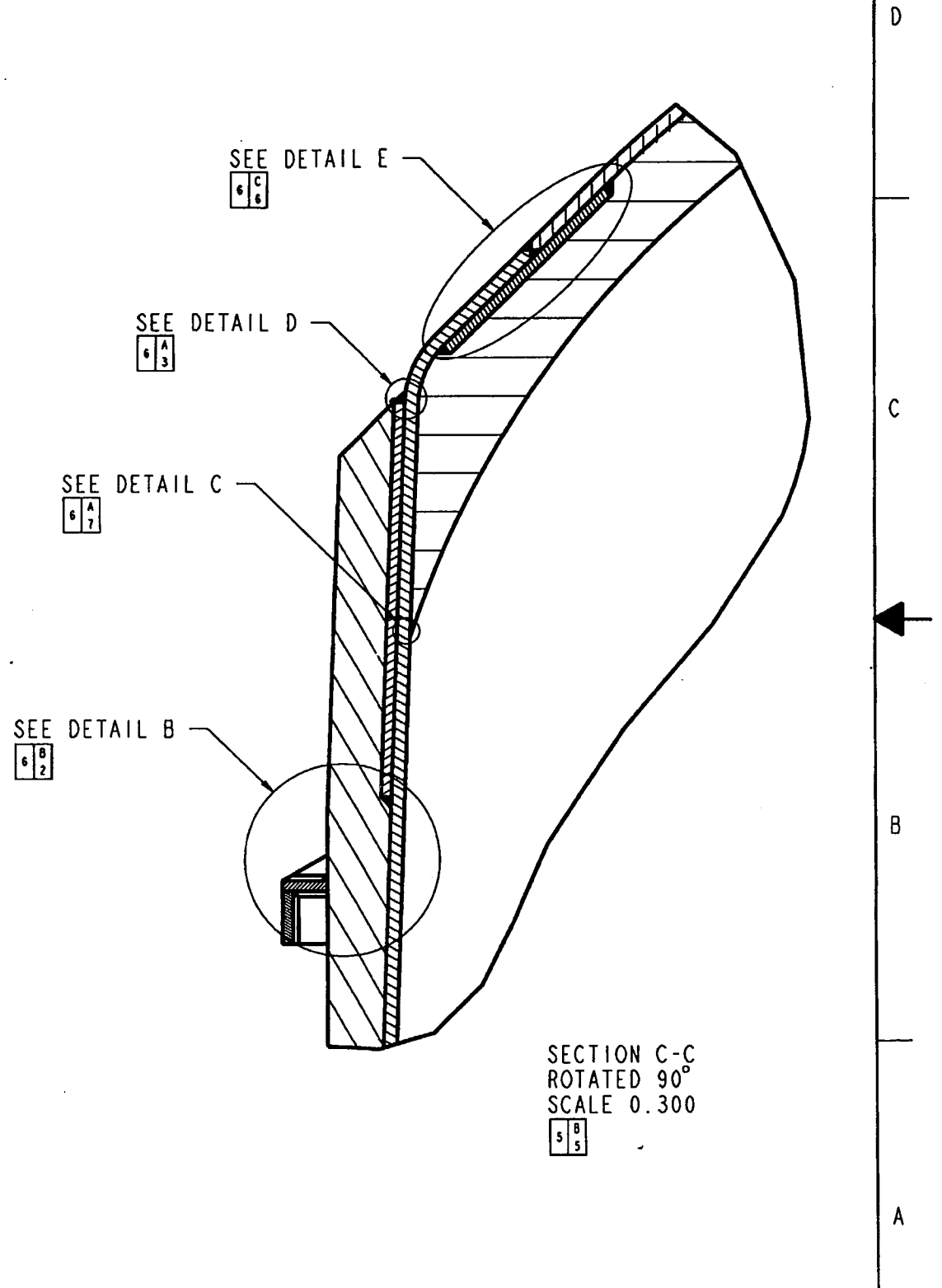
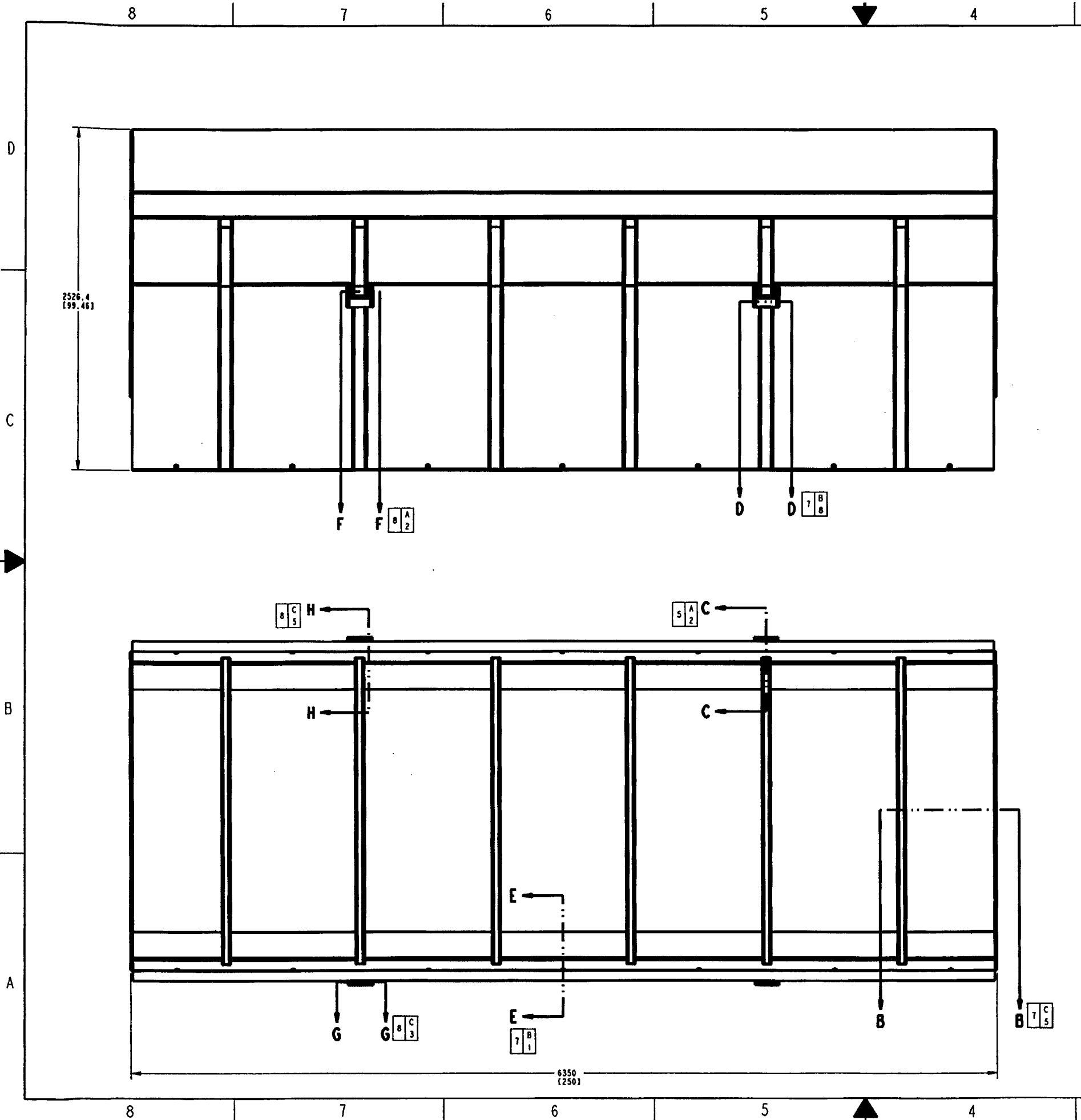
2 8  
 3 3

WASTE PACKAGE PROJECT	
<b>Bechtel SAIC Company, LLC</b>	
SKETCH NUMBER	REVISION
SK-0211	00
SCALE 0.075	SHEET 3 OF 14

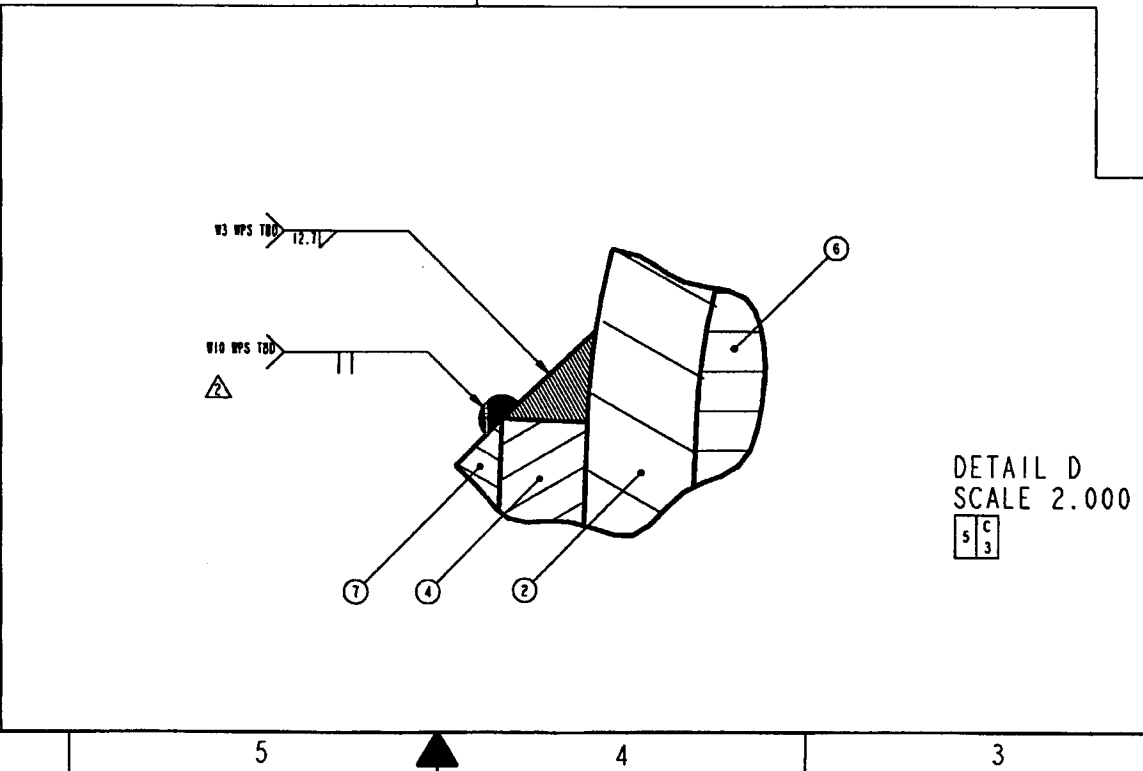
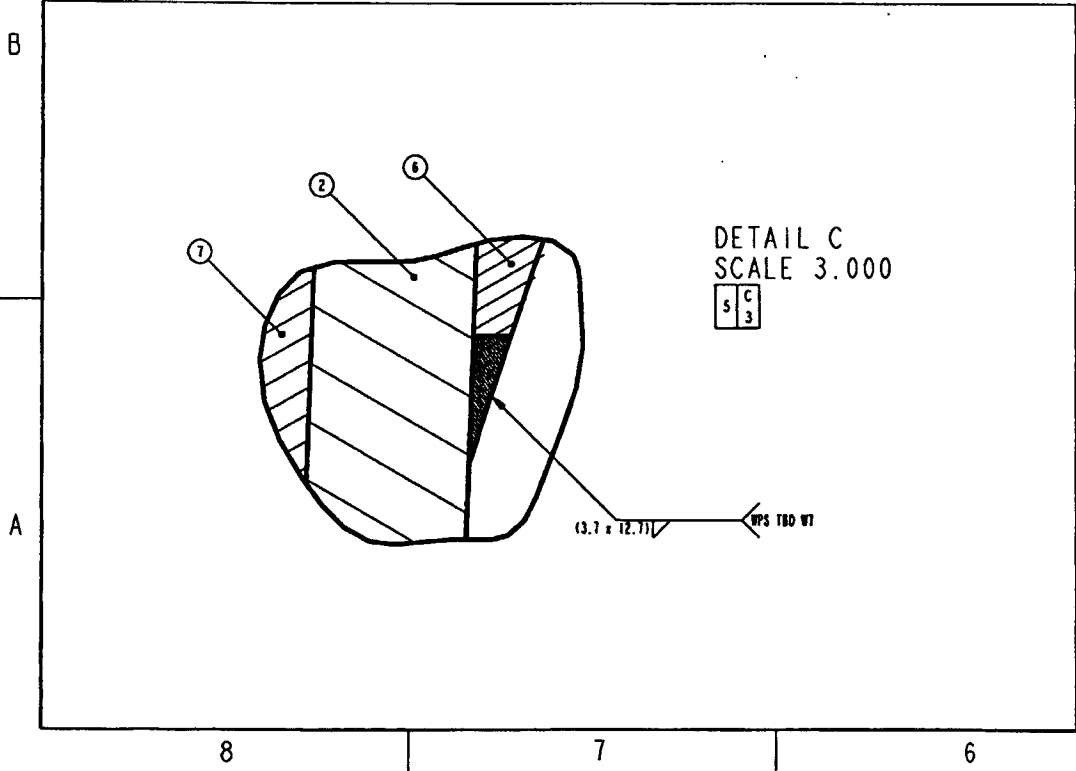
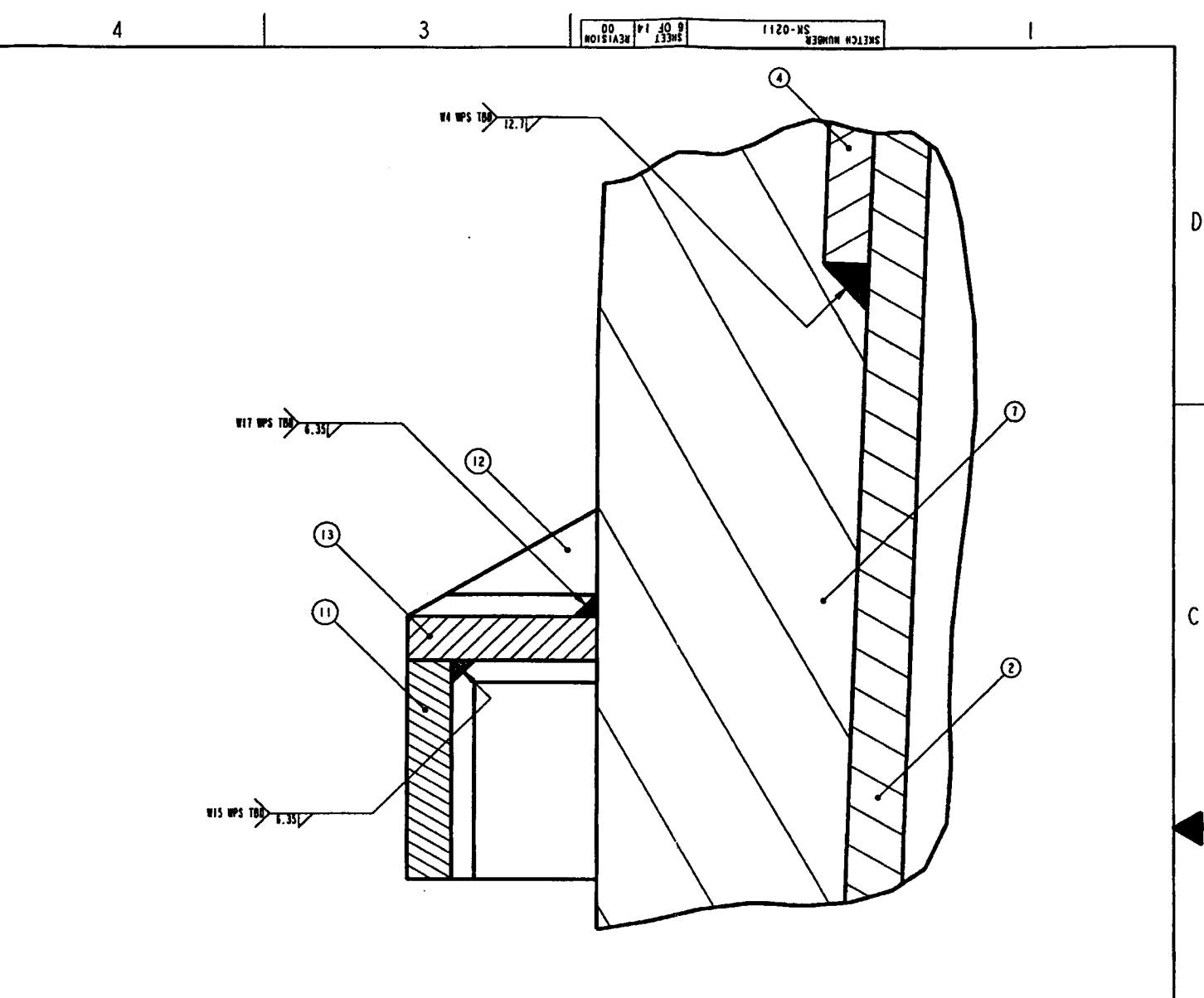
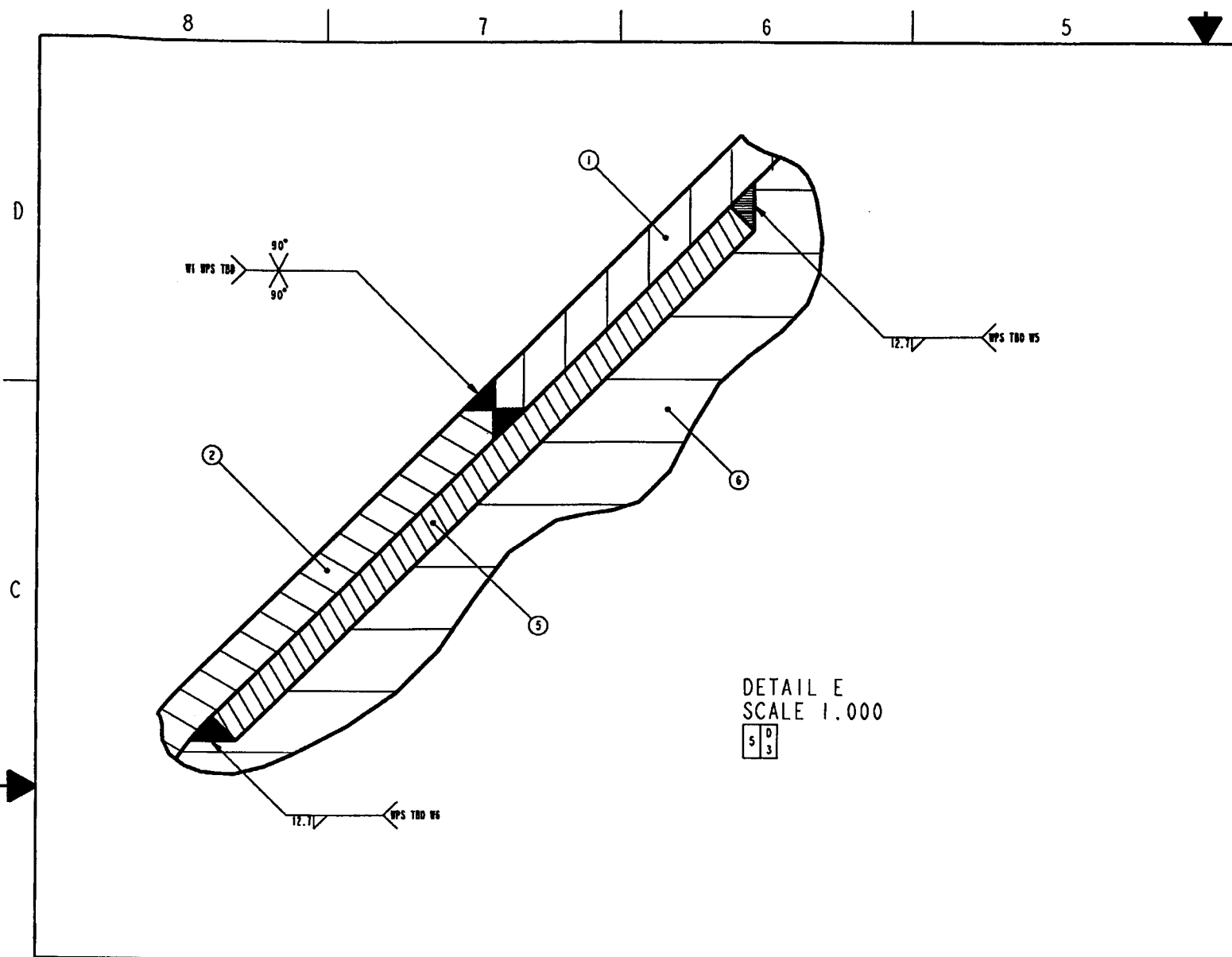


ASSEMBLY -2  
 LIFTING FEATURE ASSEMBLY  
 SCALE 1.500  
 1 B 3

WASTE PACKAGE PROJECT	
<b>Bechtel BAIC Company, LLC</b>	
SKETCH NUMBER	REVISION
SK-0211	00
SCALE 0.075	SHEET 4 OF 14



WASTE PACKAGE PROJECT	
<b>Bechtel SAIC Company, LLC</b>	
SKETCH NUMBER	REVISION
SK-0211	00
SCALE 0.075	SHEET 5 OF 14



WASTE PACKAGE PROJECT	
<b>Bchtel SAIC Company, LLC</b>	
SKETCH NUMBER	SK-0211
REVISION	00
SCALE	0.075
SHEET 6 OF 14	



8

7

6

5

4

3

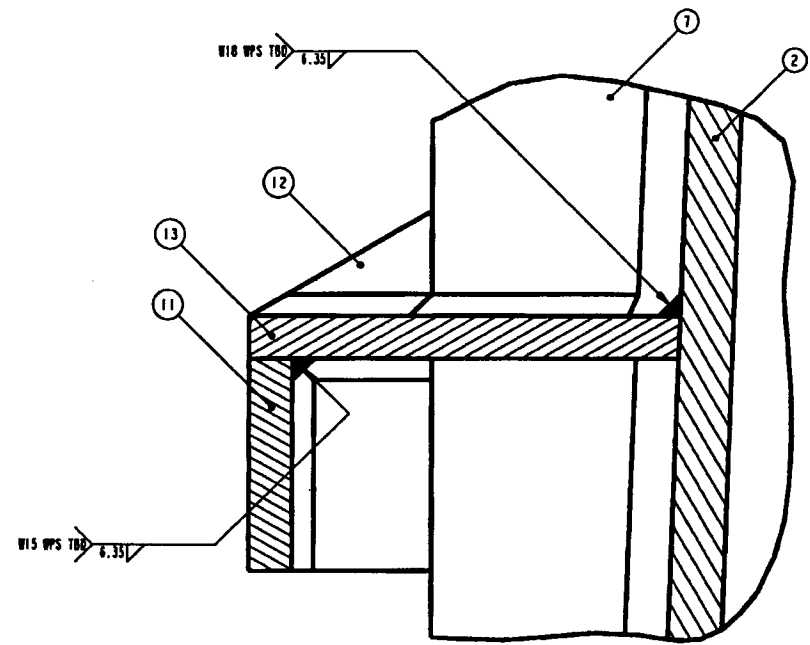
1

D

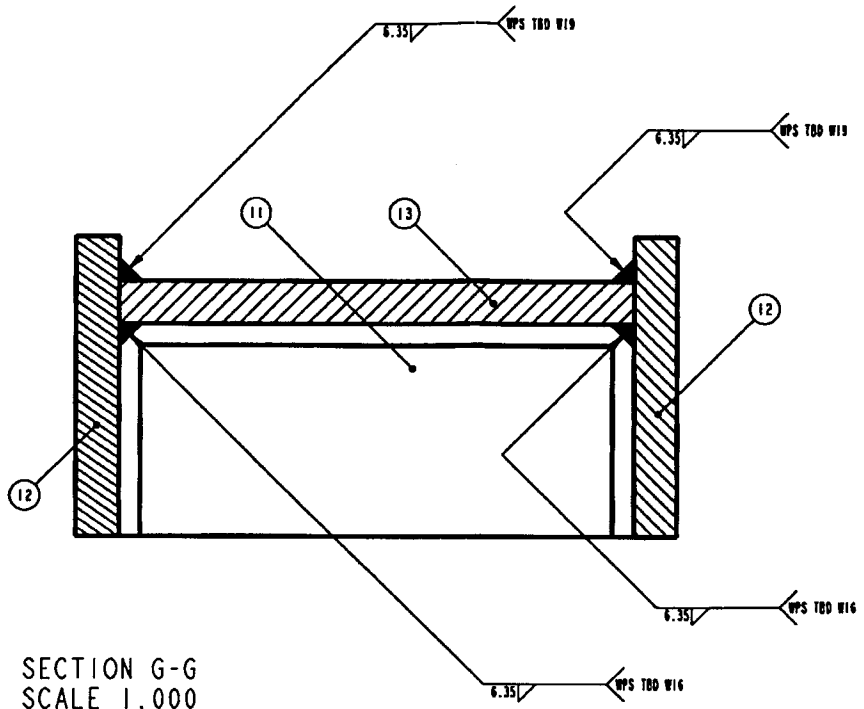
D

C

C



SECTION H-H  
 SCALE 1.000  
 5 B  
 7



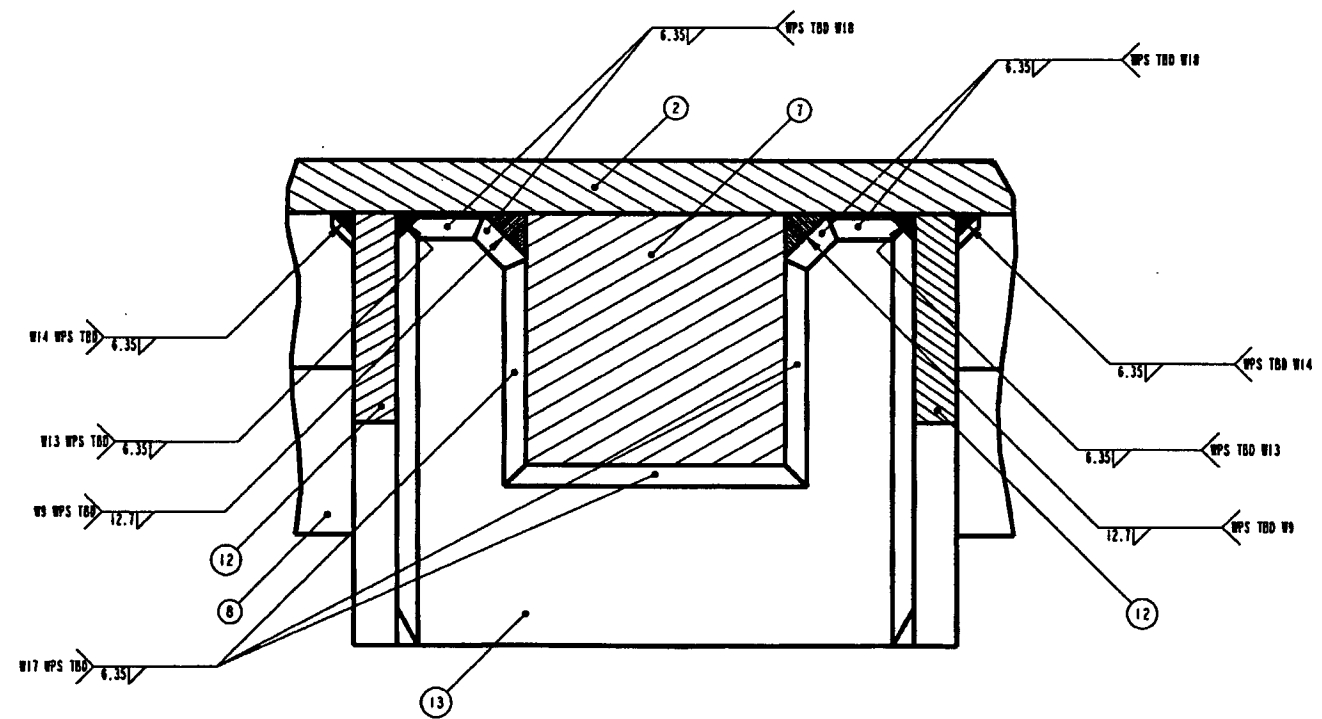
SECTION G-G  
 SCALE 1.000  
 5 A  
 7

B

B

A

A



SECTION F-F  
 SCALE 1.000  
 5 C  
 7

WASTE PACKAGE PROJECT	
<b>Bechtel SAIC Company, LLC</b>	
SKETCH NUMBER SK-0211	REVISION 00
SCALE 0.075	SHEET 8 OF 14

8

7

6

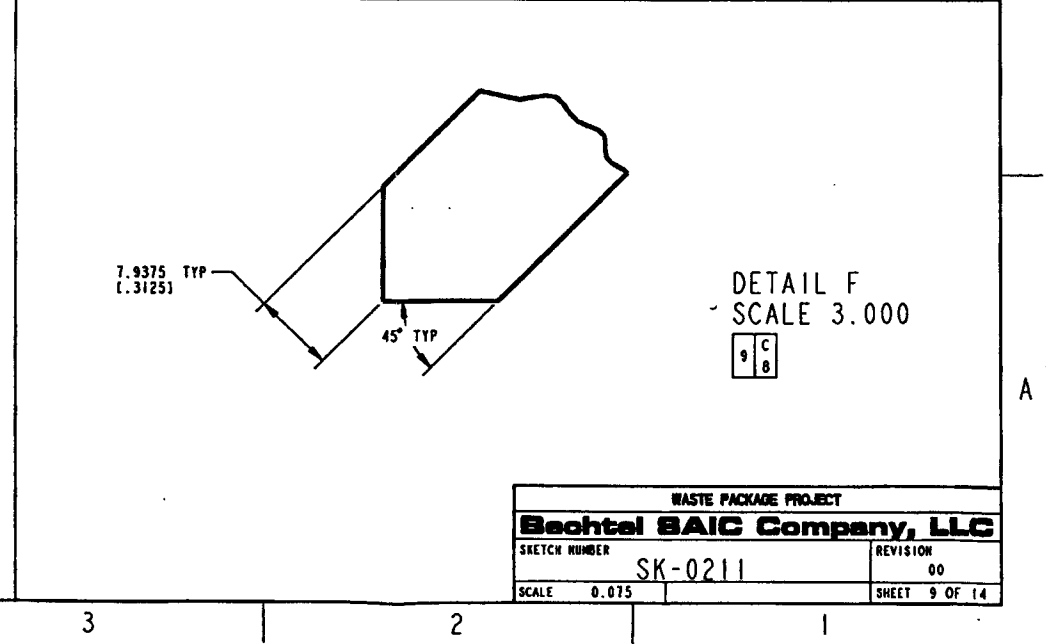
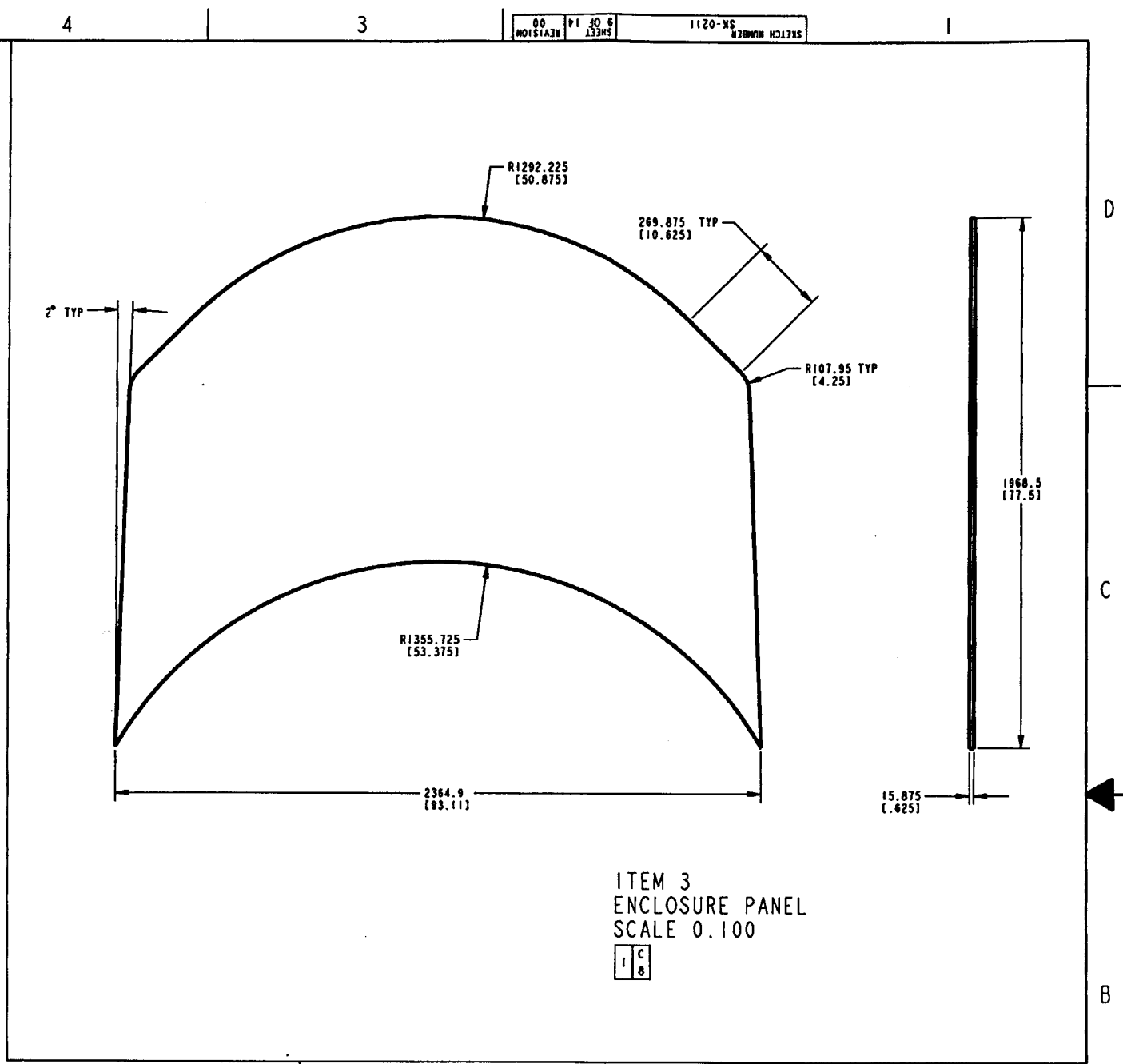
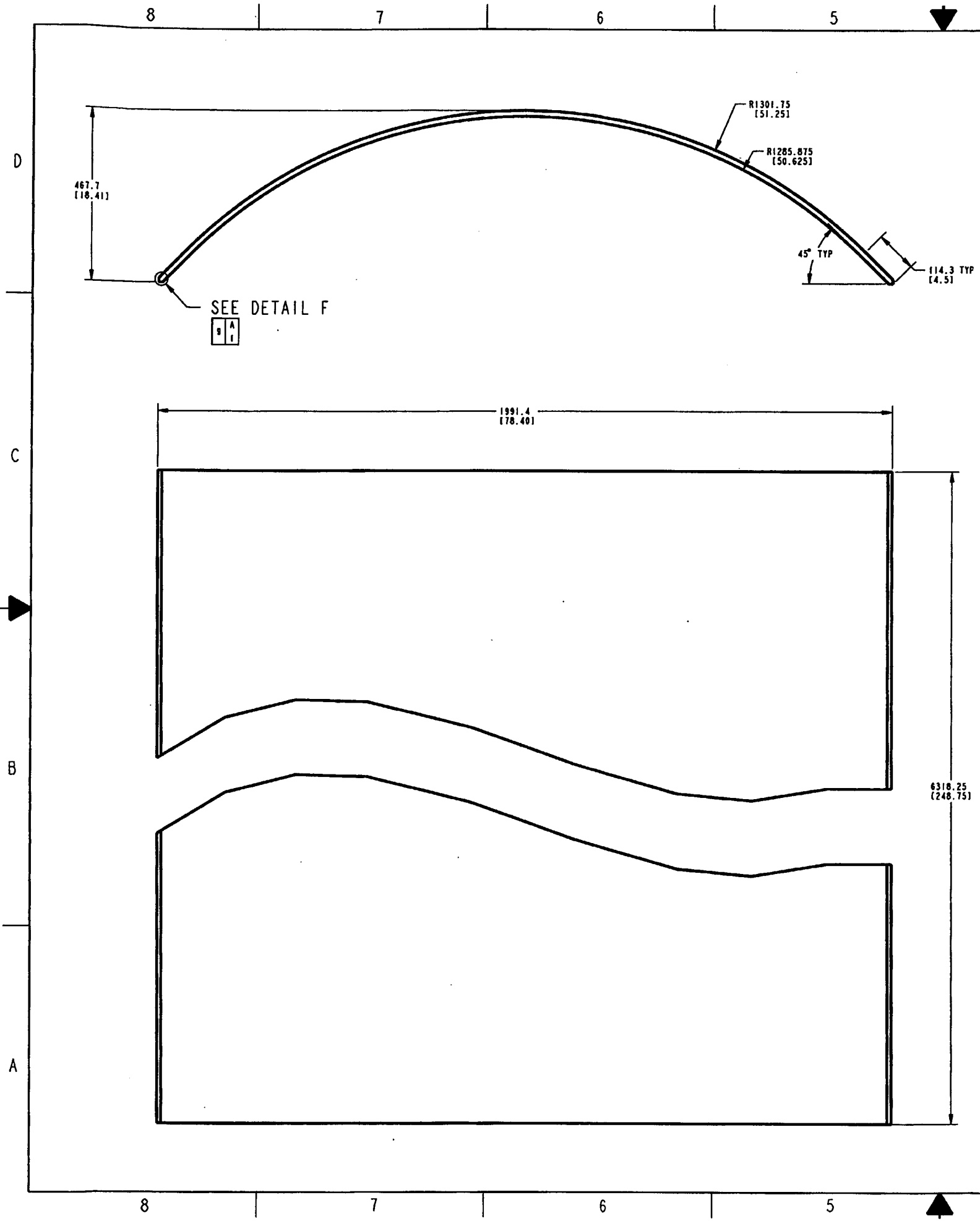
5

4

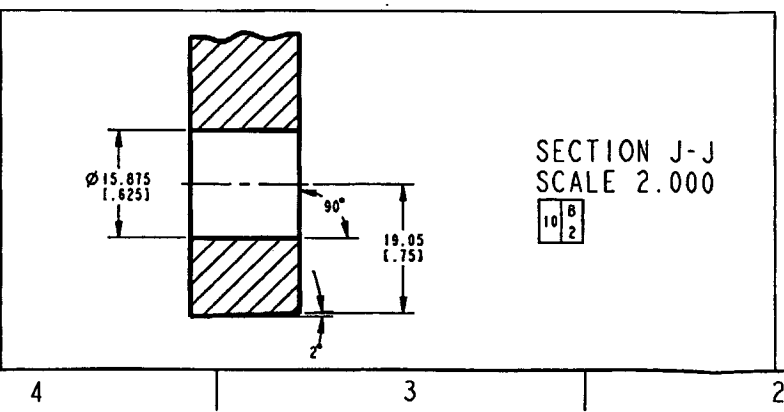
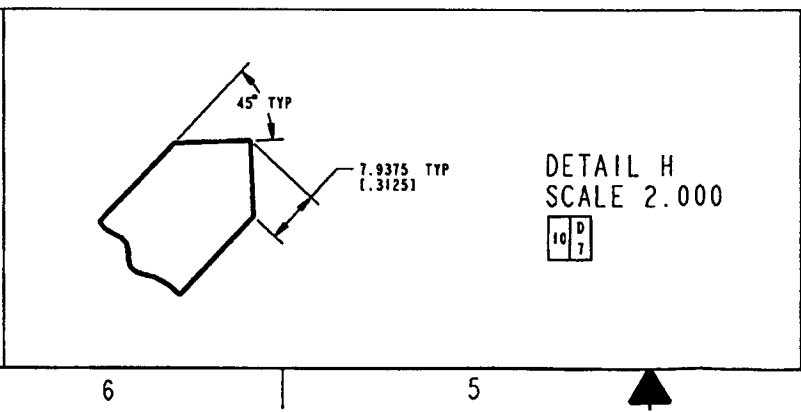
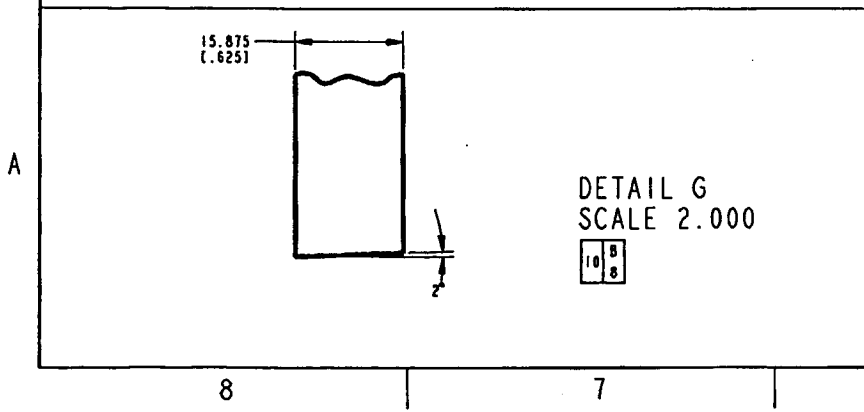
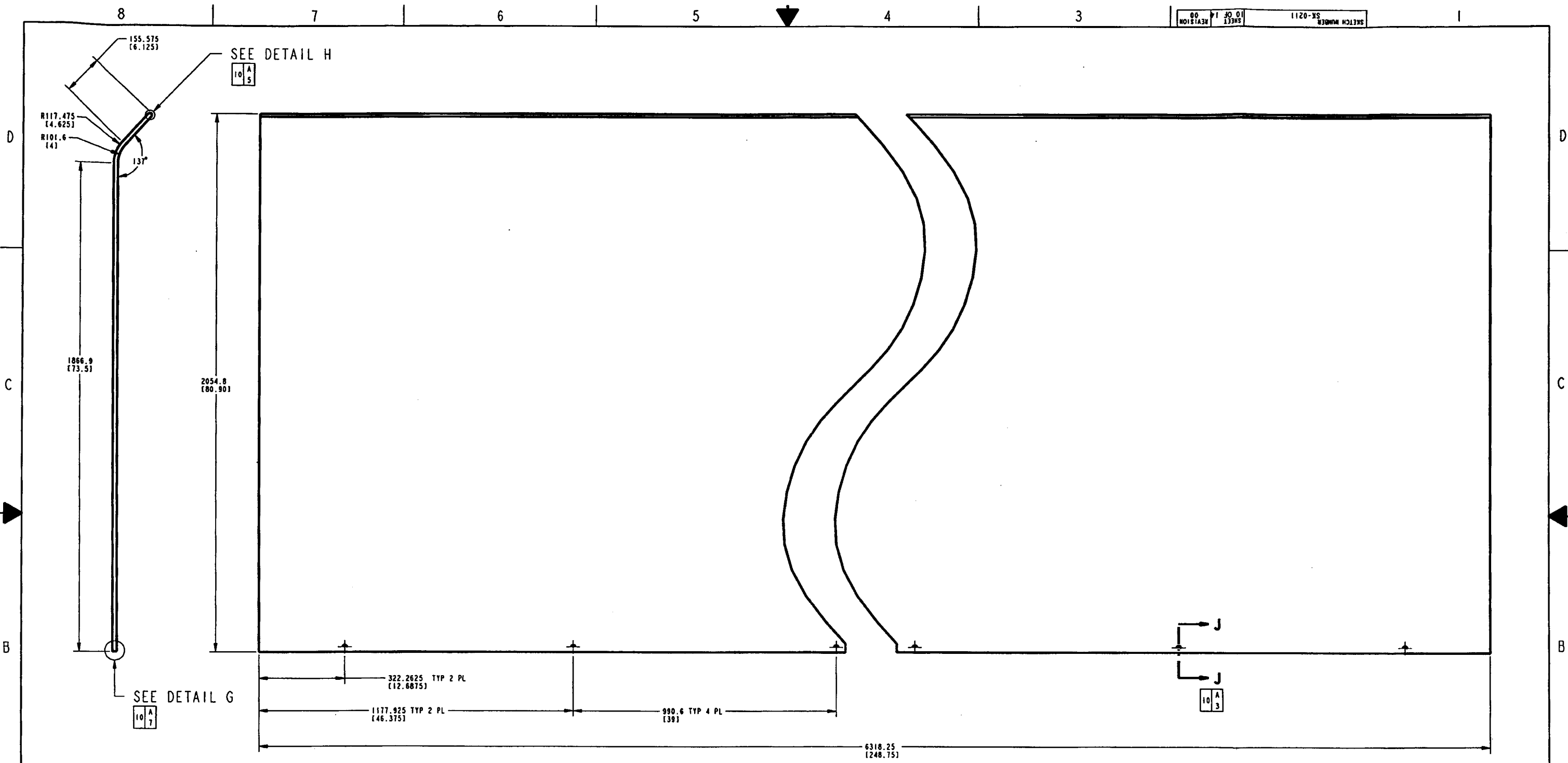
3

2

1



WASTE PACKAGE PROJECT	
<b>Bechtel SAIC Company, LLC</b>	
SKETCH NUMBER	REVISION
SK-0211	00
SCALE 0.075	SHEET 9 OF 14



ITEM 2  
 PLATE-2  
 SCALE 0.150

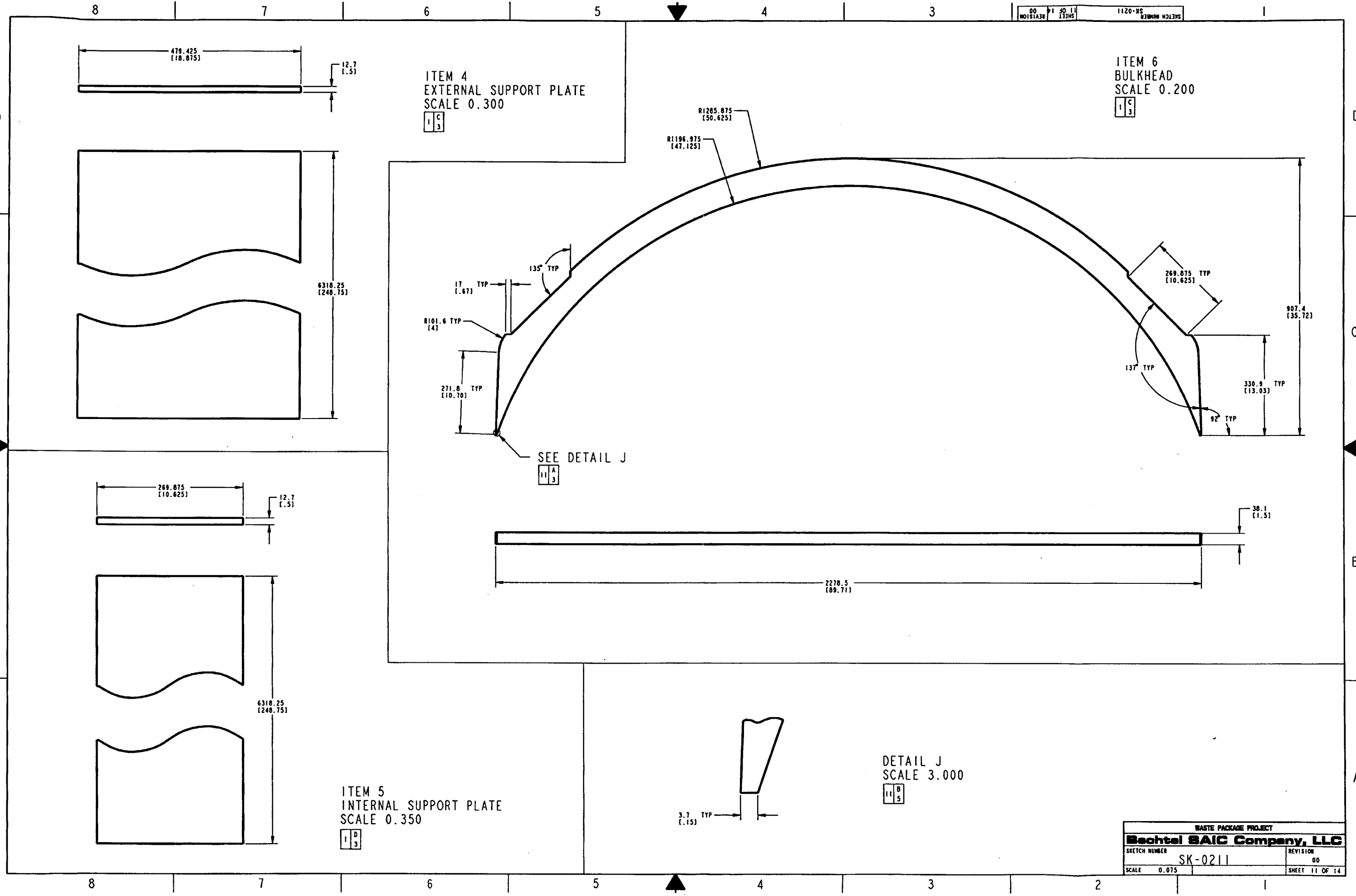
WASTE PACKAGE PROJECT	
<b>Bechtel SAIC Company, LLC</b>	
SKETCH NUMBER	REVISION
SK-0211	00
SCALE 0.075	SHEET 10 OF 14

ITEM 6  
 BULKHEAD  
 SCALE 0.200  
 11C3

ITEM 4  
 EXTERNAL SUPPORT PLATE  
 SCALE 0.300  
 11C3

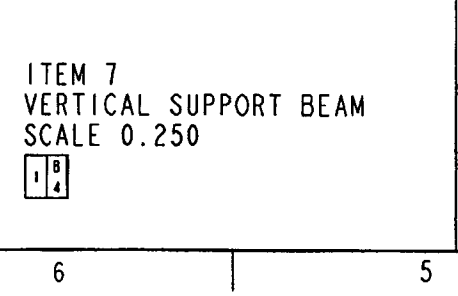
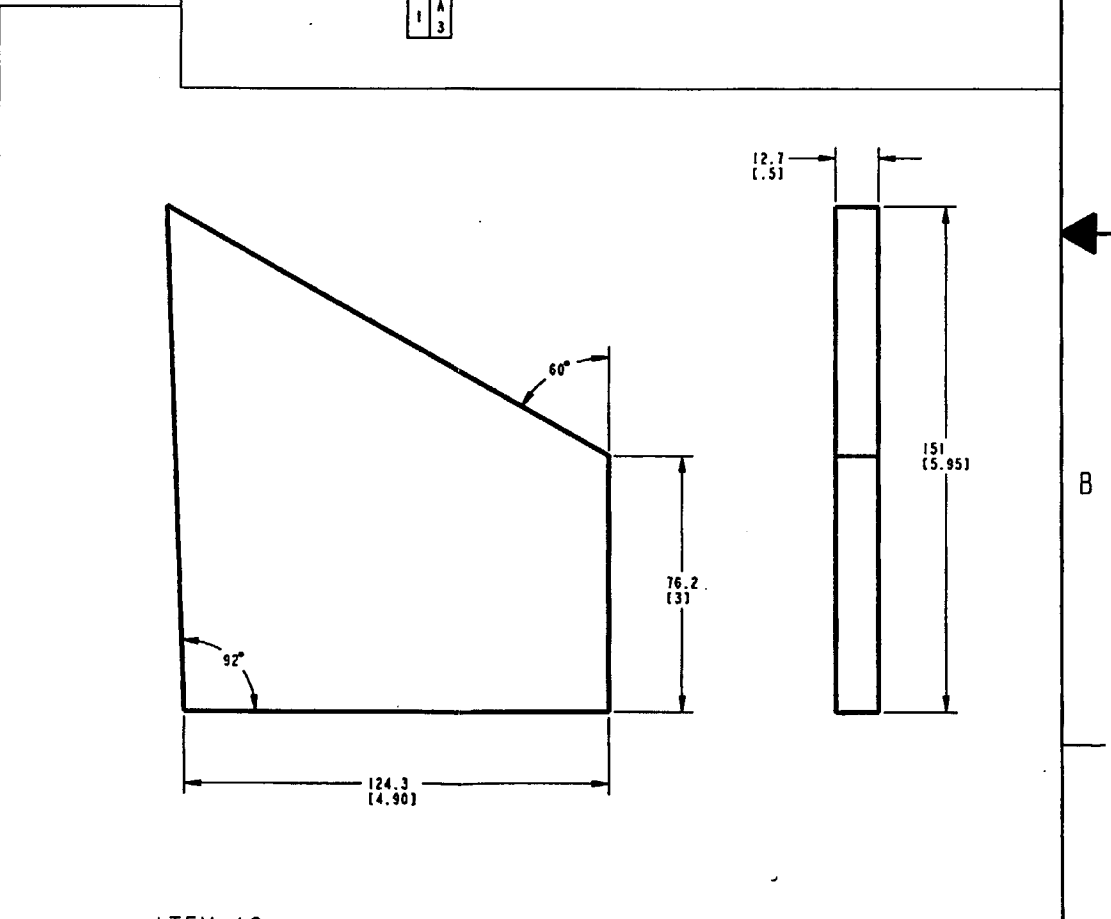
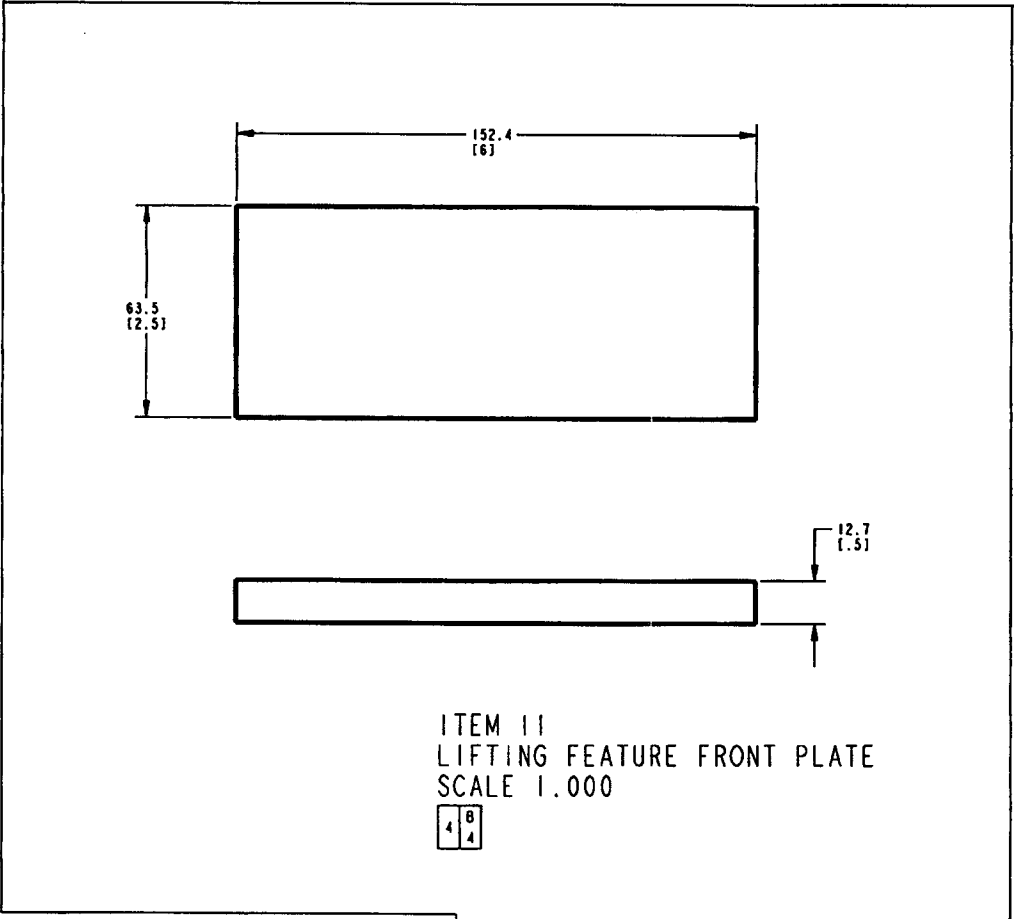
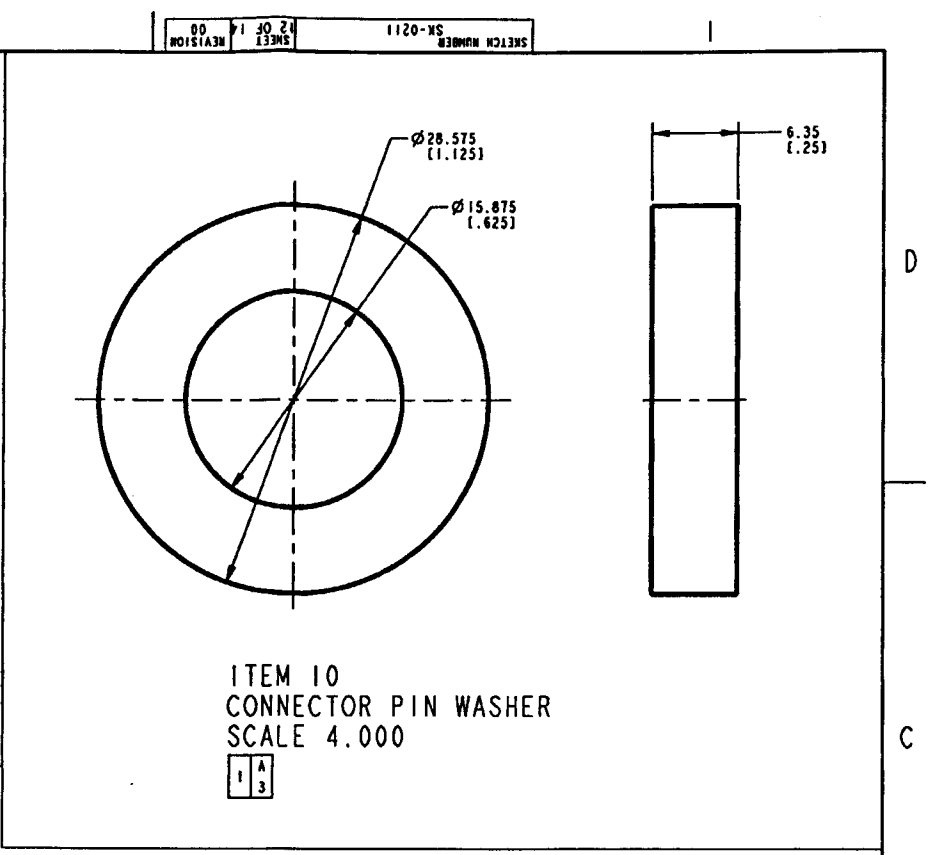
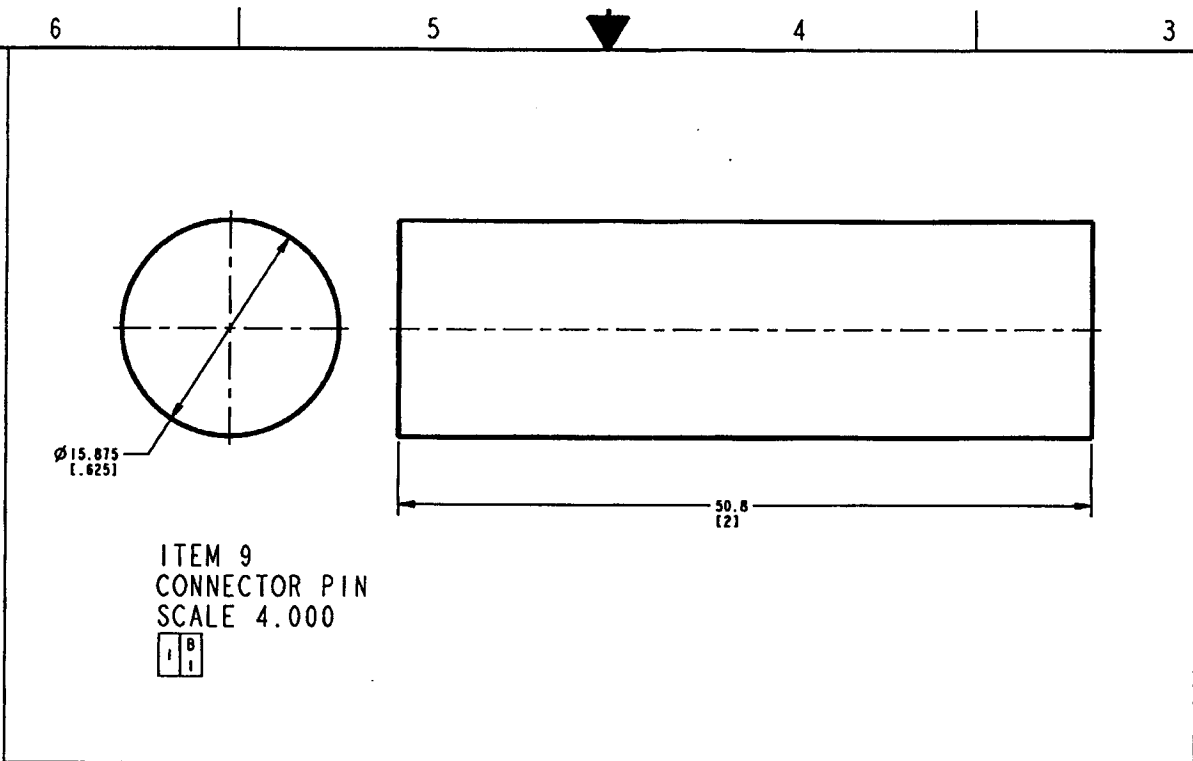
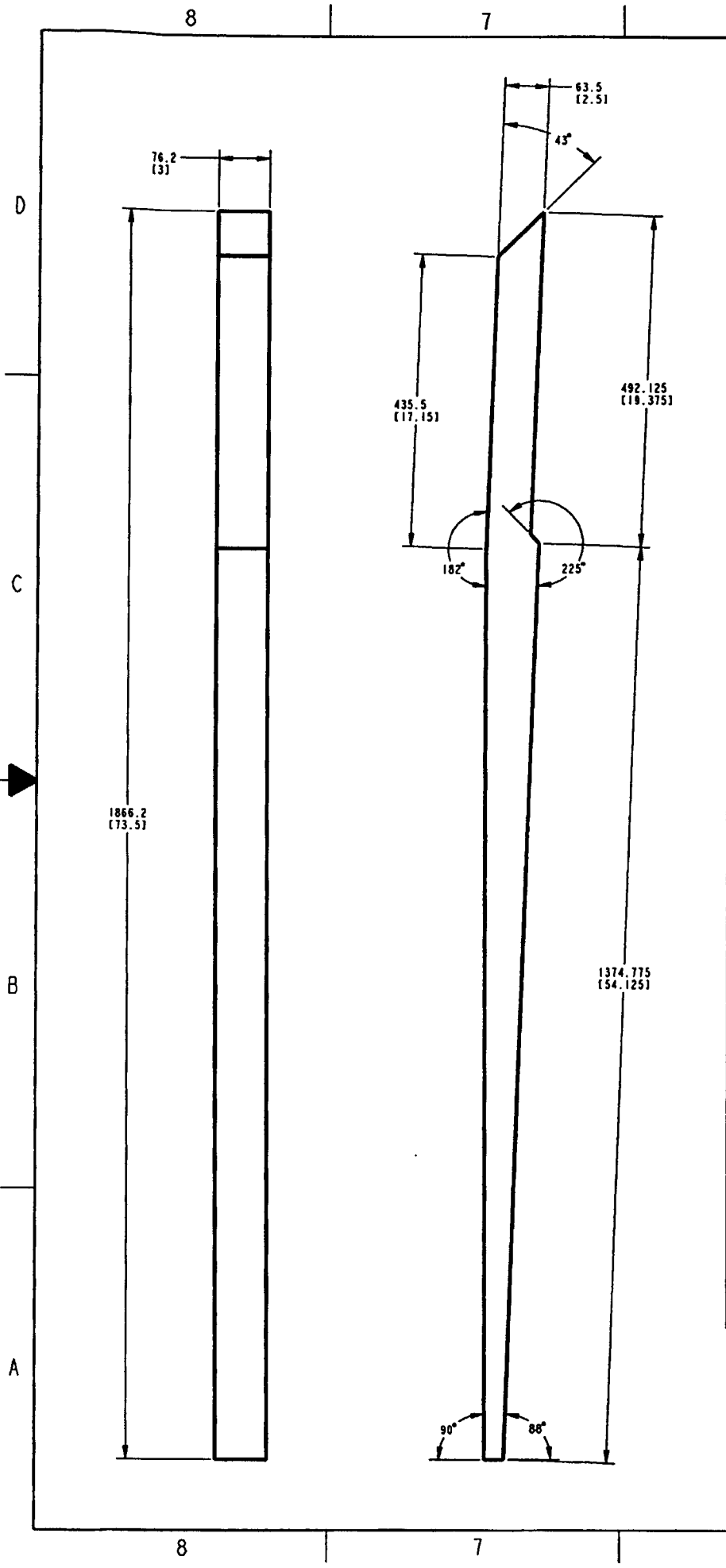
ITEM 5  
 INTERNAL SUPPORT PLATE  
 SCALE 0.350  
 11D3

DETAIL J  
 SCALE 3.000  
 11B5



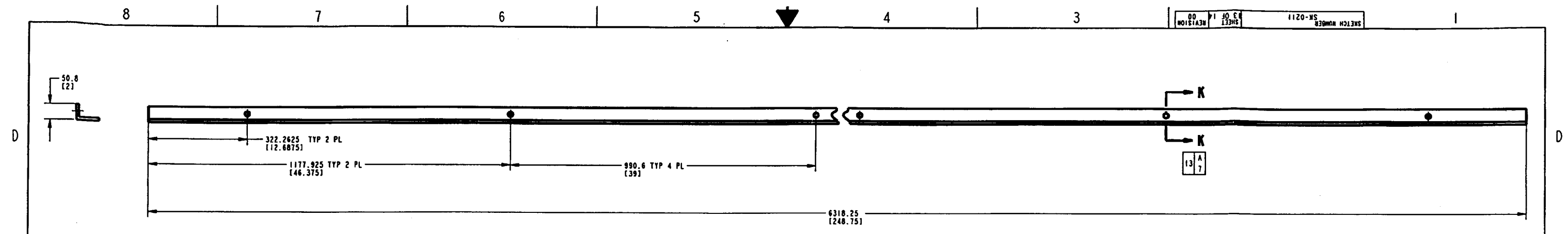
SEE DETAIL J  
 11A3

WASTE PACKAGE PROJECT	
<b>Bechtel SAIC Company, LLC</b>	
SKETCH NUMBER SK-0211	REVISION 00
SCALE 0.075	SHEET 11 OF 14

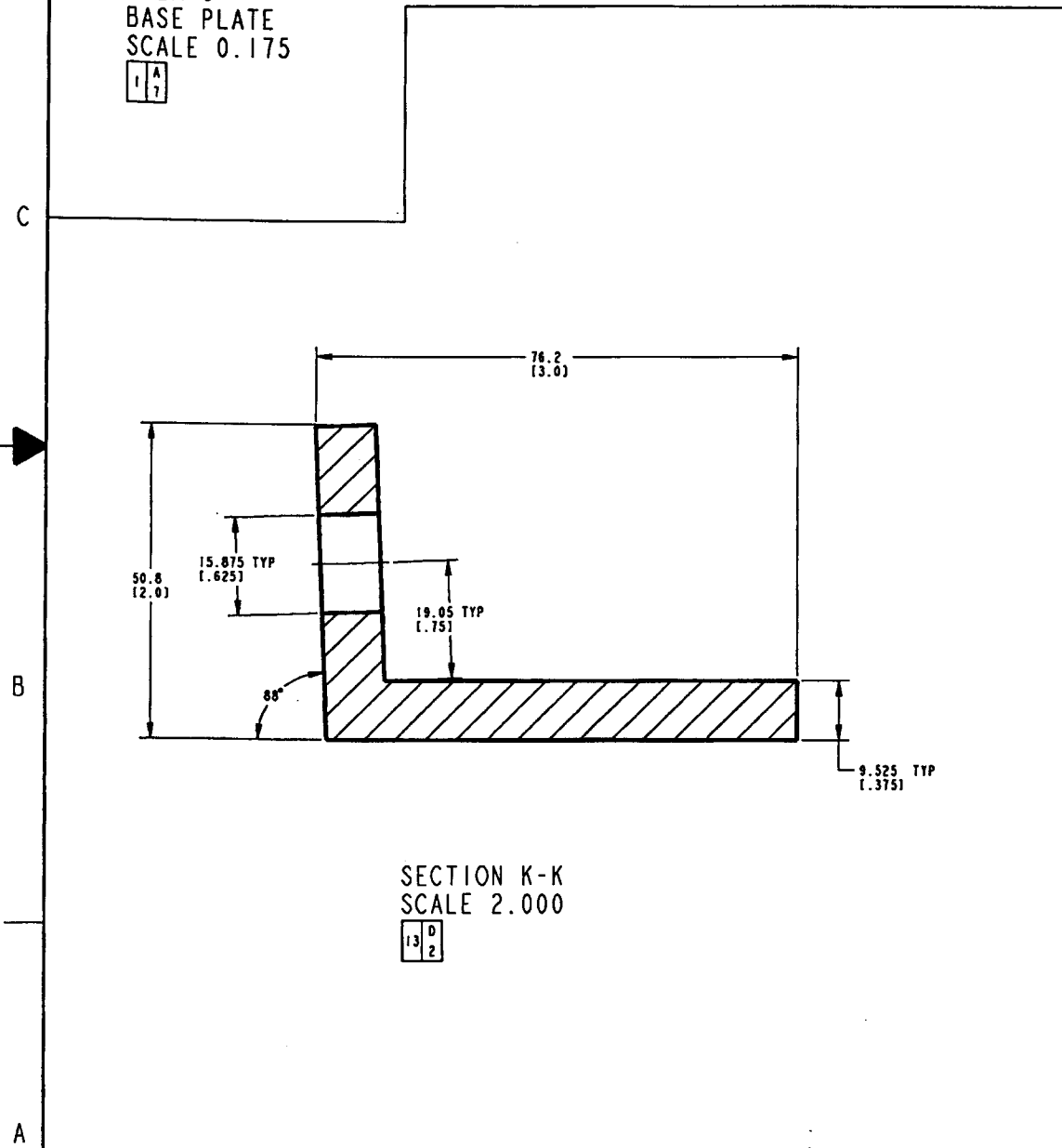


ITEM 12 LIFTING FEATURE SIDE PLATE SCALE 1.000

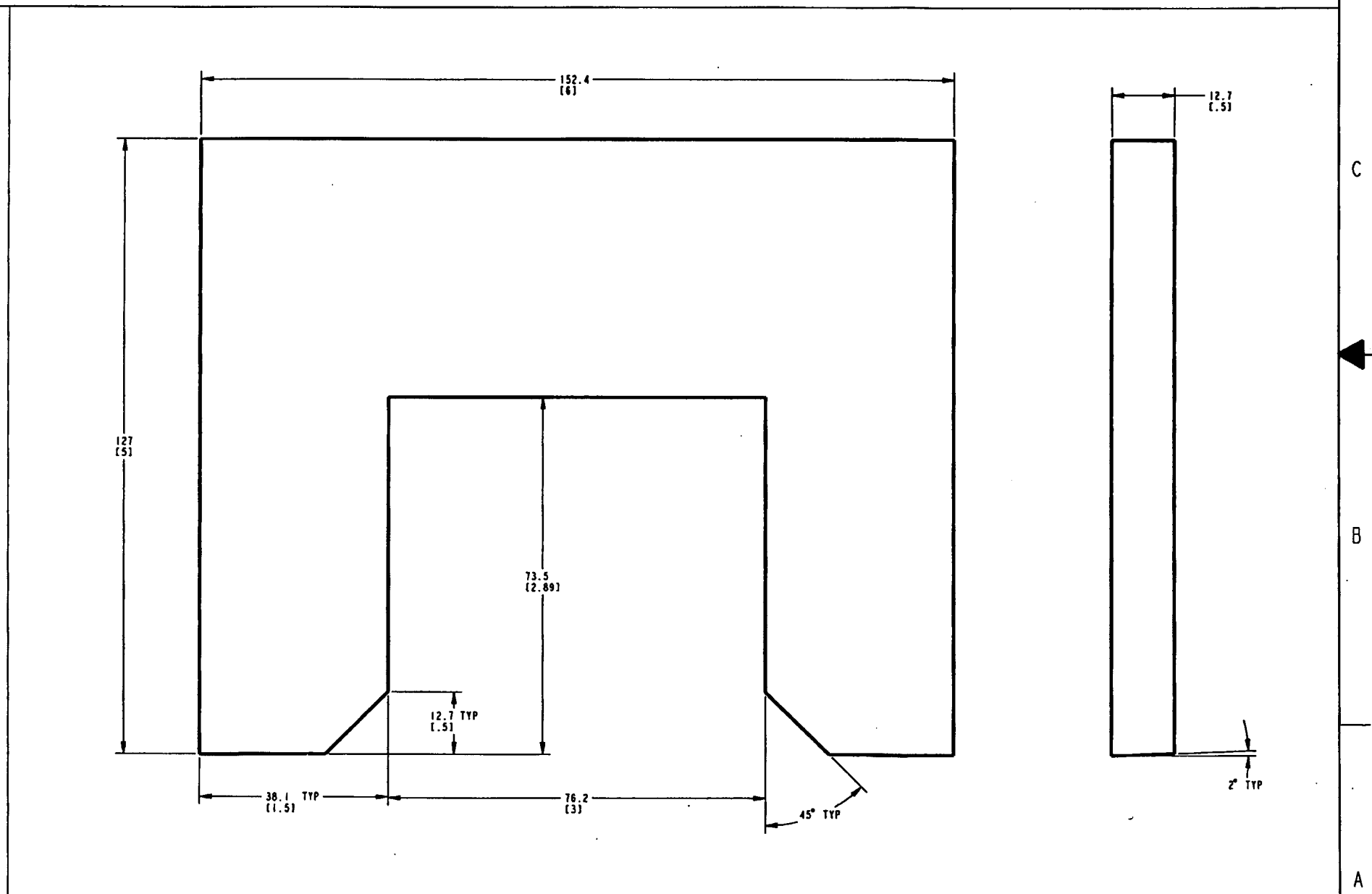
WASTE PACKAGE PROJECT	
<b>Bechtel SAIC Company, LLC</b>	
SKETCH NUMBER	REVISION
SK-0211	00
SCALE 0.075	SHEET 12 OF 14



ITEM 8  
BASE PLATE  
SCALE 0.175  
13 A 1



SECTION K-K  
SCALE 2.000  
13 D 2



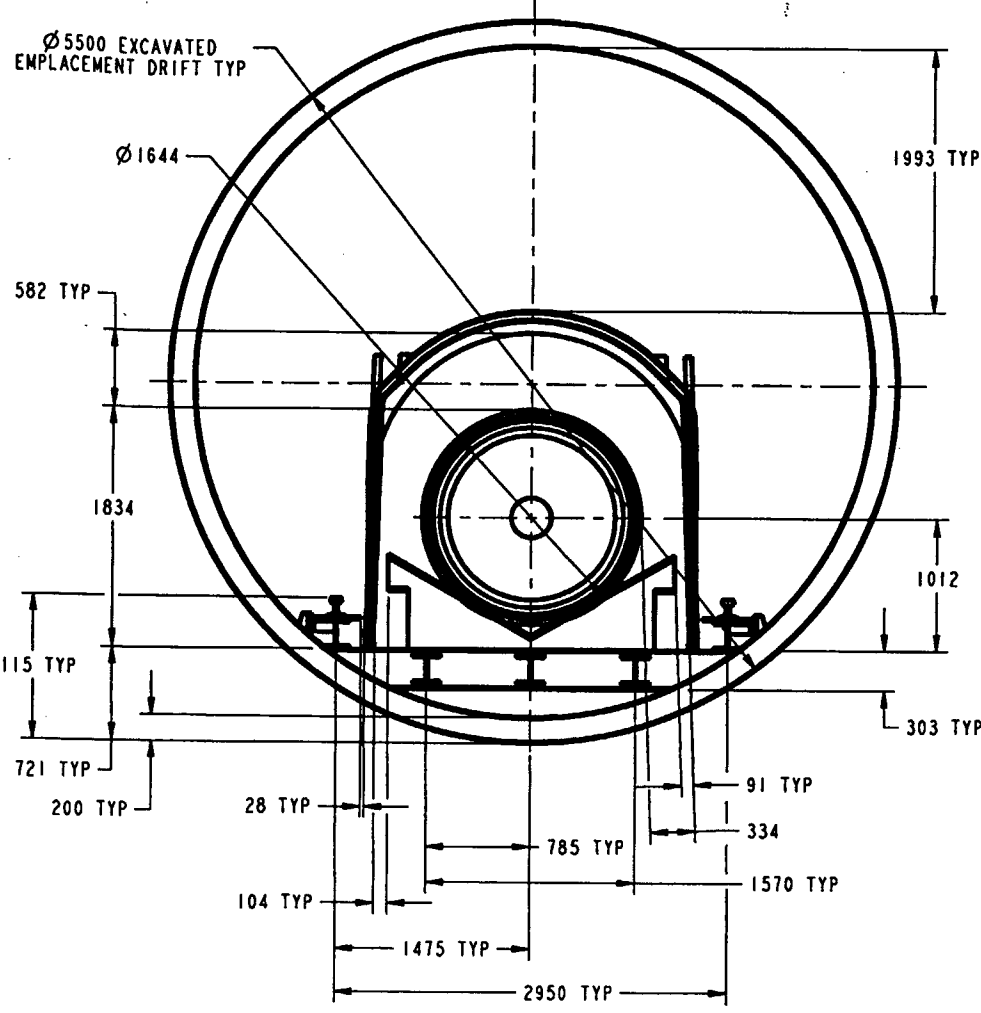
ITEM 13  
LIFTING FEATURE TOP PLATE  
SCALE 2.000  
4 D 2

WASTE PACKAGE PROJECT	
<b>Bechtel SAIC Company, LLC</b>	
SKETCH NUMBER	REVISION
SK-0211	00
SCALE 0.075	SHEET 13 OF 14

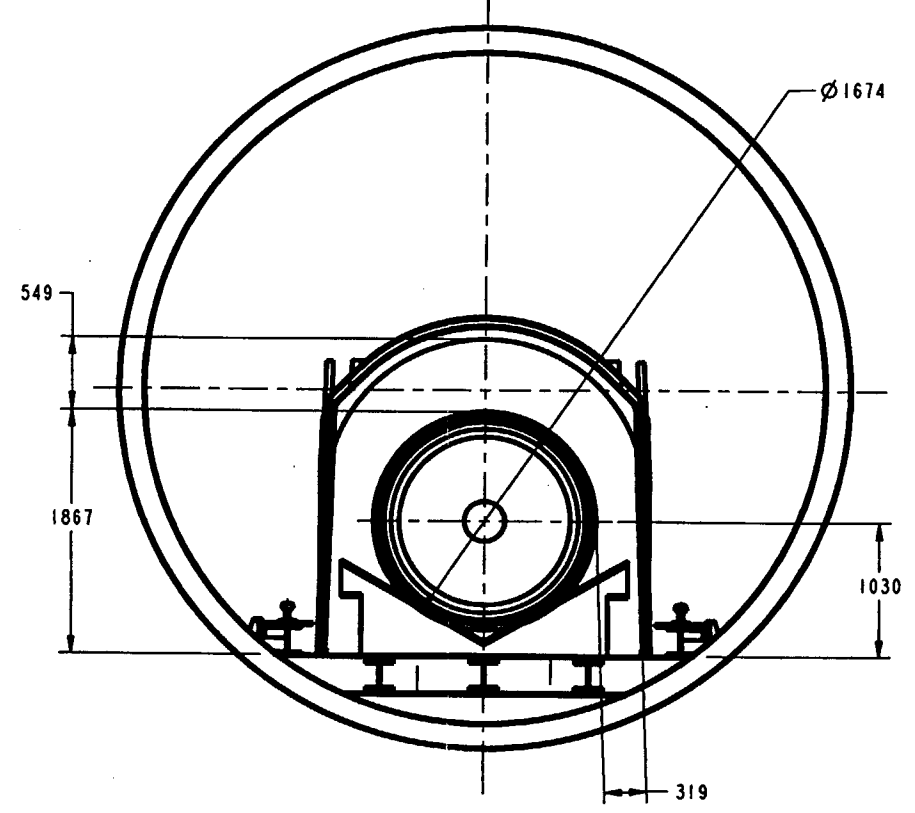
COMPONENT LIST							
ITEM NUMBER	ASSEMBLY	SUBASSEMBLY	COMPONENT NAME	MATERIAL	THICKNESS	BASE DIM	QTY REQD
-1	STAND ALONE DRIP SHIELD-LONG ASSEMBLY	-	-	-	-	4740	1
1	-	-	PLATE-1	SB-265 R52400	15.875 (.625)	1020	1
2	-	-	PLATE-2	SB-265 R52400	15.875 (.625)	950	2
3	-	-	ENCLOSURE PANEL	SB-265 R52400	15.875 (.625)	210	2
4	-	-	EXTERNAL SUPPORT PLATE	SB-265 R56405	12.7 (.5)	170	2
5	-	-	INTERNAL SUPPORT PLATE	SB-265 R56405	12.7 (.5)	96	2
6	-	-	BULKHEAD	SB-265 R56405	38.1 (1.5)	43	6
7	-	-	VERTICAL SUPPORT BEAM	SB-265 R56405	76.2 (3)	34	12
8	-	-	BASE PLATE	SB-575 N06022	9.525 (.375)	60	2
9	-	-	CONNECTOR PIN	SB-575 N06022	15.875 (.625)	0.09	14
10	-	-	CONNECTOR PIN WASHER	SB-575 N06022	6.35 (.25)	0.02	28
-2	-	LIFTING FEATURE ASSEMBLY	-	-	-	3.0	4
11	-	-	LIFTING FEATURE FRONT PLATE	SB-265 R56405	12.7 (.5)	0.54	4
12	-	-	LIFTING FEATURE SIDE PLATE	SB-265 R56405	12.7 (.5)	0.81	8
13	-	-	LIFTING FEATURE TOP PLATE	SB-265 R56405	12.7 (.5)	0.76	4
-	-	-	TOTAL TITANIUM GRADE 7 WELDS	SFA-5.16 R52401	-	59	-

WELD LIST				
WELD NUMBER	WELD TYPE	MATERIAL	BASE DIM	QTY REQD
1	GROOVE	SFA-5.16 R52401	1.8	4
2	FILLET	SFA-5.16 R52401	1.1	2
3	FILLET	SFA-5.16 R52401	2.4	2
4	FILLET	SFA-5.16 R52401	2.3	2
5	FILLET	SFA-5.16 R52401	2.3	2
6	FILLET	SFA-5.16 R52401	2.2	2
7	FILLET	SFA-5.16 R52401	0.004	12
8	FILLET	SFA-5.16 R52401	1.2	12
9	FILLET	SFA-5.16 R52401	0.68	24
10	SQUARE	SFA-5.16 R52401	0.006	12
11	FILLET	SFA-5.16 R52401	0.01	28
12	FILLET	SFA-5.16 R52401	0.006	8
13	FILLET	SFA-5.16 R52401	0.006	8
14	FILLET	SFA-5.16 R52401	0.01	8
15	FILLET	SFA-5.16 R52401	0.01	4
16	FILLET	SFA-5.16 R52401	0.01	8
17	FILLET	SFA-5.16 R52401	0.02	4
18	FILLET	SFA-5.16 R52401	0.003	8
19	FILLET	SFA-5.16 R52401	0.01	8
TOTAL TITANIUM GRADE 7 WELDS			59	-

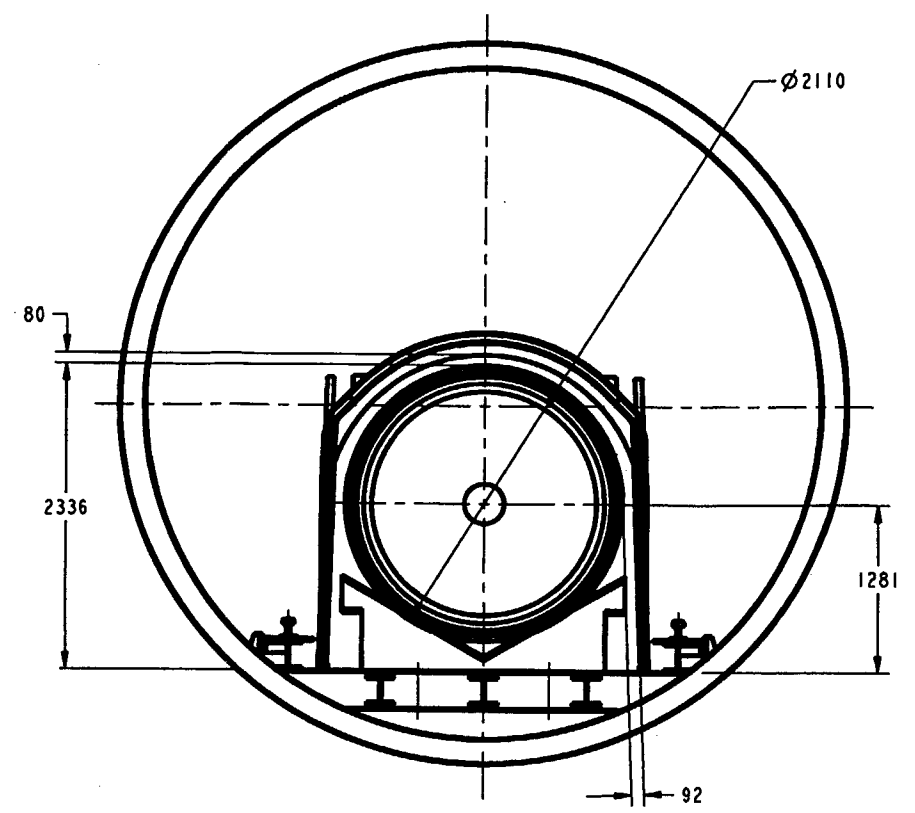
WASTE PACKAGE PROJECT  
**Bechtel SAIC Company, LLC**  
 SKETCH NUMBER SK-0211 REVISION 00  
 SCALE 0.075 SHEET 14 OF 14



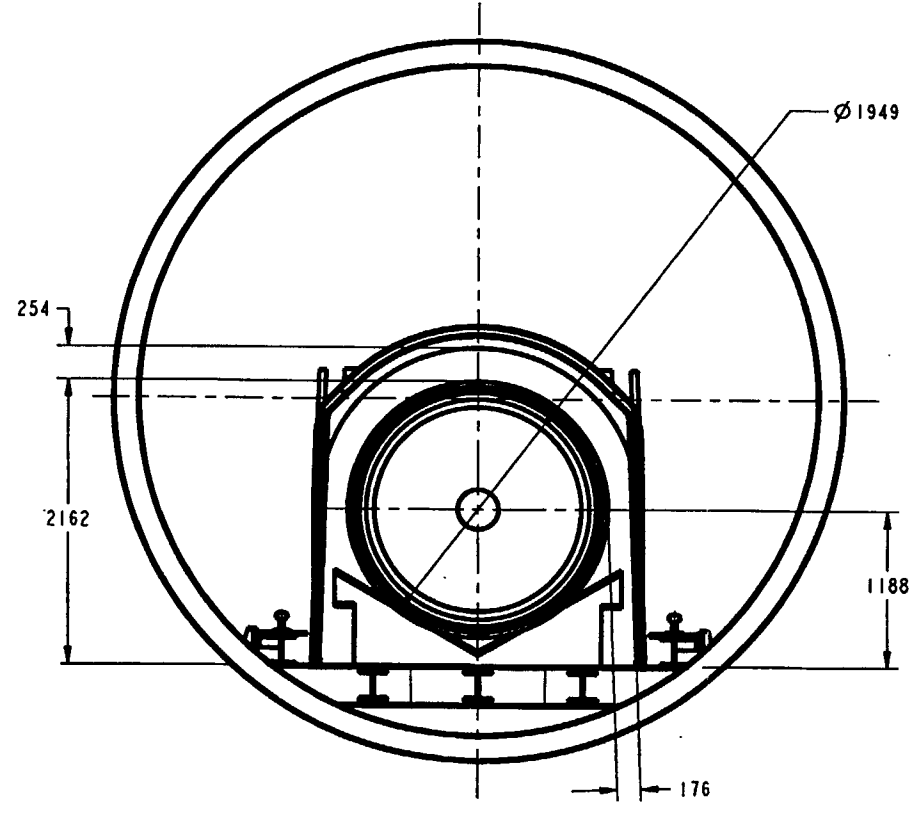
21 PWR



44 BWR



5 DHLW



NAVAL

UNITS: mm

DO NOT SCALE FROM SKETCH

**"FOR INFORMATION ONLY"**

**DRIFT CROSS SECTION SHOWING  
EMPLACED PACKAGE AND DRIP SHIELD**

SKETCH NUMBER:	SK-0154 REV 02
SKETCHED BY:	GENE CONNELL <i>GC</i> <i>SMB</i>
DATE:	01/28/00 <i>2/2/00</i> <i>02/03/00</i> <i>2.8.00</i>
FILE:	/home/pro-library/checkout/sketches/drift/drift_SK-0133rev02.dwg

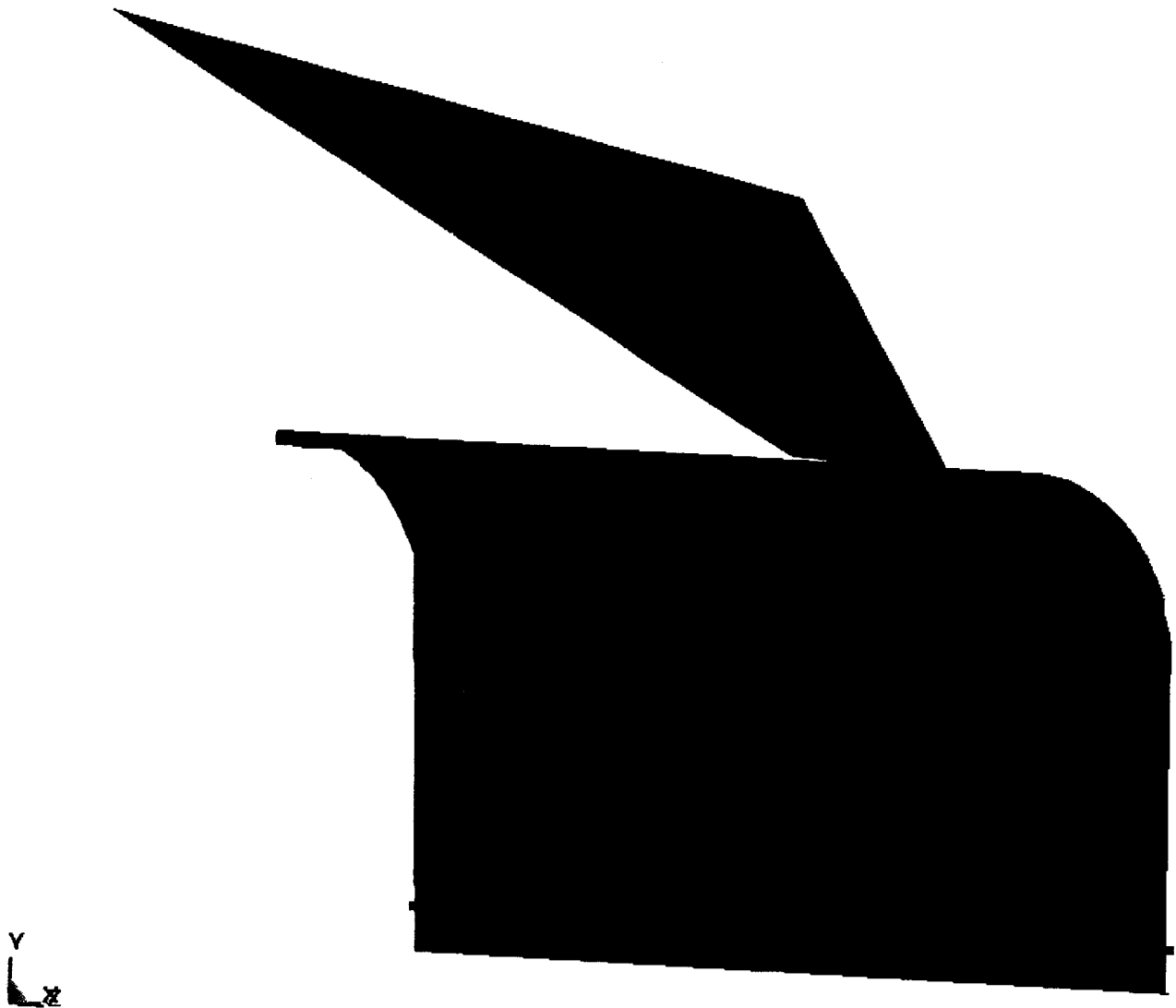
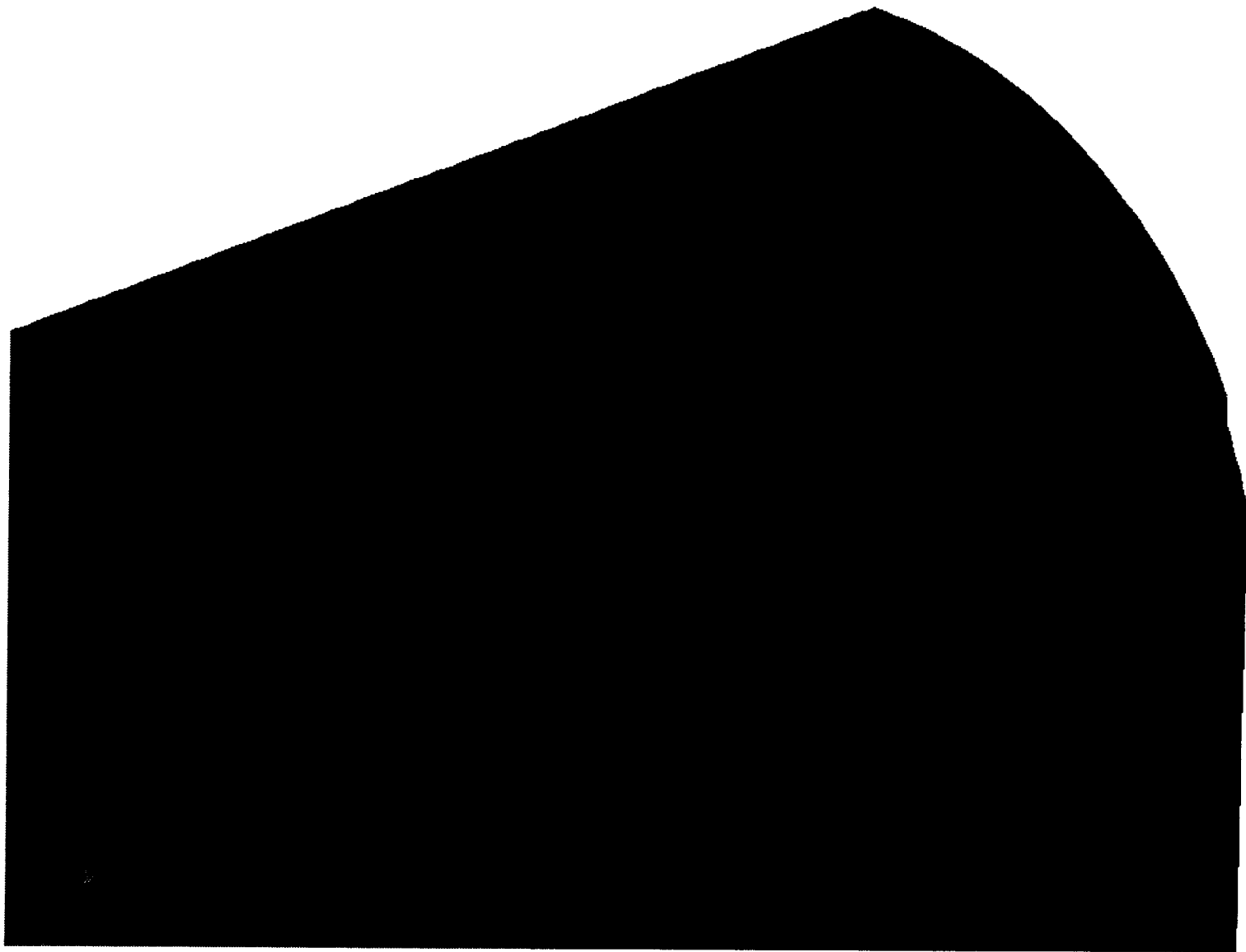
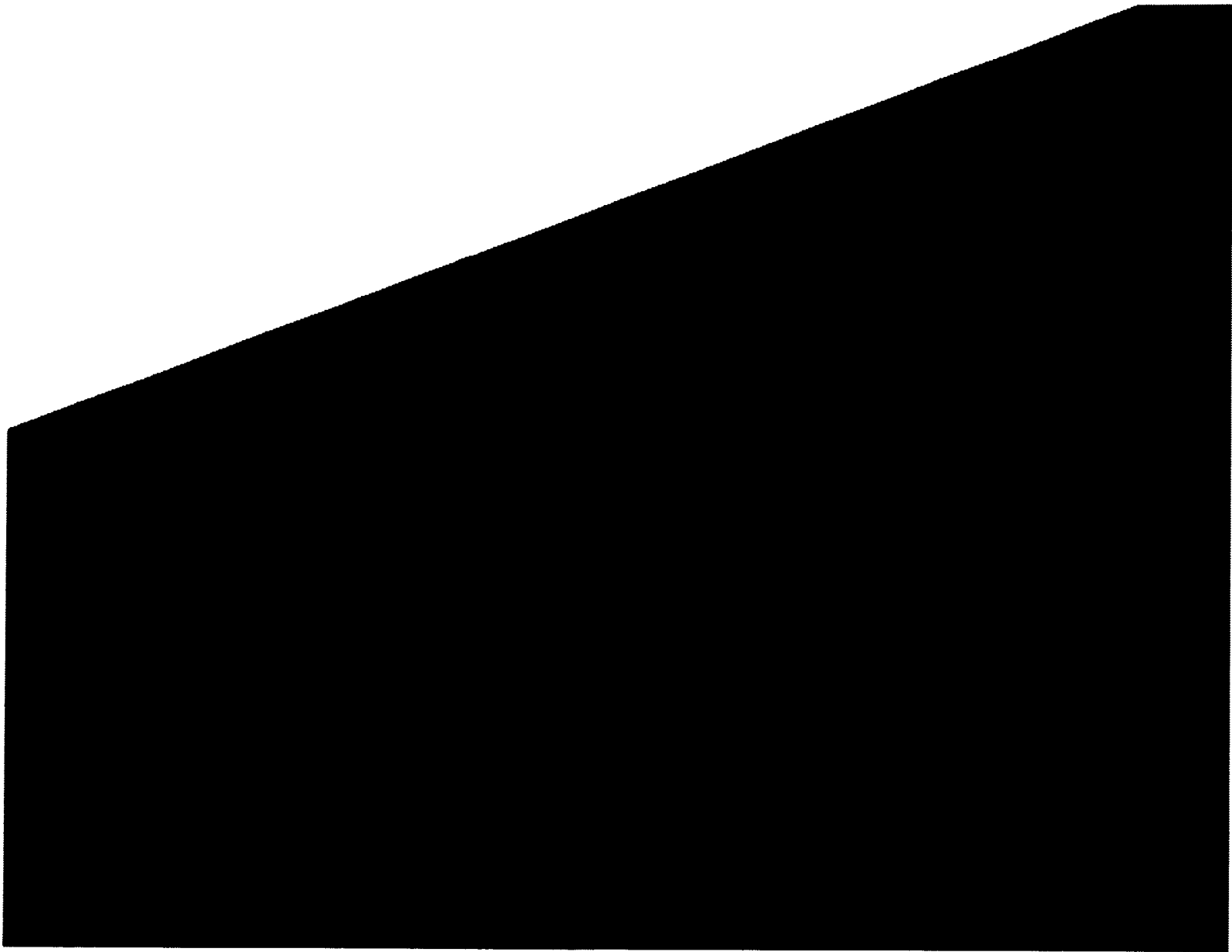


Figure II-1. Finite Element Representation of 6-MT Rock Fall on Drip Shield (FE mesh is not shown for clarity)



**Figure II-2.** Longitudinal Stiffeners and Bulkhead Stiffener Plates Located Below the Top Plate



**Figure II-3.** Detailed View of Longitudinal Stiffeners and Bulkhead Stiffener Plates

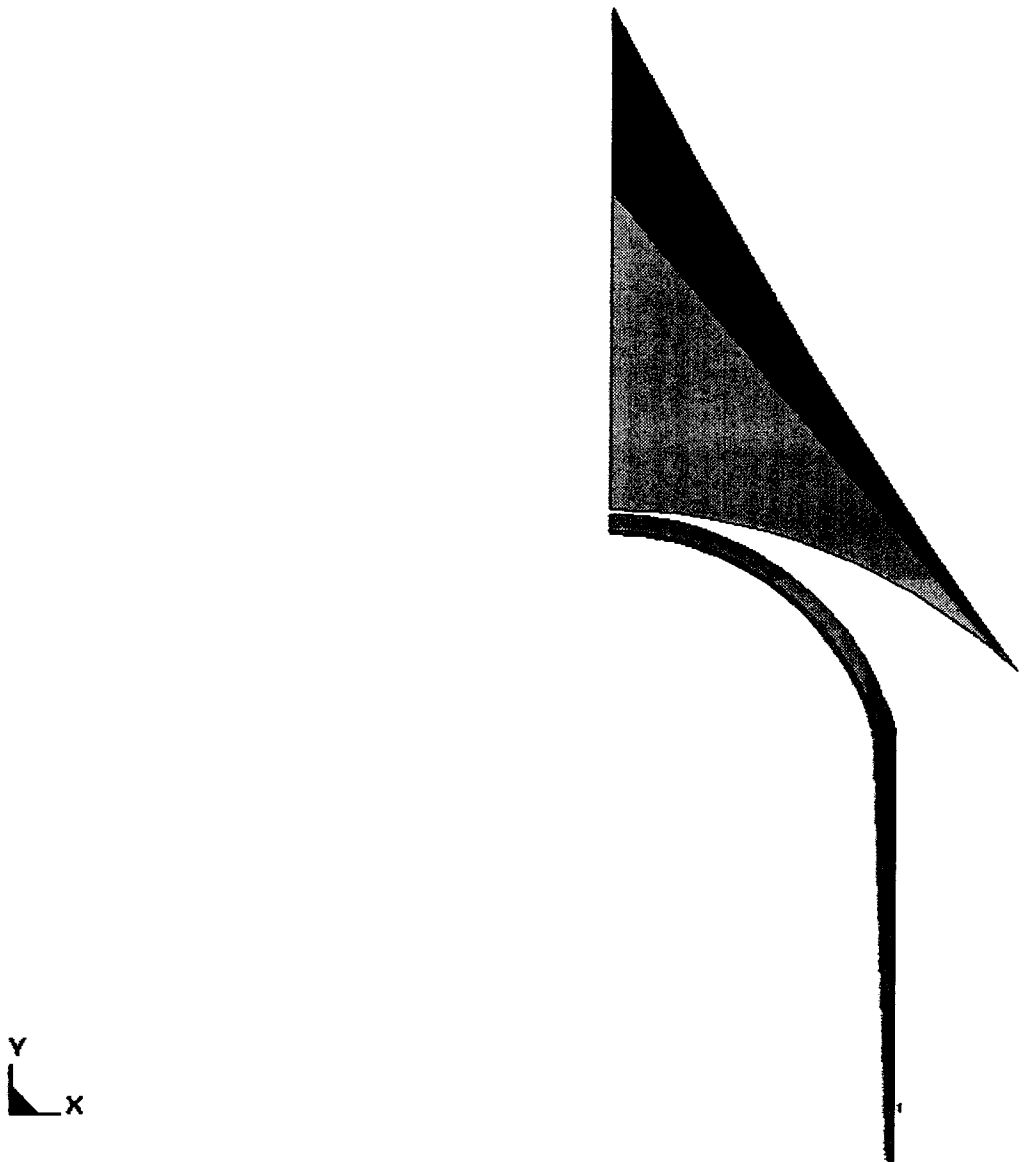


**Figure II-4.** End-view of the 6-MT Rock Fall on Drip Shield

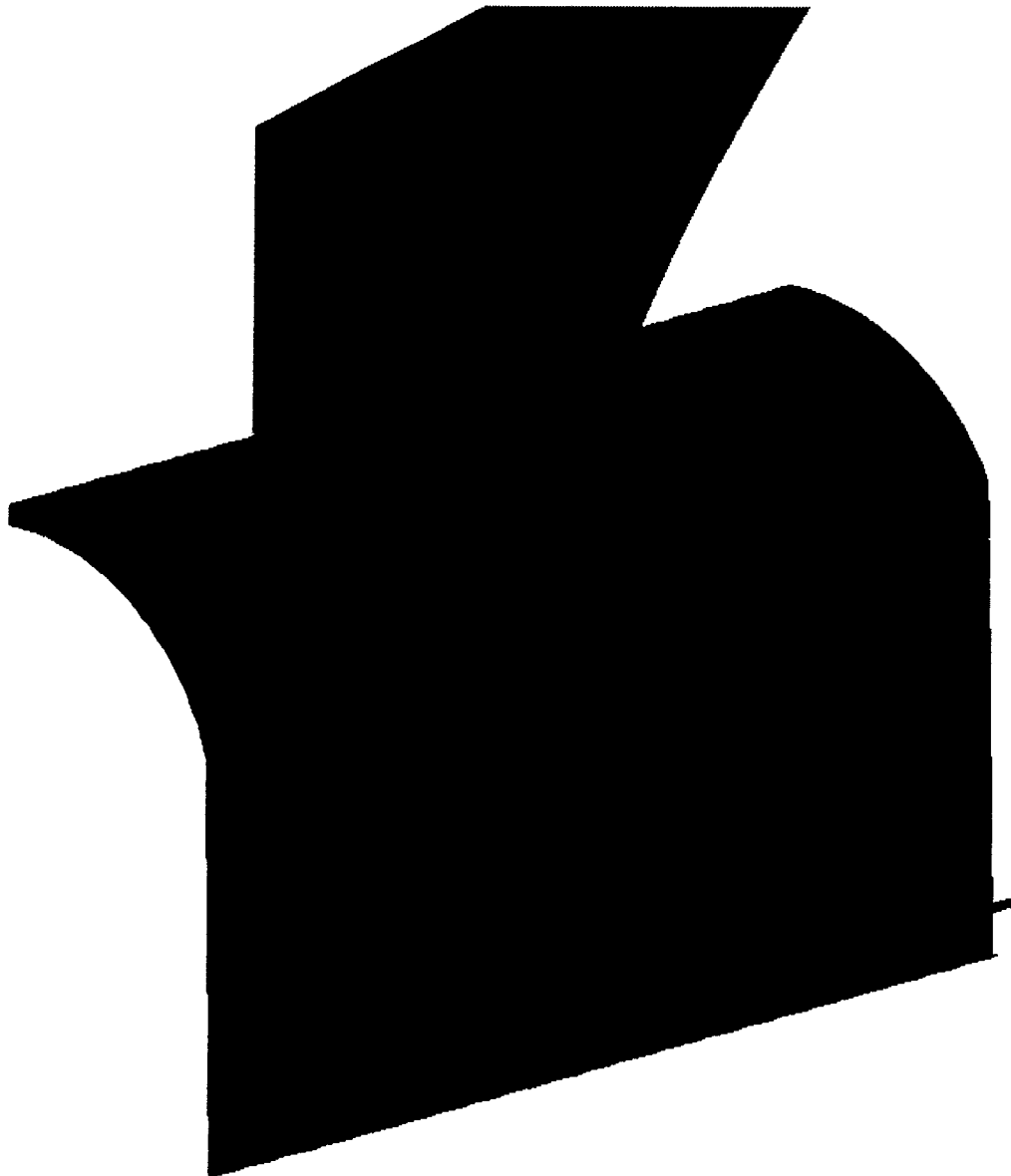


Figure II-5. Isometric View of the 6-MT Rock Fall on Drip Shield

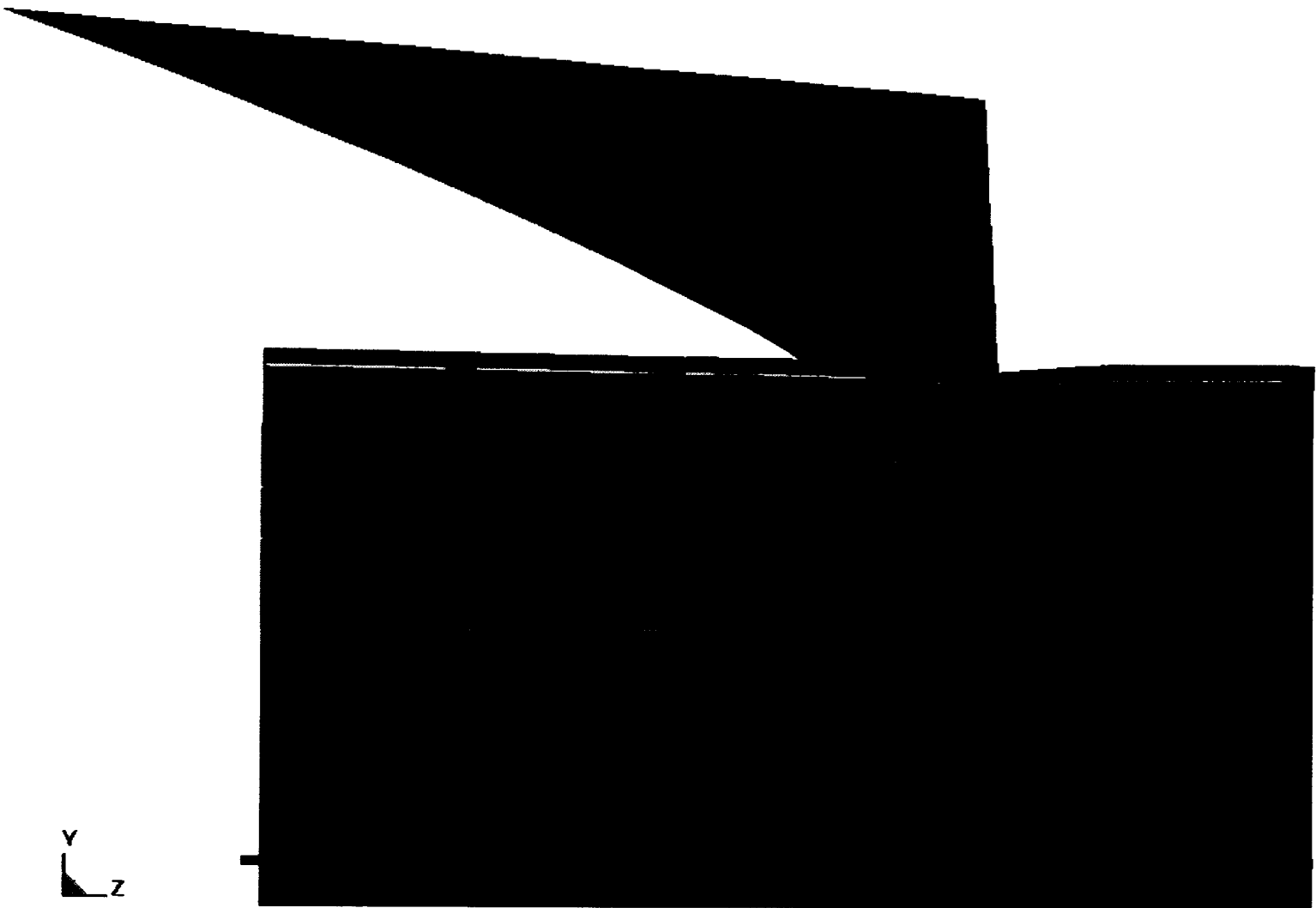


Figure II-6. Illustration of deformation for 6-MT Rock Fall on Drip Shield

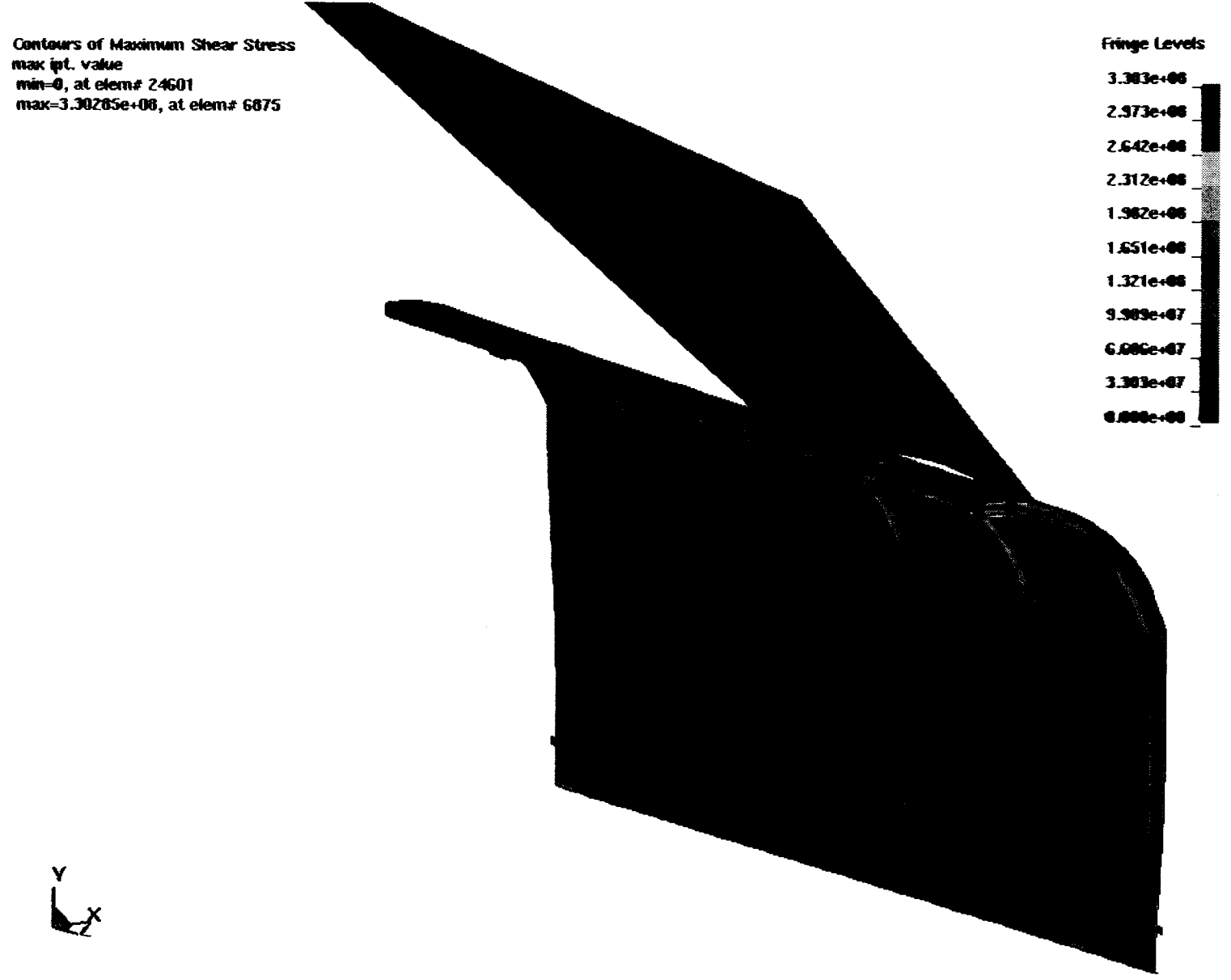
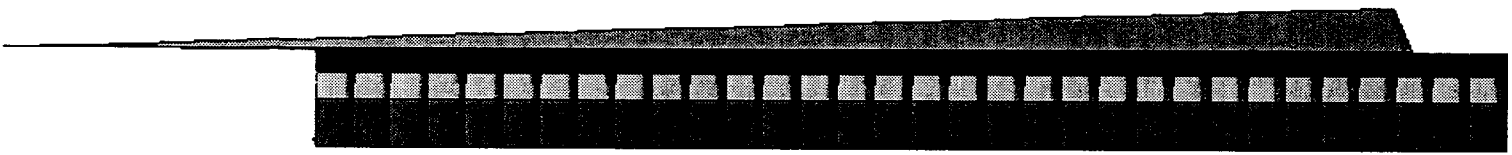


Figure II-7. Illustration of a Typical Stress Contour for 6-MT Rock Fall on Drip Shield



**Figure II-8.** Finite Element Representation of 52-MT Horizontal Rock Fall on Drip Shield (FE mesh is not shown for clarity)



**Figure II-9. Finite Element Representation of 52-MT Pointed-edge Rock Fall on Drip Shield**

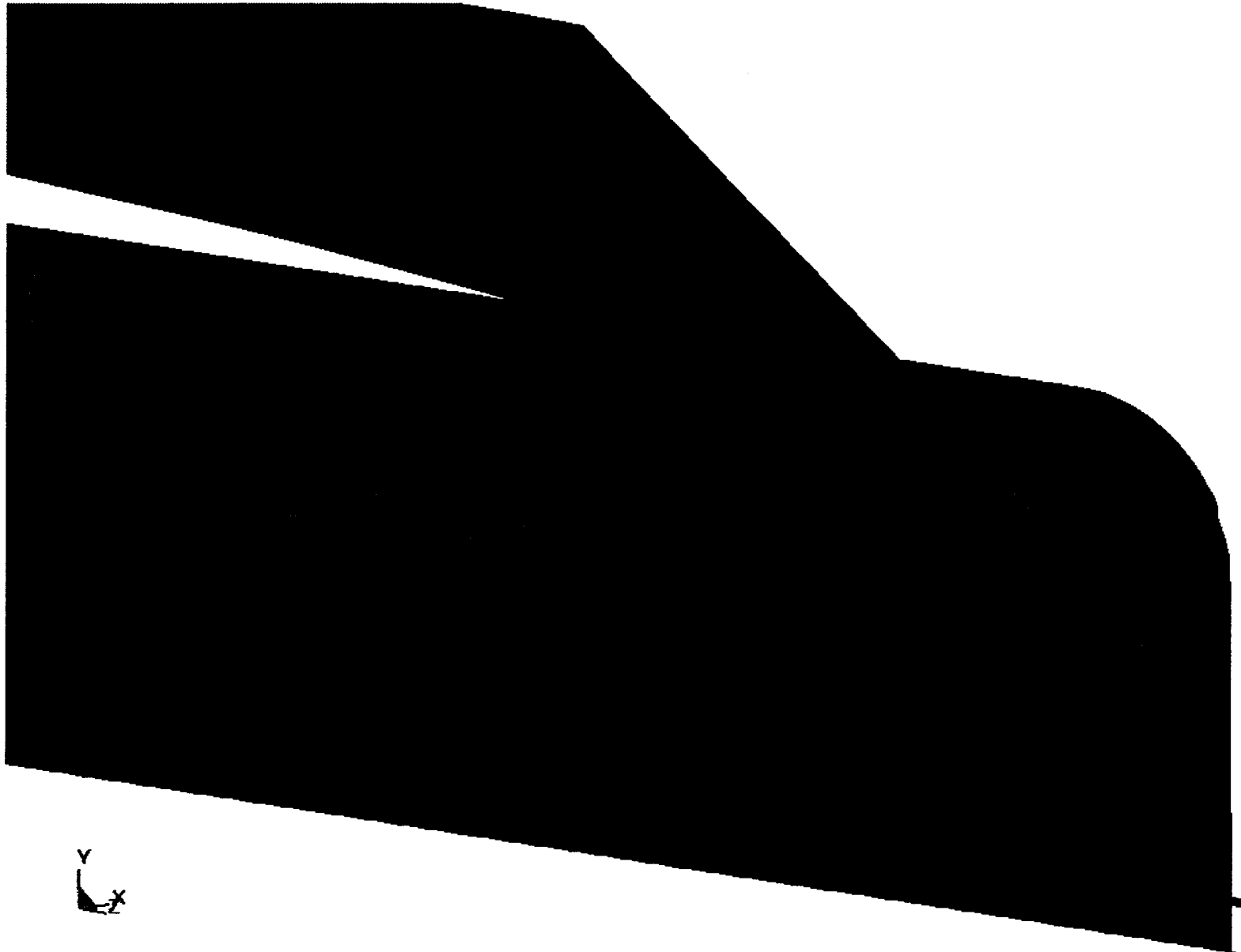
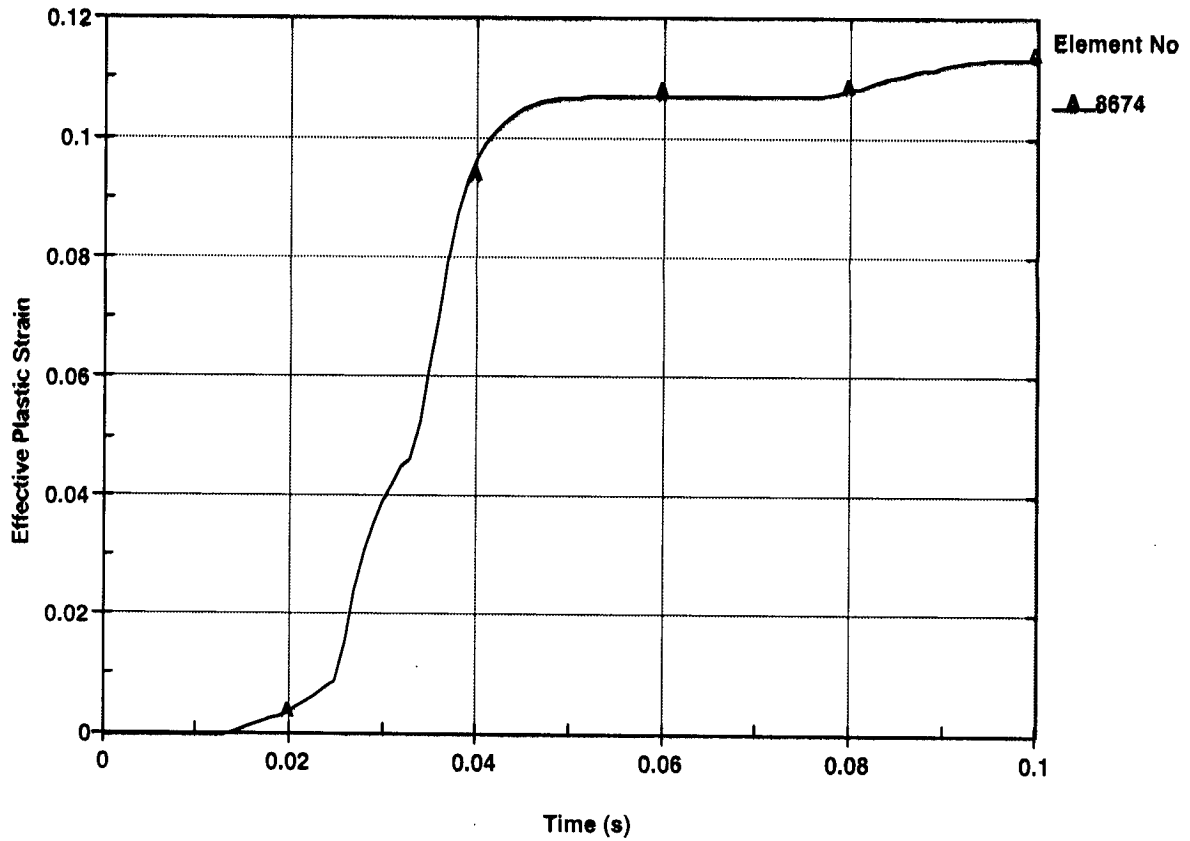


Figure II-10. Finite Element Mesh for 52-MT Rock Fall on Drip Shield



**Figure II-11.** Maximum Effective Plastic Strain in the Top Plate  
(52-MT pointed-edge rock fall)

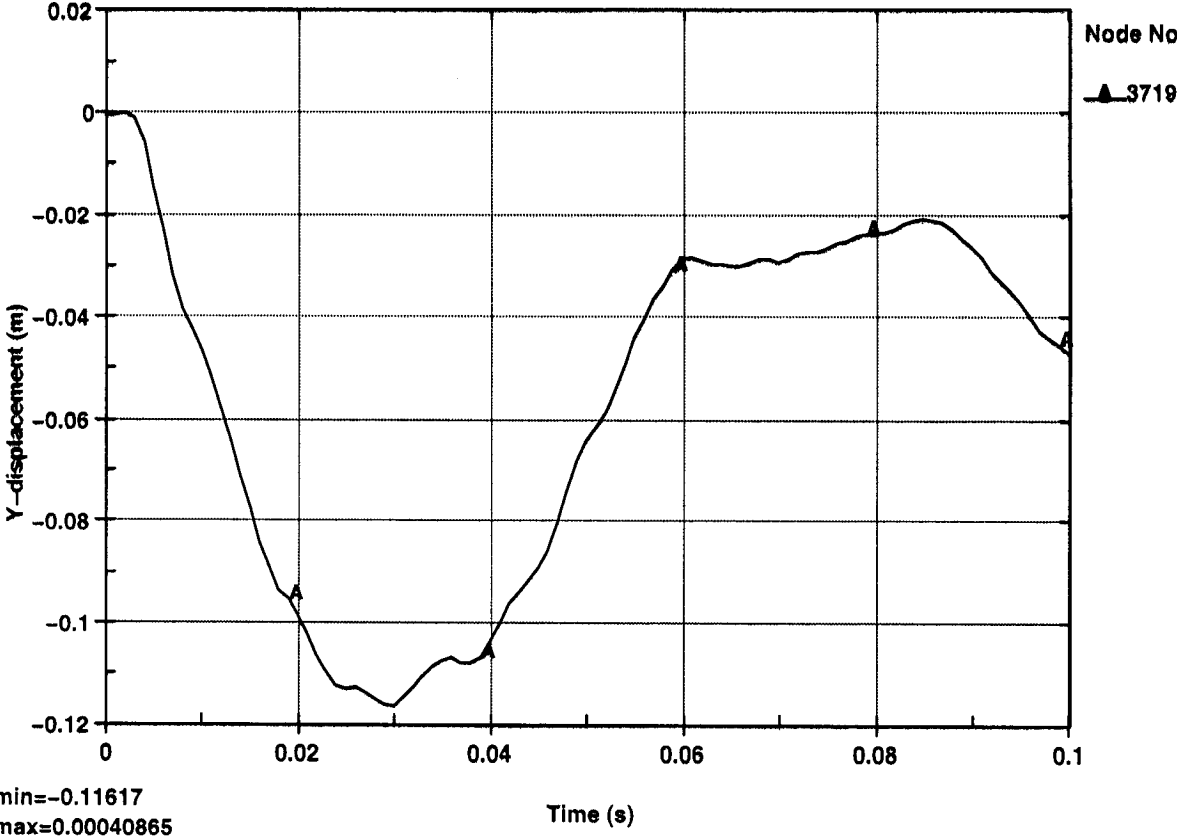


Figure II-12. Maximum Displacement for 6-MT Horizontal Rock Fall (Bulkhead stiffeners)

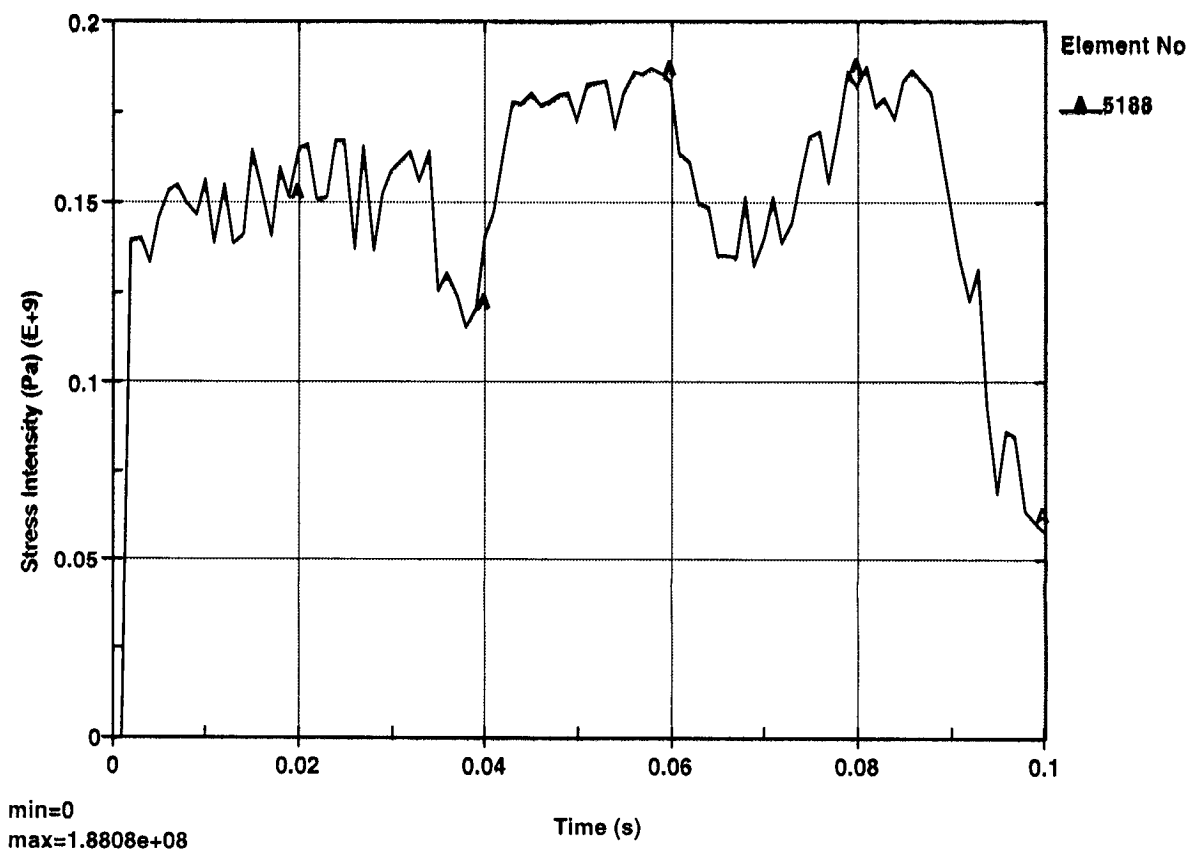


Figure II-13. Maximum Stress Intensity for 6-MT Horizontal Rock Fall (Top plate)

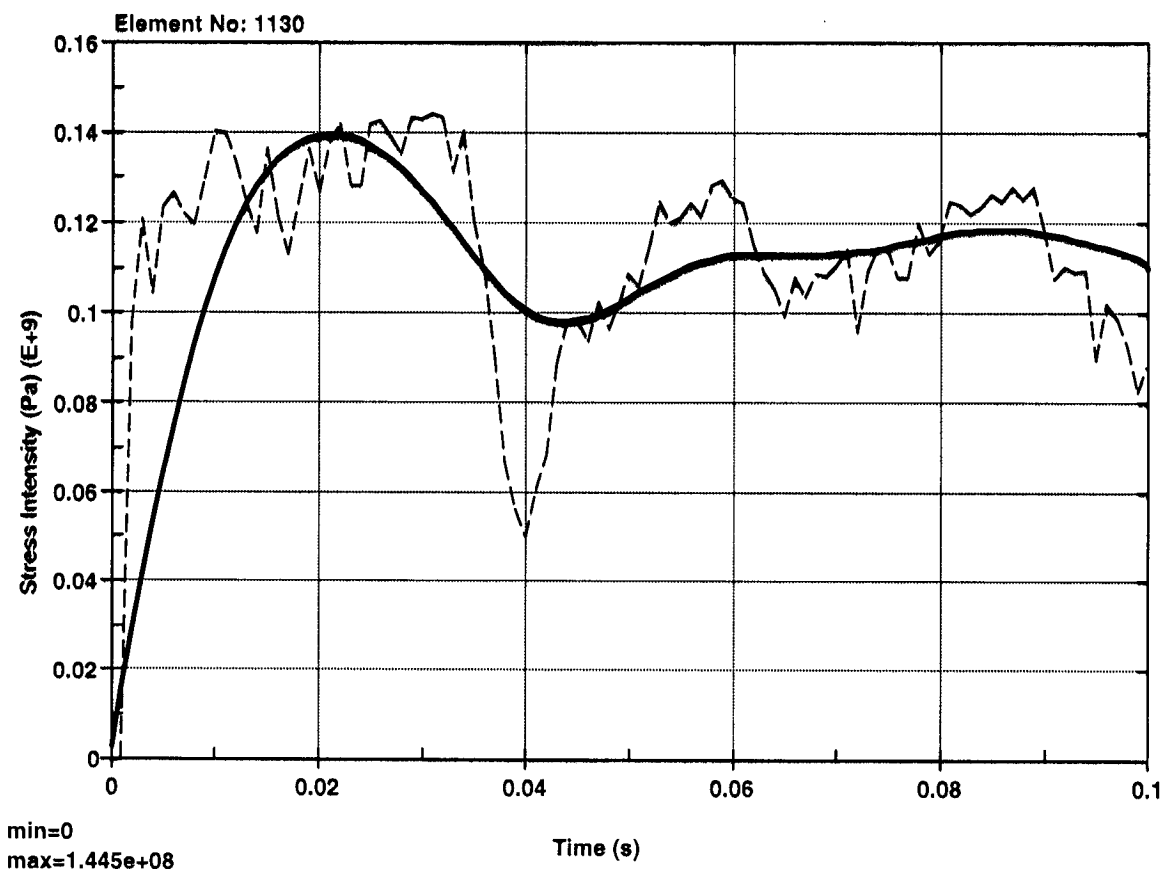


Figure II-14. Maximum Residual Stress for 6-MT Horizontal Rock Fall (Top plate)

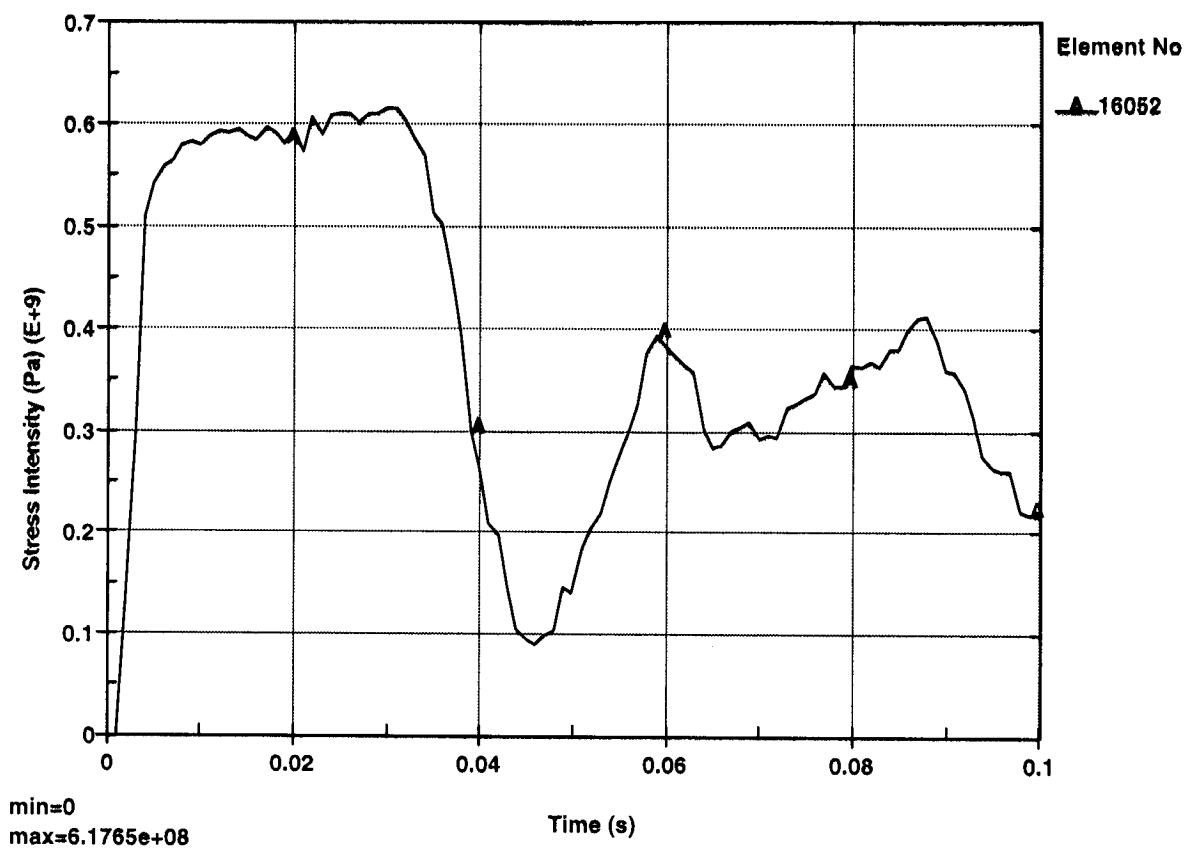


Figure II-15. Maximum Stress Intensity for 6-MT Horizontal Rock Fall (Bulkheads)

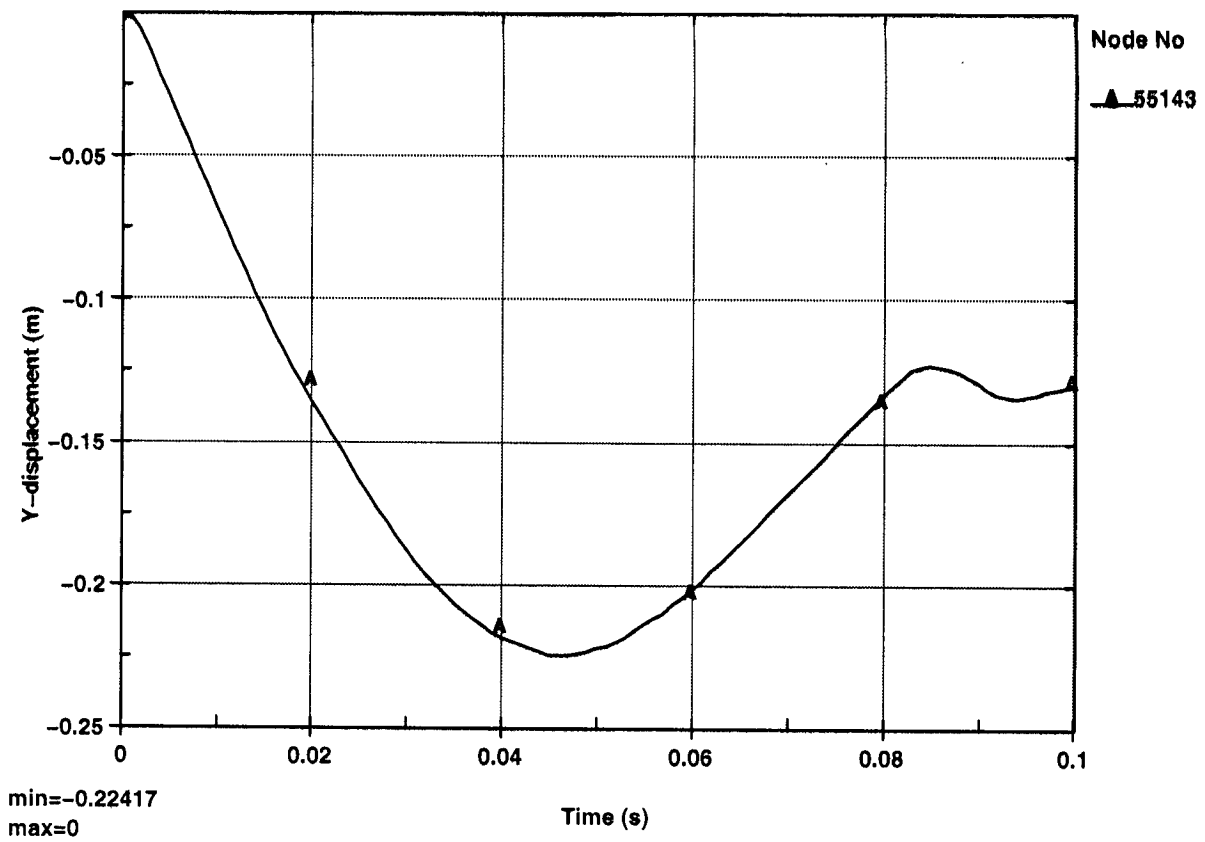


Figure II-16. Maximum Displacement for 52-MT Horizontal Rock Fall (Bulkhead stiffeners)

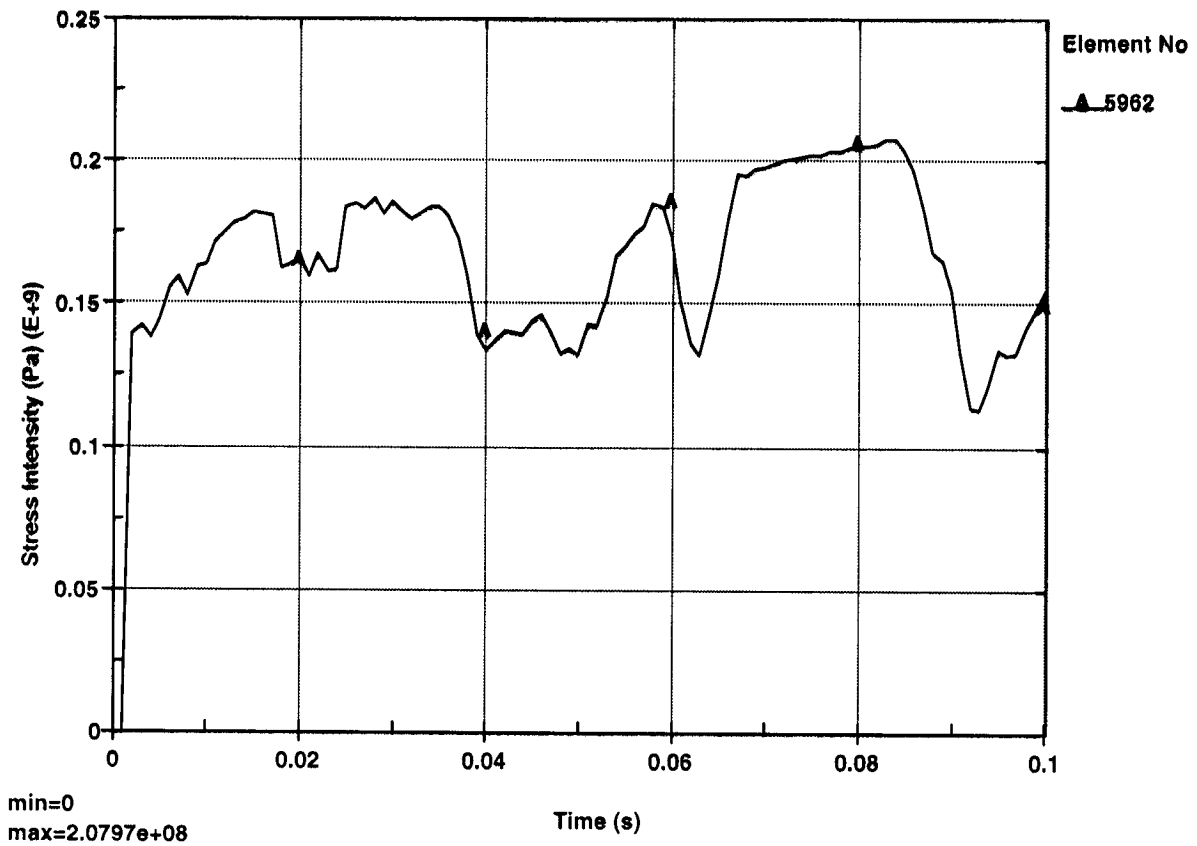


Figure II-17. Maximum Stress Intensity for 52-MT Horizontal Rock Fall (Top plate)

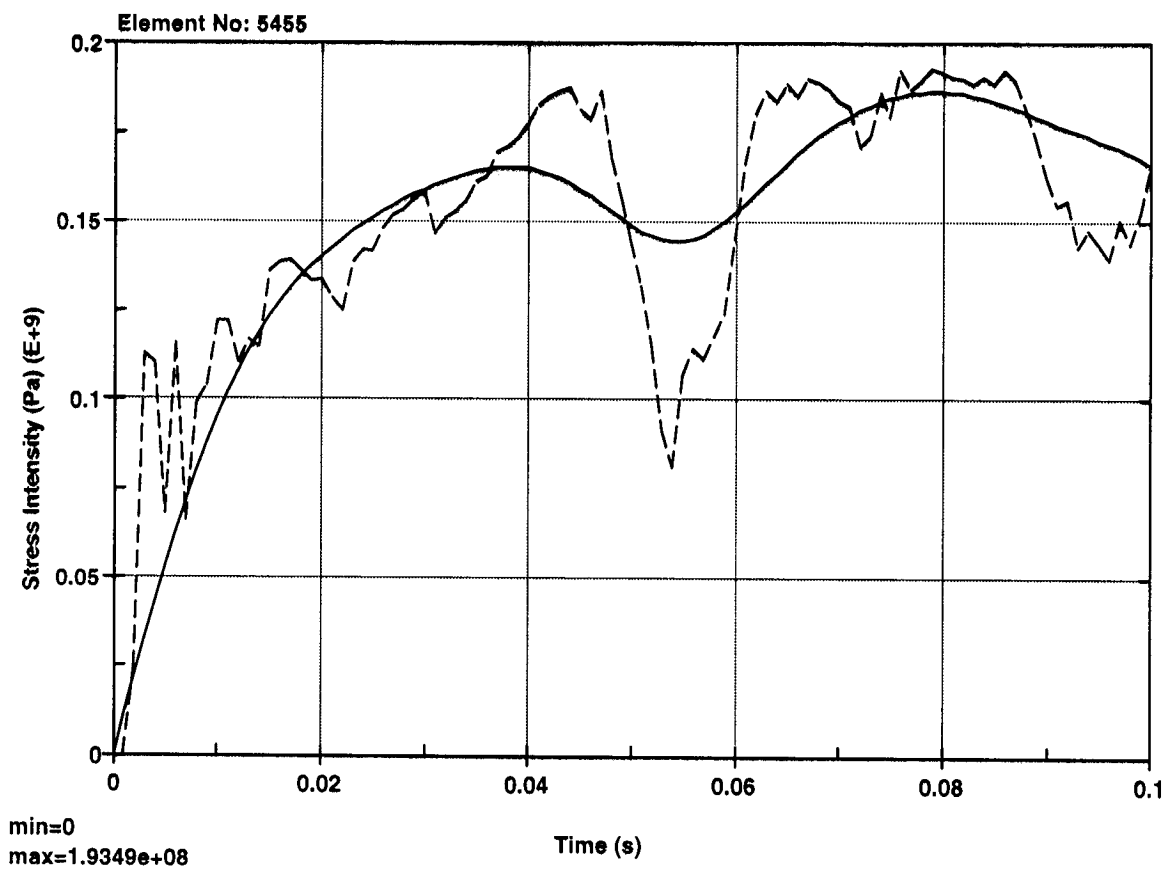


Figure II-18. Maximum Residual Stress for 52-MT Horizontal Rock Fall (Top plate)

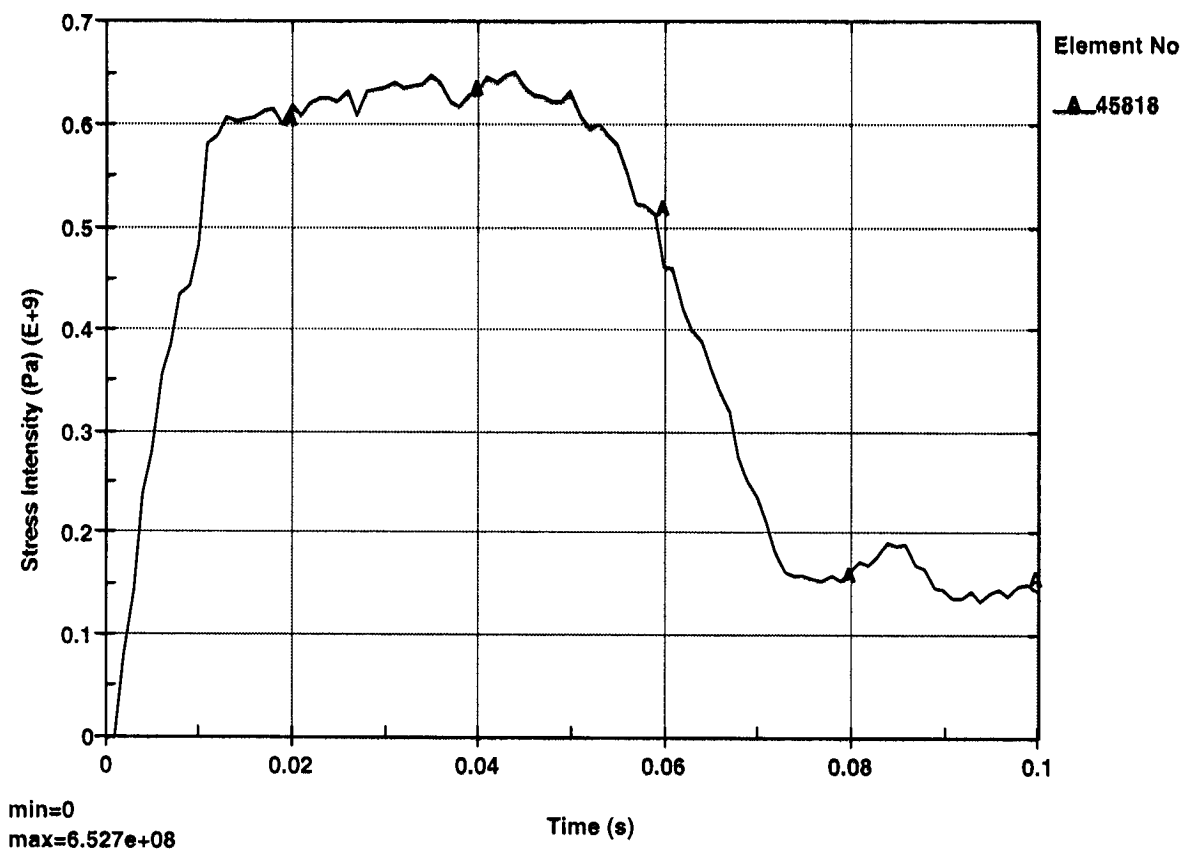


Figure II-19. Maximum Stress Intensity for 52-MT Horizontal Rock Fall (Bulkheads)

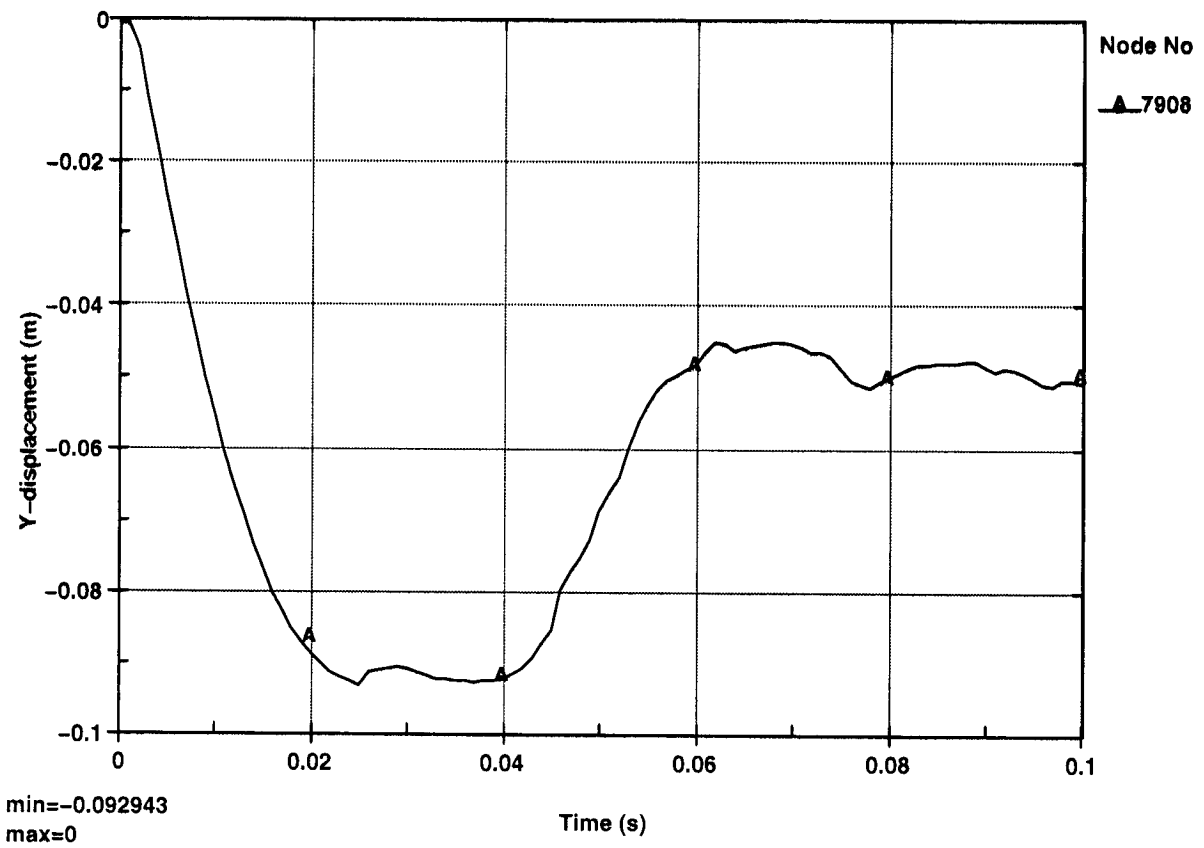


Figure II-20. Maximum Displacement for 6-MT Pointed-edge Rock Fall (Bulkhead stiffeners)

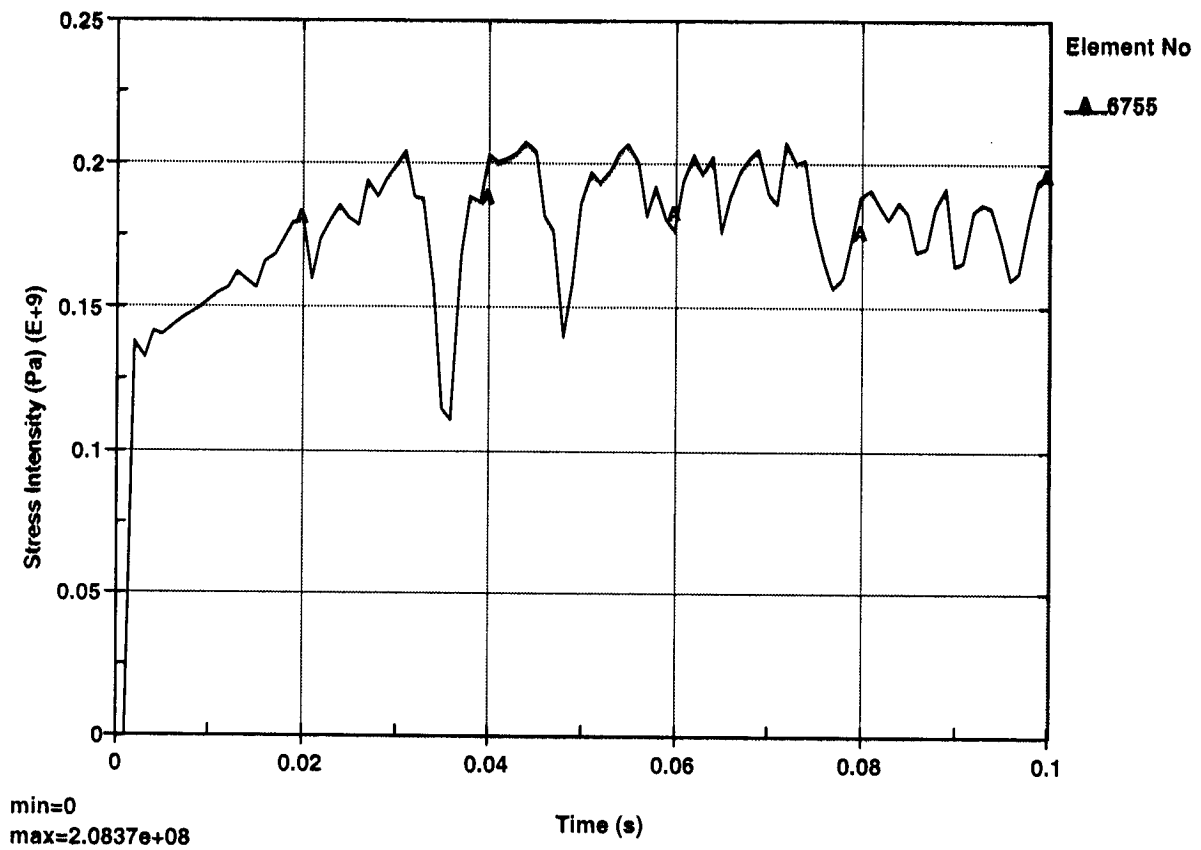


Figure II-21. Maximum Stress Intensity for 6-MT Pointed-edge Rock Fall (Top plate)

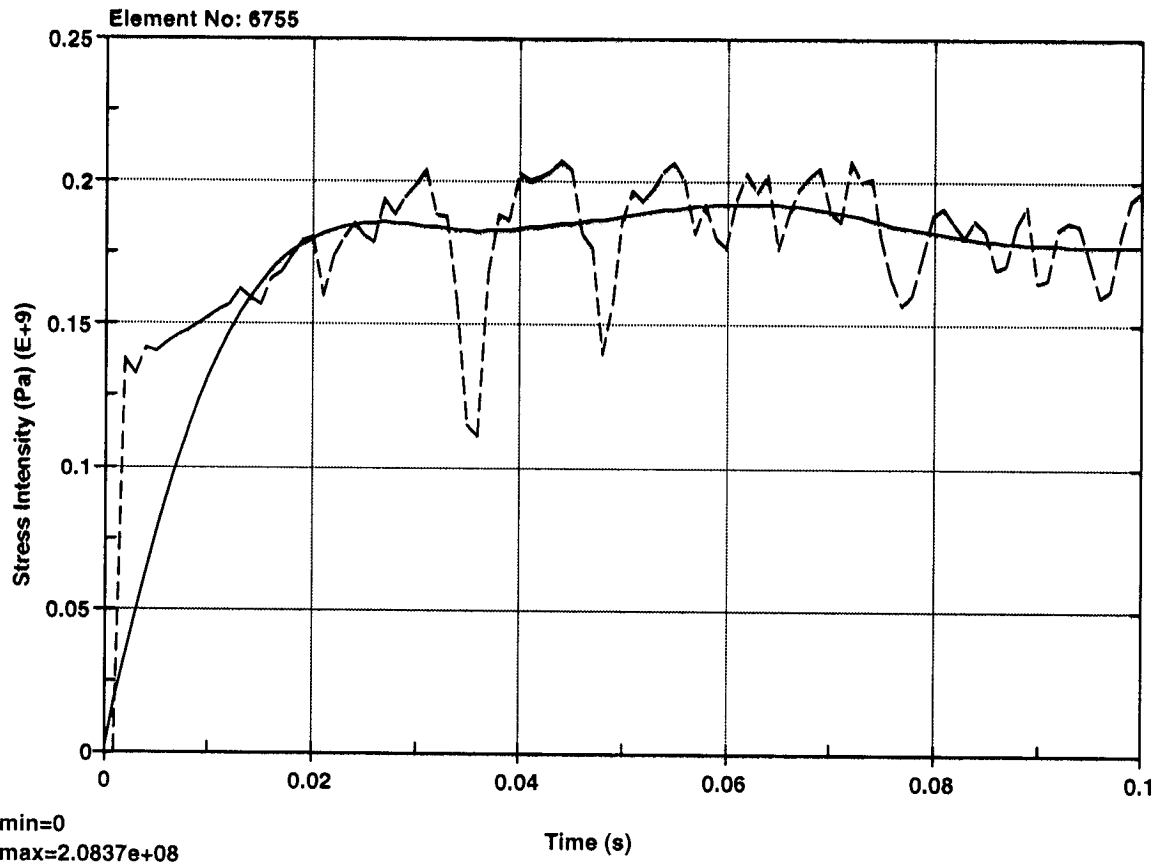


Figure II-22. Maximum Residual Stress for 6-MT Pointed-edge Rock Fall (Top plate)

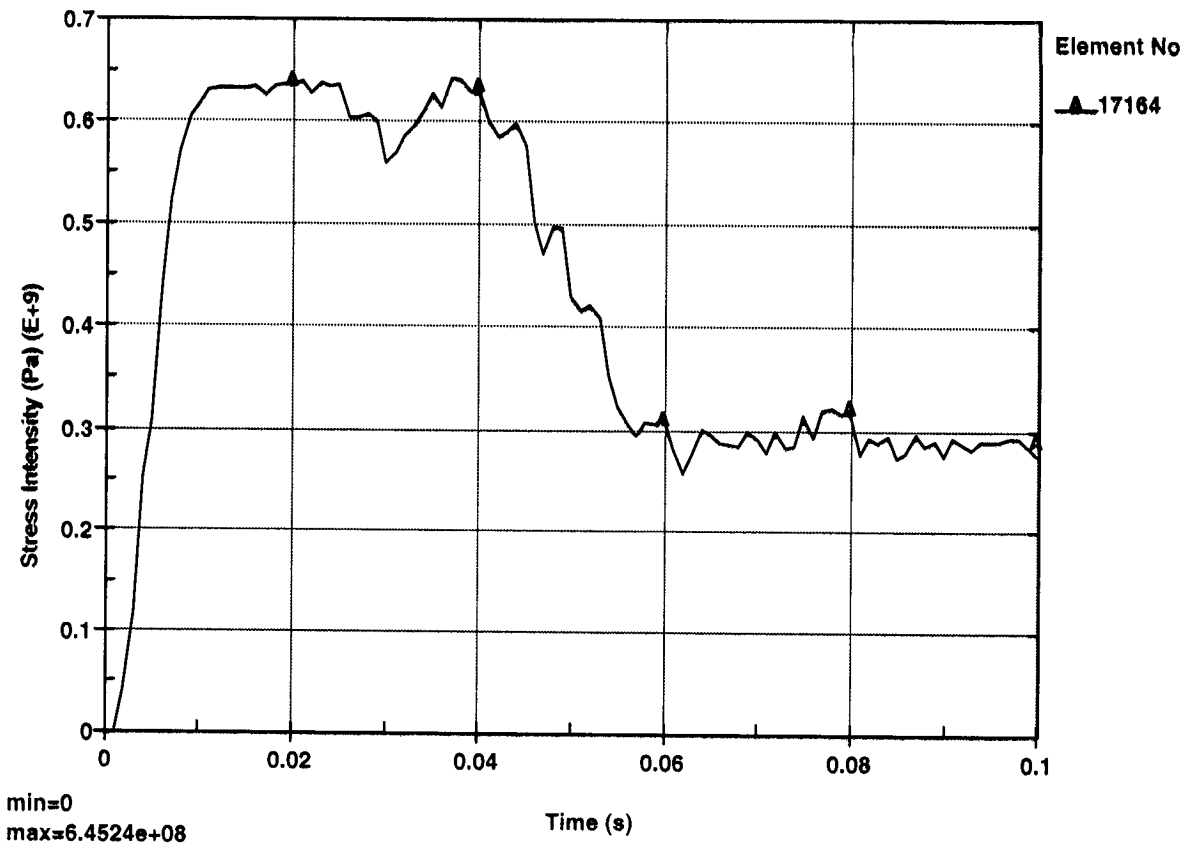


Figure II-23. Maximum Stress Intensity for 6-MT Pointed-edge Rock Fall (Bulkheads)

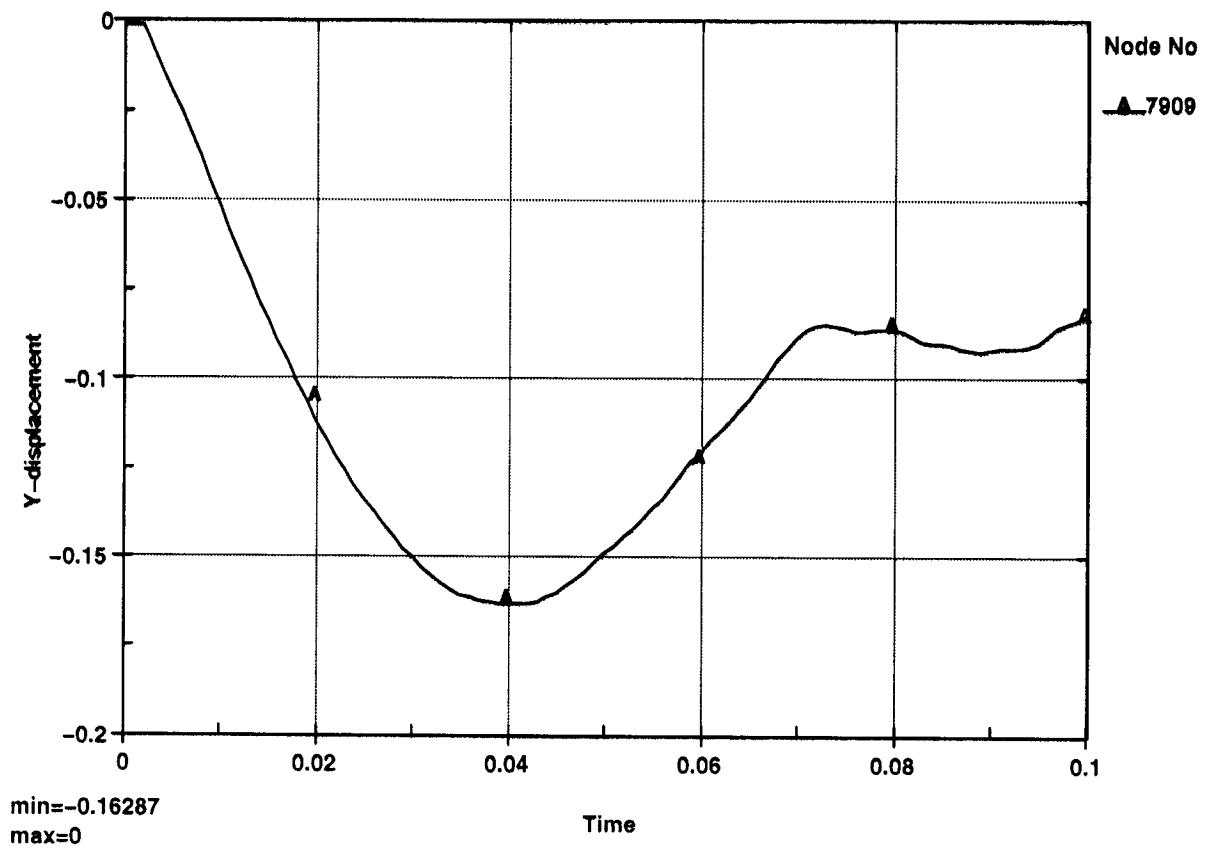


Figure II-24. Maximum Displacement for 15-MT Pointed-edge Rock Fall (Bulkhead stiffeners)

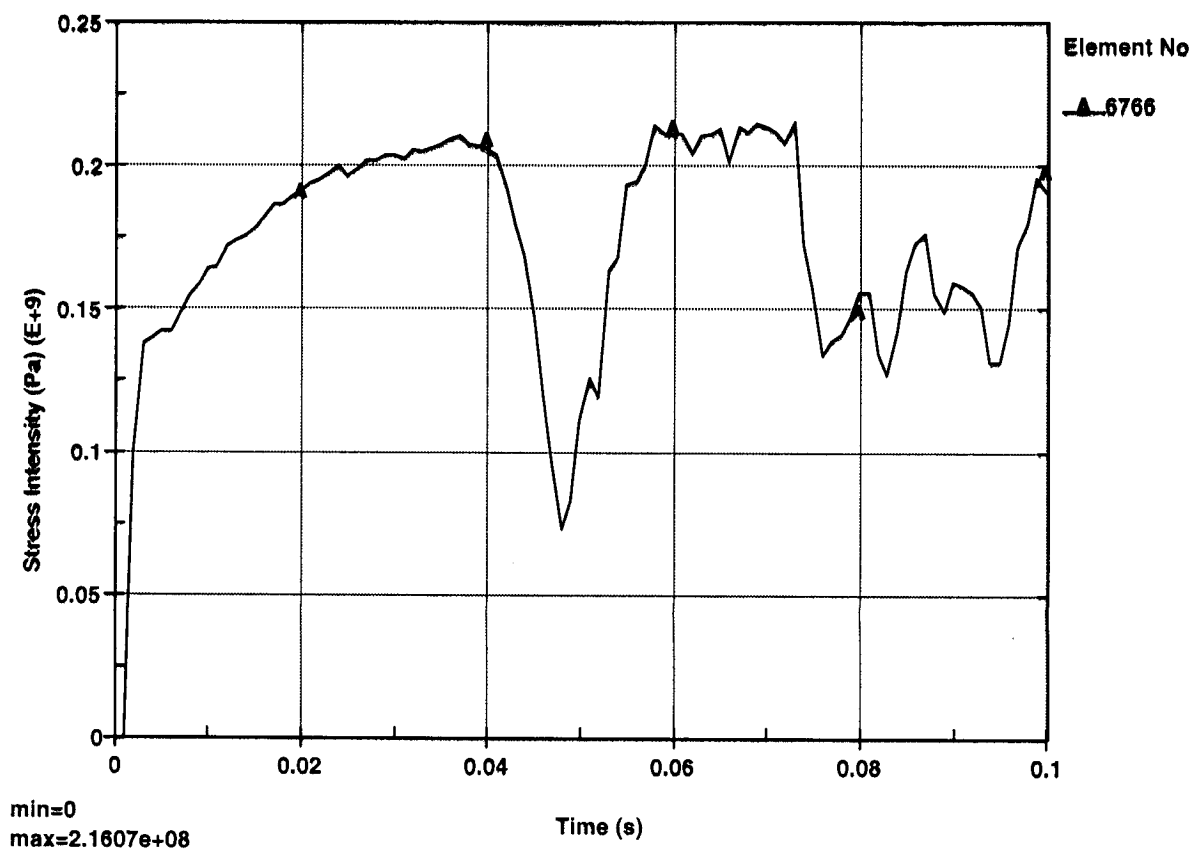


Figure II-25. Maximum Stress Intensity for 15-MT Pointed-edge Rock Fall (Top plate)

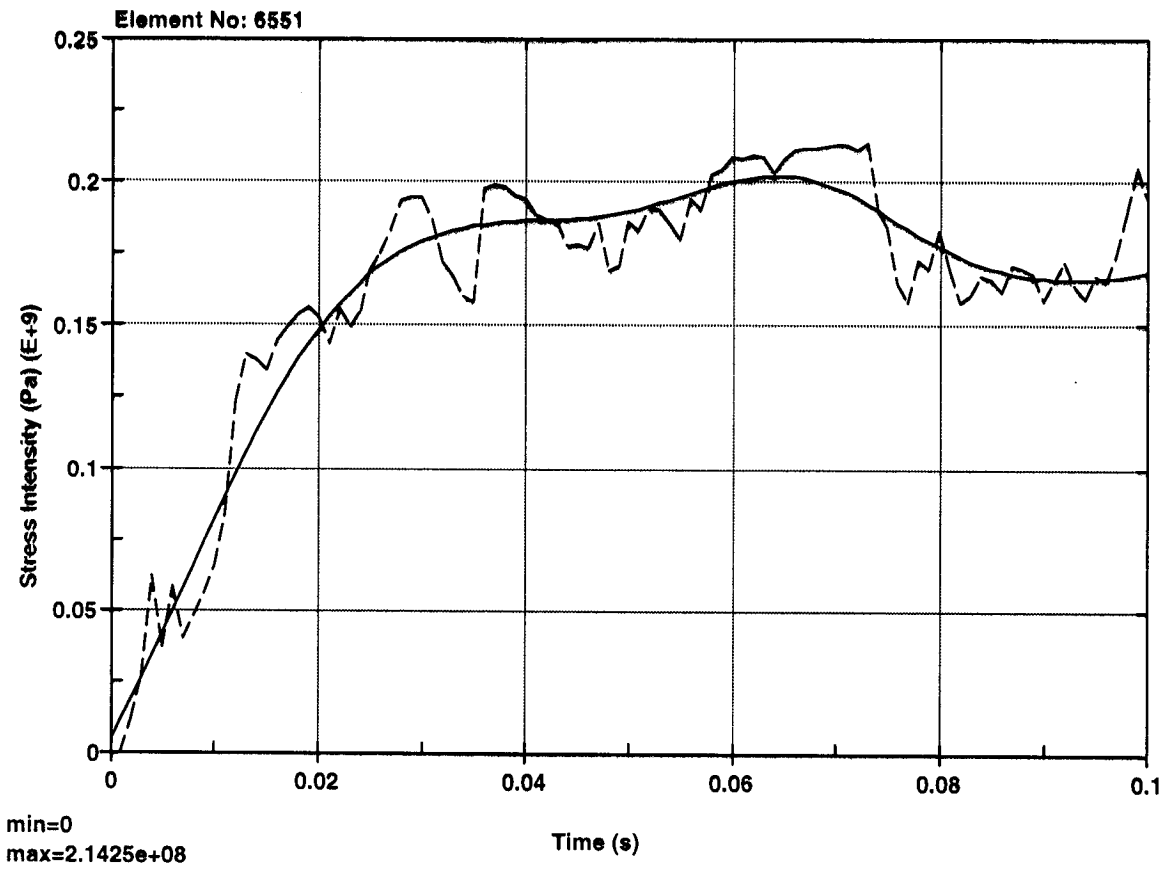


Figure II-26. Maximum Residual Stress for 15-MT Pointed-edge Rock Fall (Top plate)

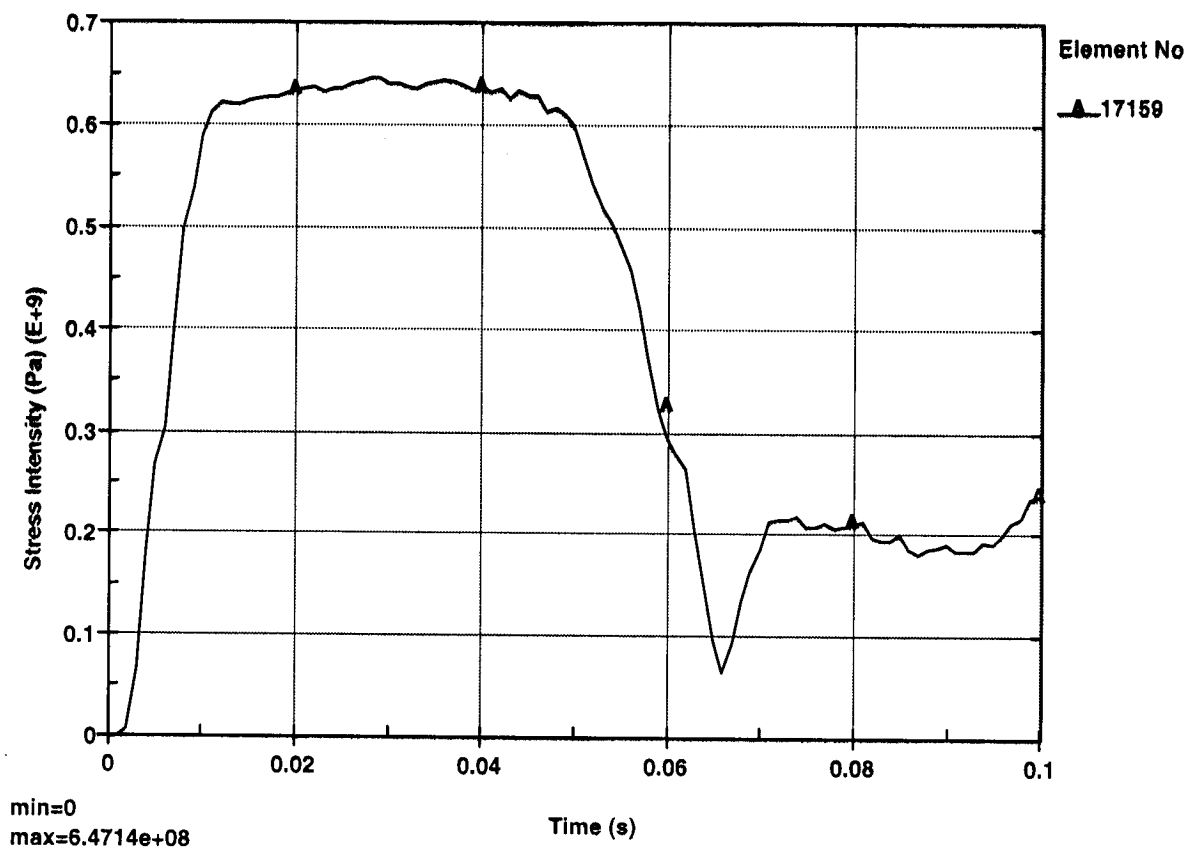


Figure II-27. Maximum Stress Intensity for 15-MT Pointed-edge Rock Fall (Bulkheads)

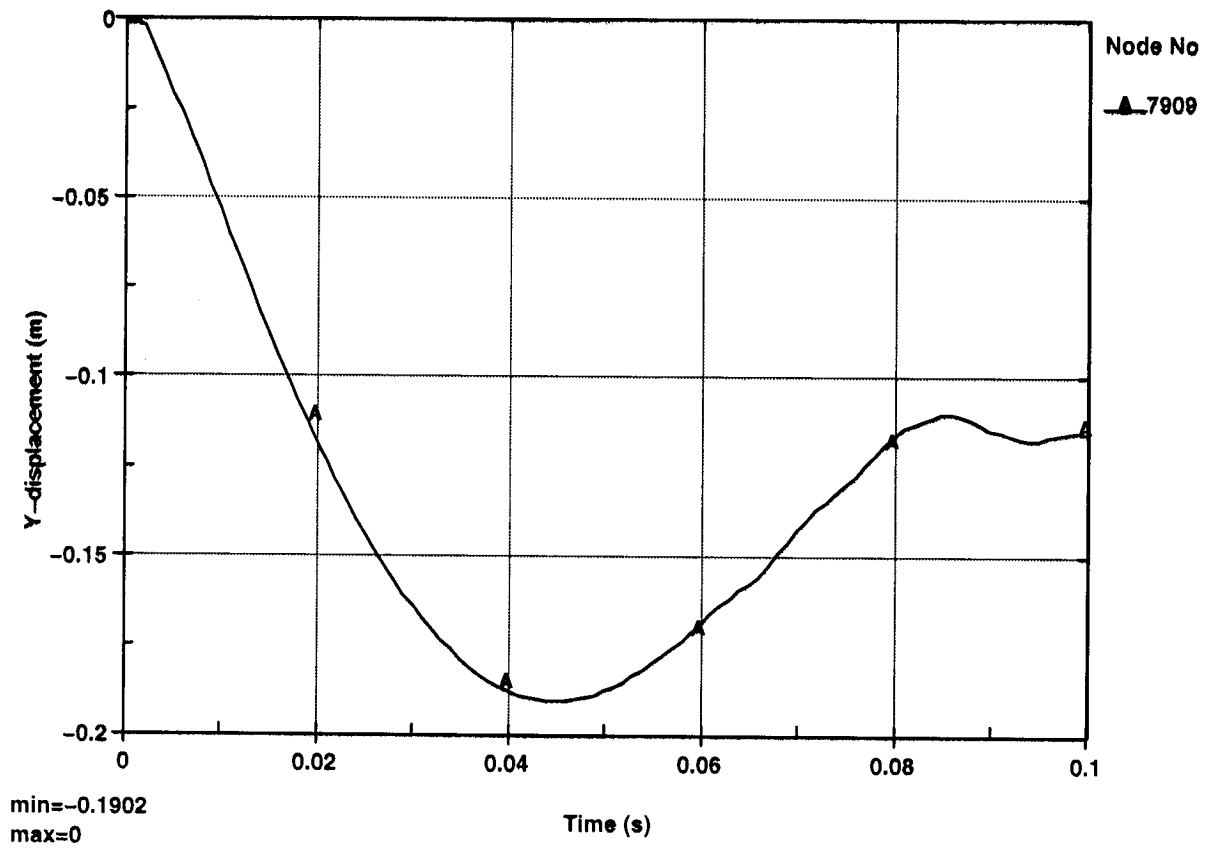


Figure II-28. Maximum Displacement for 19-MT Pointed-edge Rock Fall (Bulkhead stiffeners)

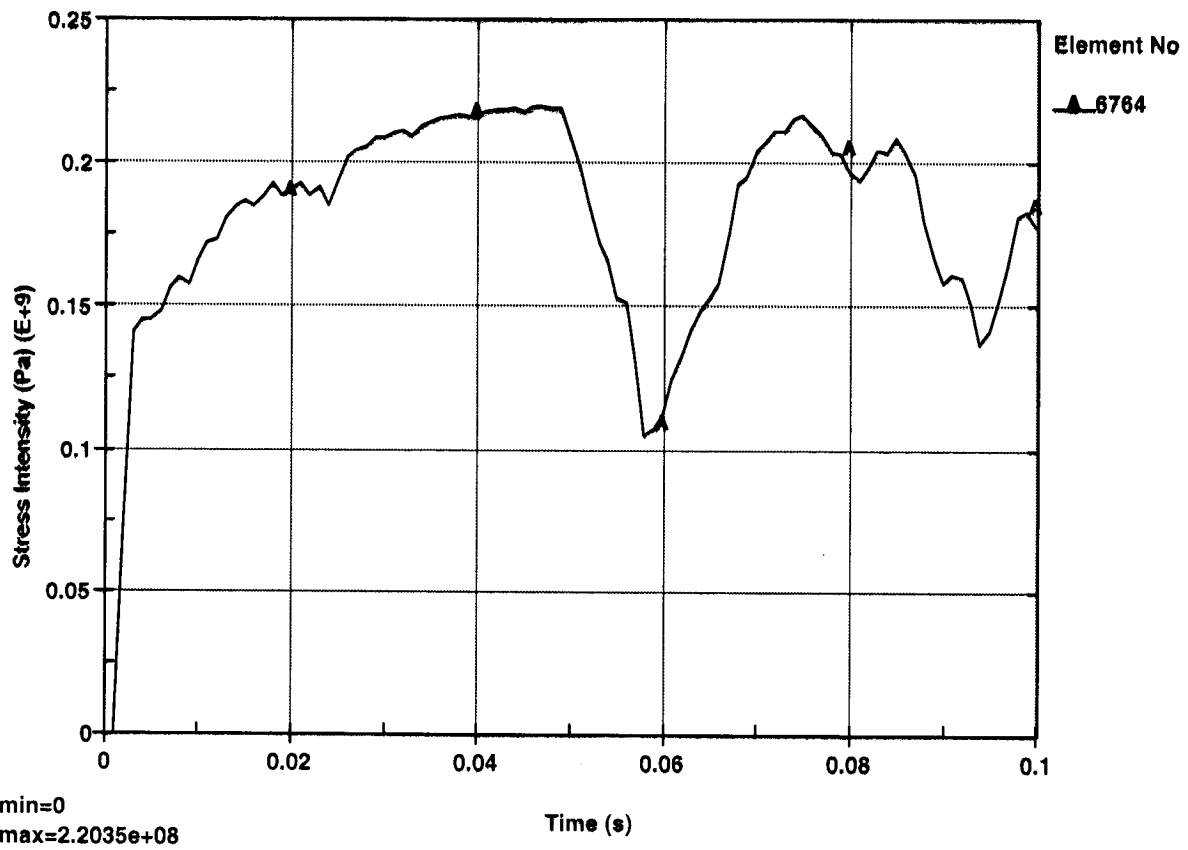


Figure II-29. Maximum Stress Intensity for 19-MT Pointed-edge Rock Fall (Top plate)

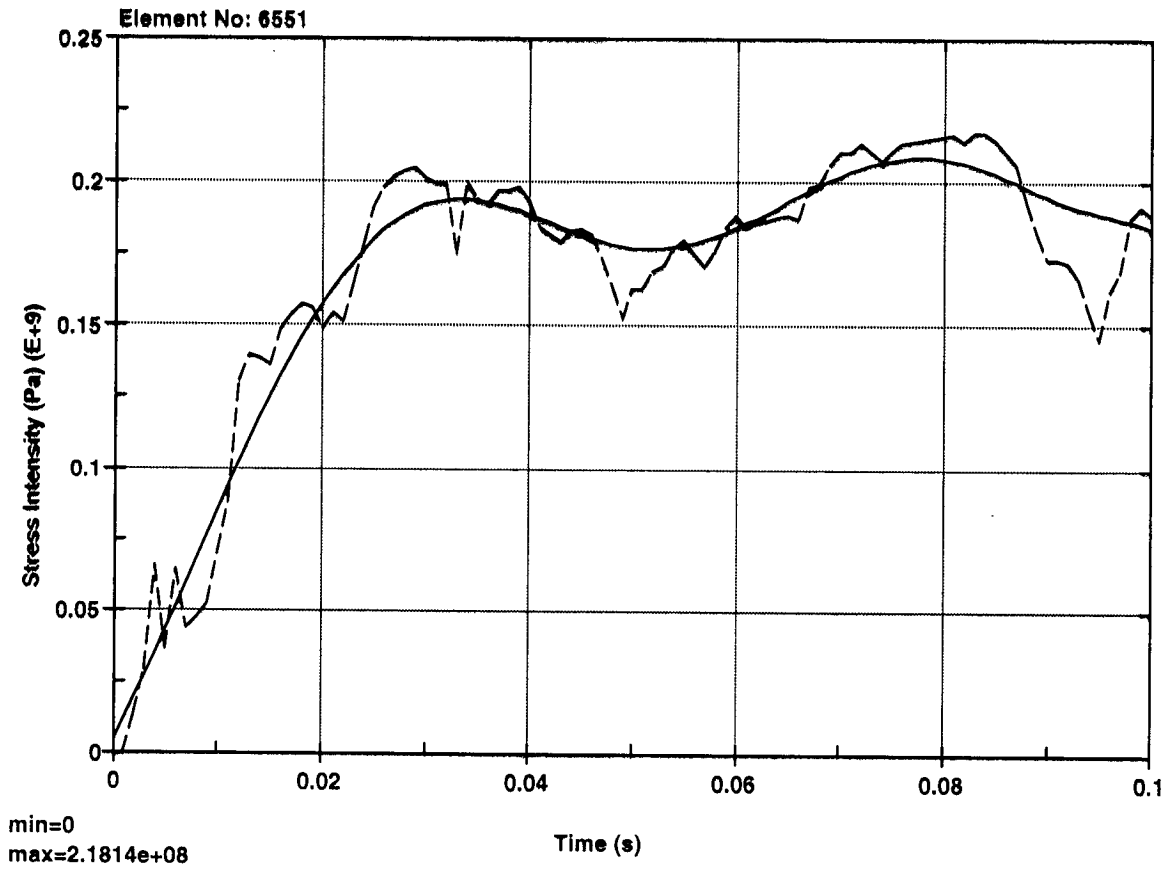


Figure II-30. Maximum Residual Stress for 19-MT Pointed-edge Rock Fall (Top plate)

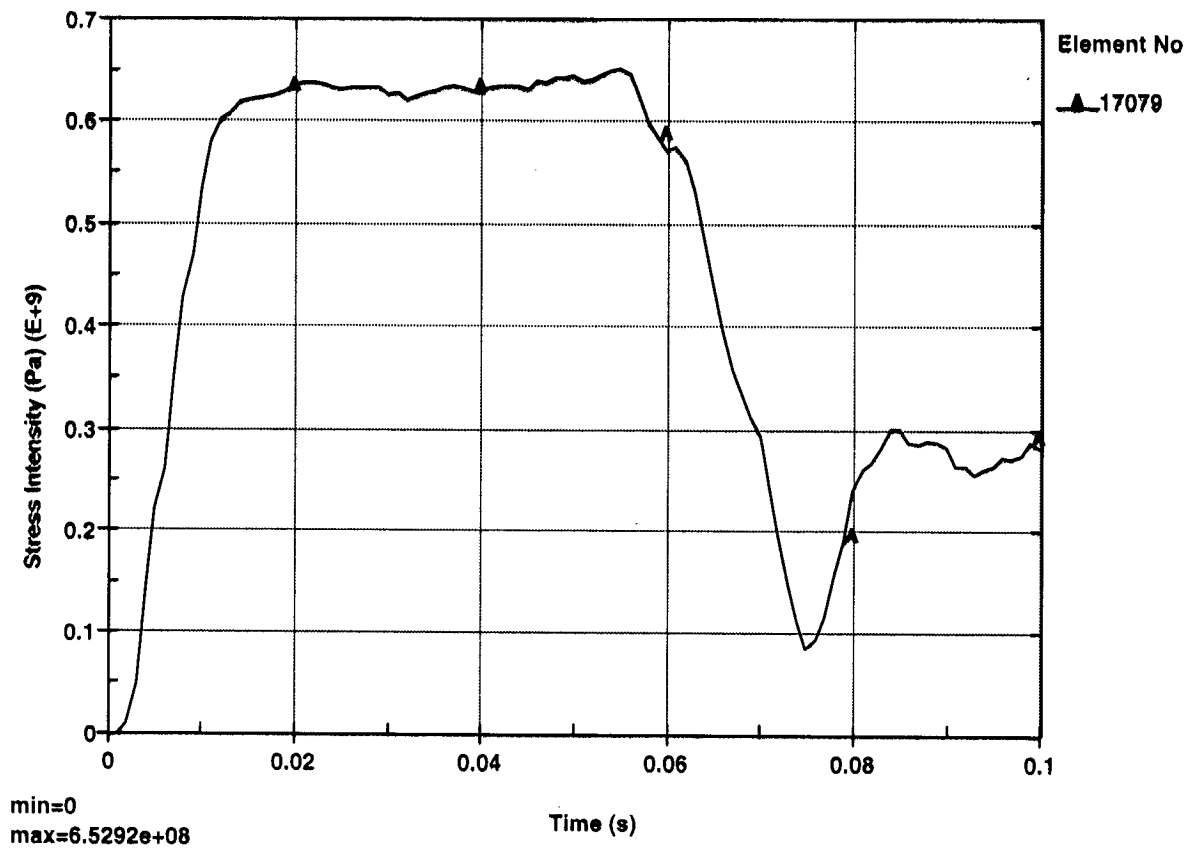


Figure II-31. Maximum Stress Intensity for 19-MT Pointed-edge Rock Fall (Bulkheads)

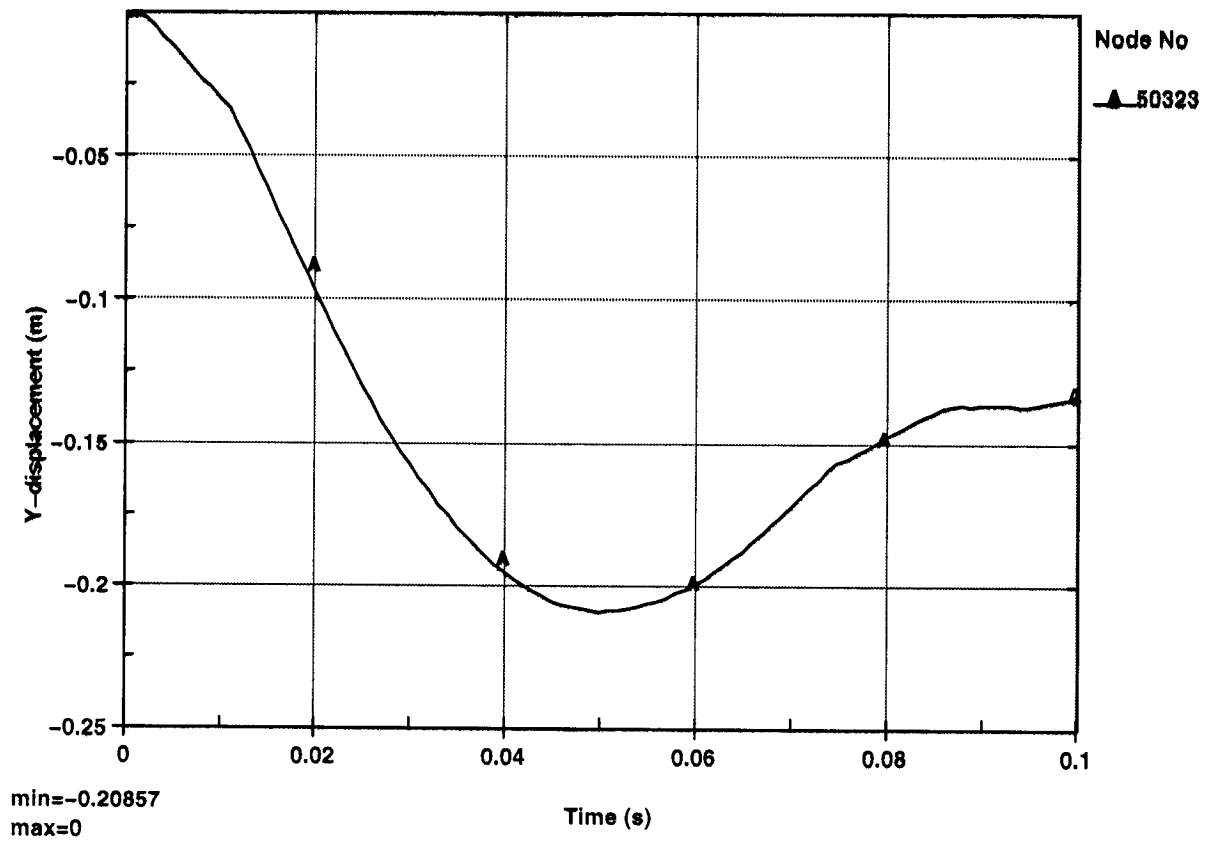


Figure II-32. Maximum Displacement for 30-MT Pointed-edge Rock Fall (Bulkhead stiffeners)

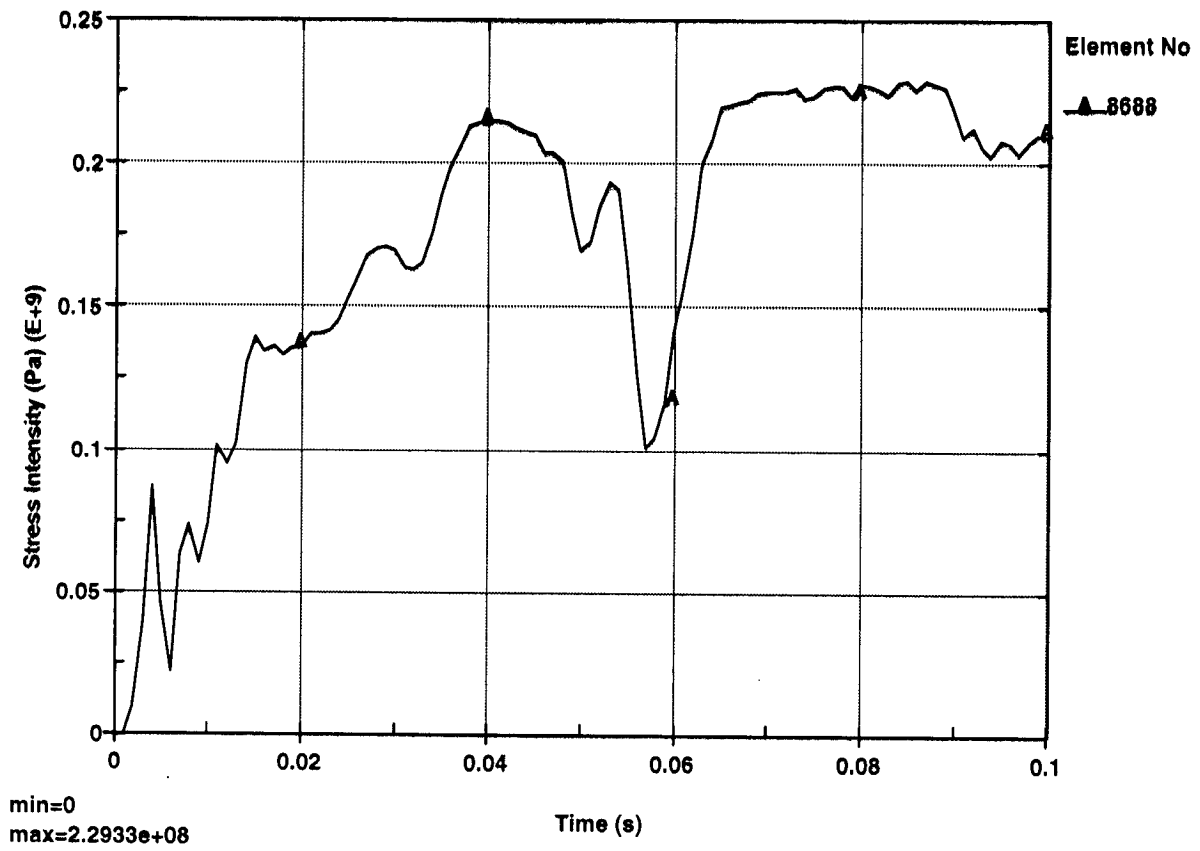


Figure II-33. Maximum Stress Intensity for 30-MT Pointed-edge Rock Fall (Top plate)

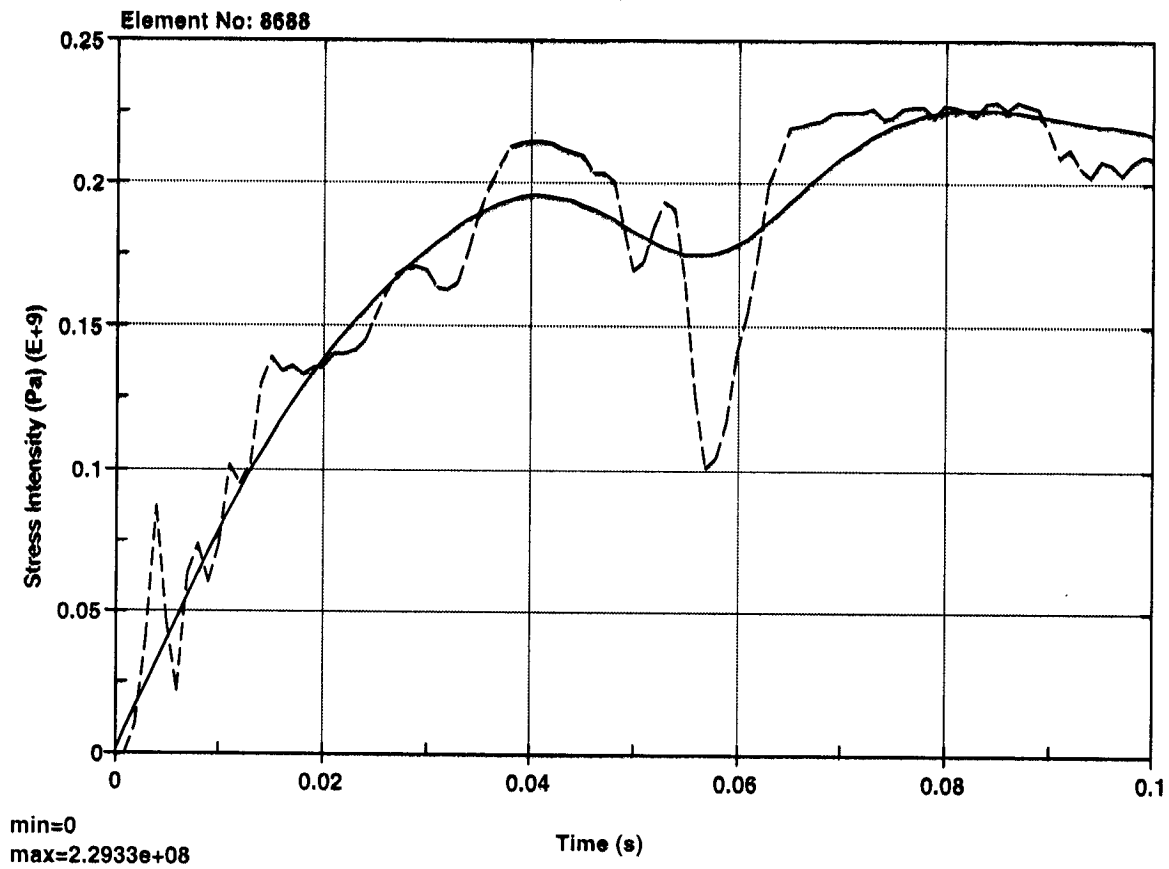


Figure II-34. Maximum Residual Stress for 30-MT Pointed-edge Rock Fall (Top plate)

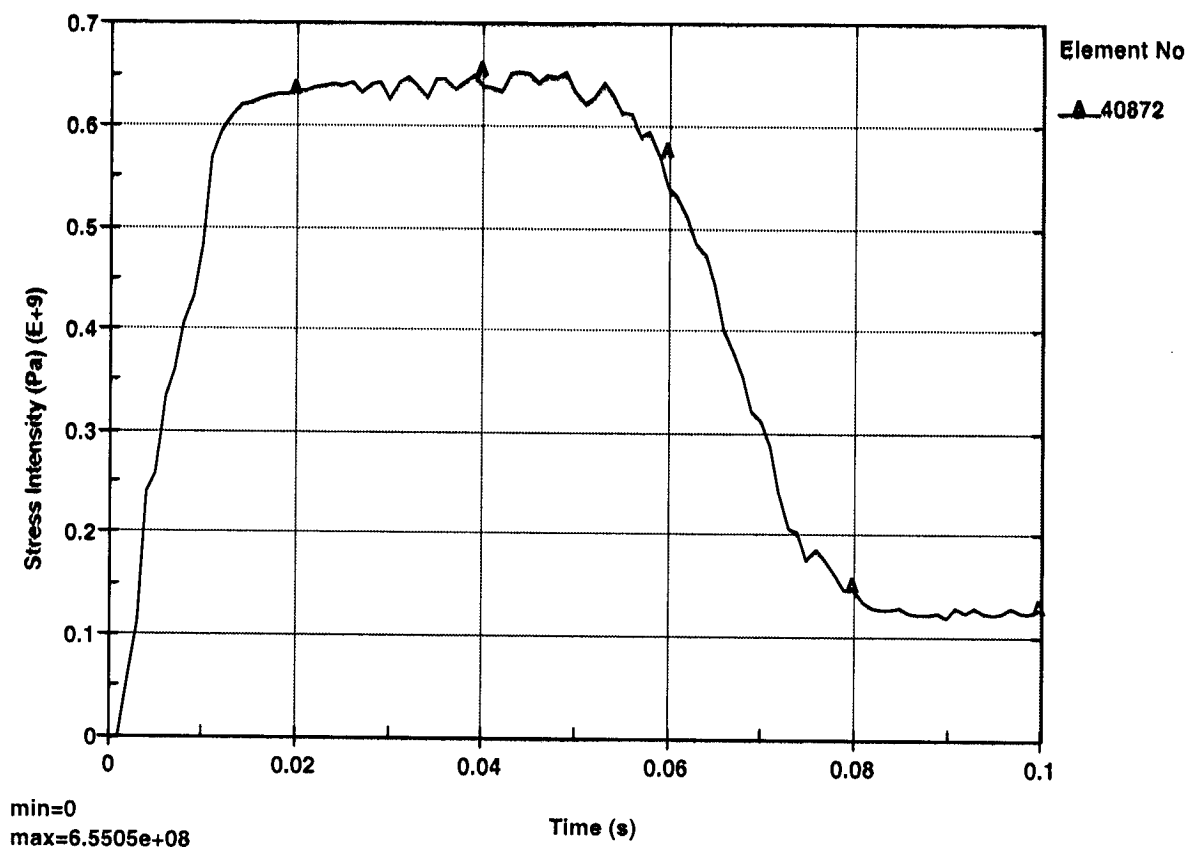


Figure II-35. Maximum Stress Intensity for 30-MT Pointed-edge Rock Fall (Bulkheads)

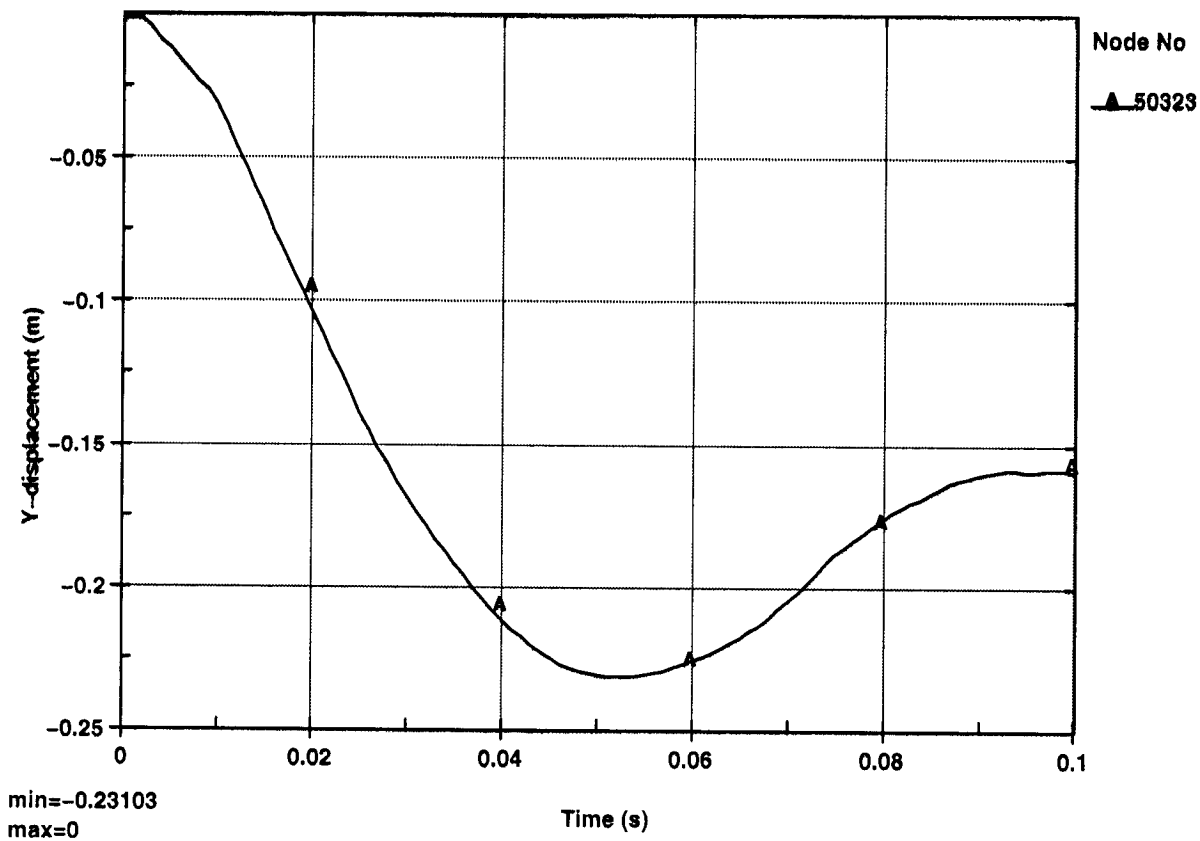


Figure II-36. Maximum Displacement for 36-MT Pointed-edge Rock Fall (Bulkhead stiffeners)

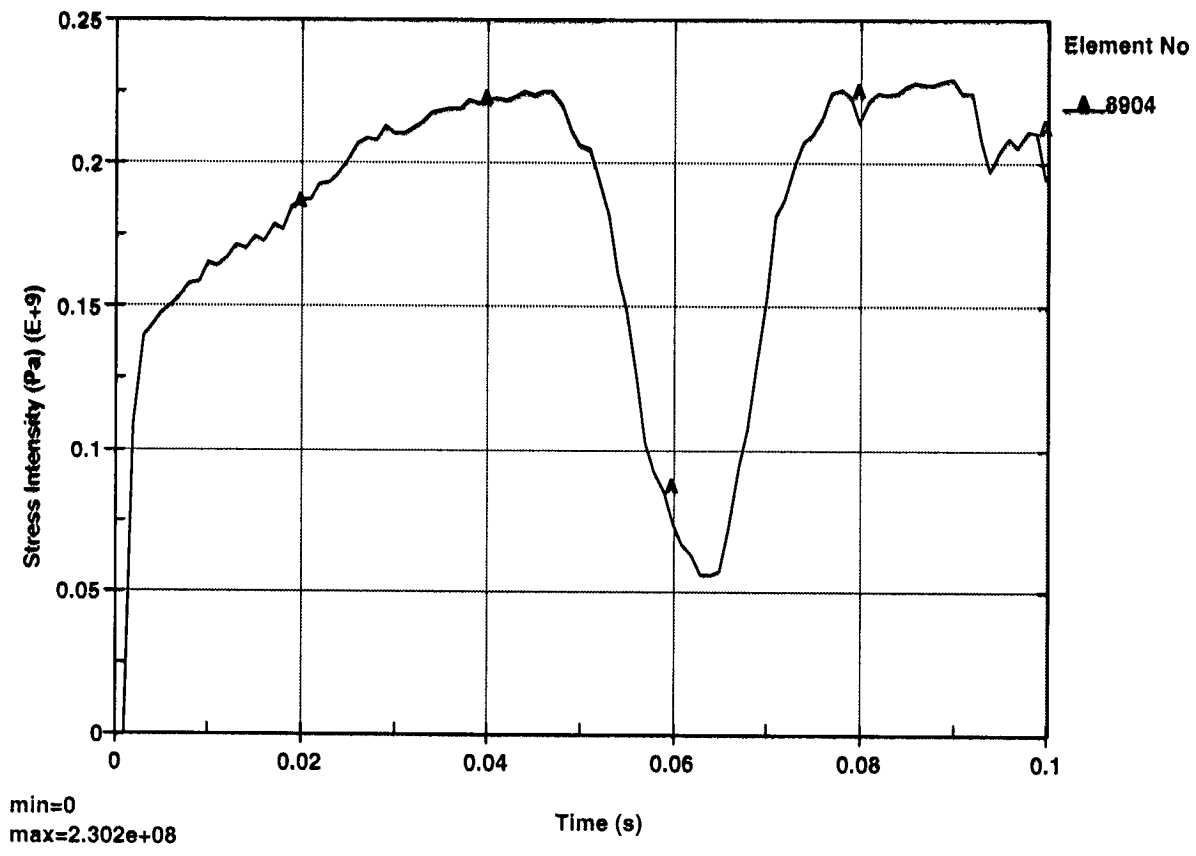


Figure II-37. Maximum Stress Intensity for 36-MT Pointed-edge Rock Fall (Top plate)

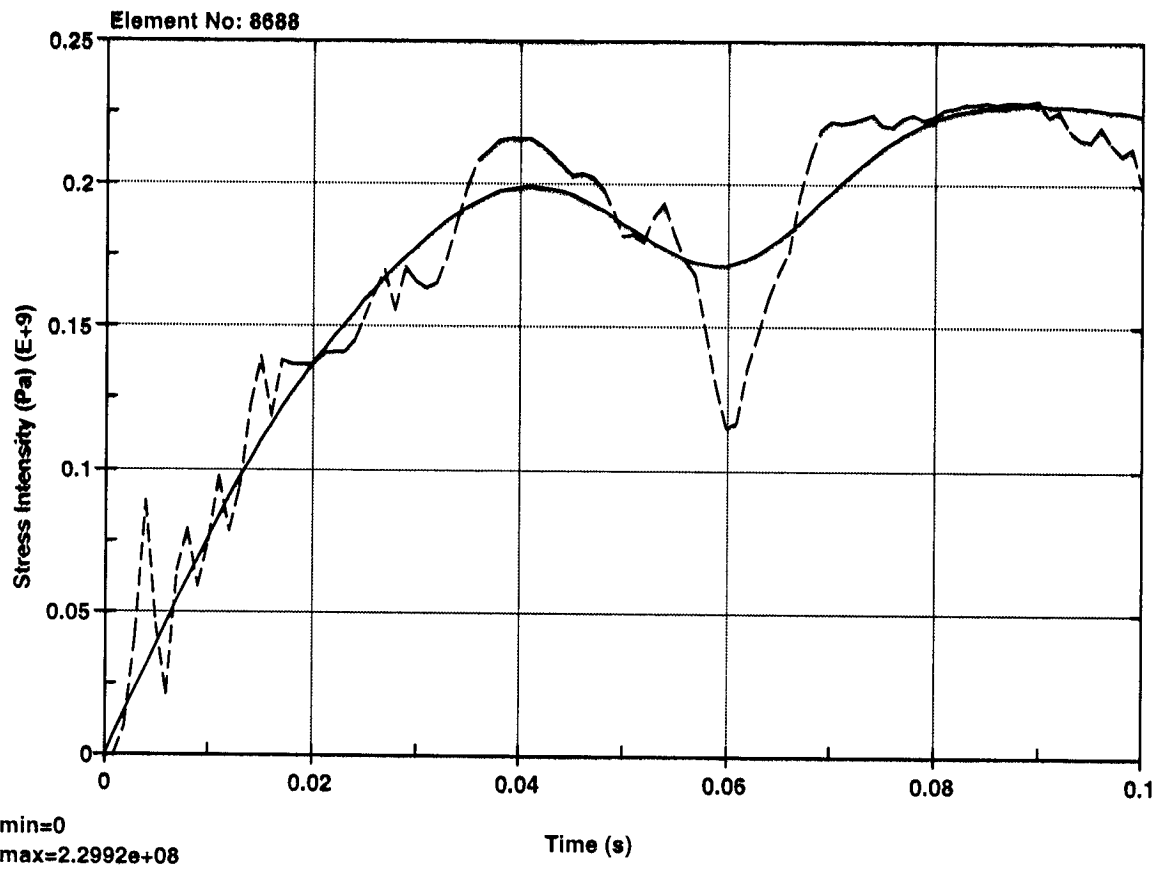


Figure II-38. Maximum Residual Stress for 36-MT Pointed-edge Rock Fall (Top plate)

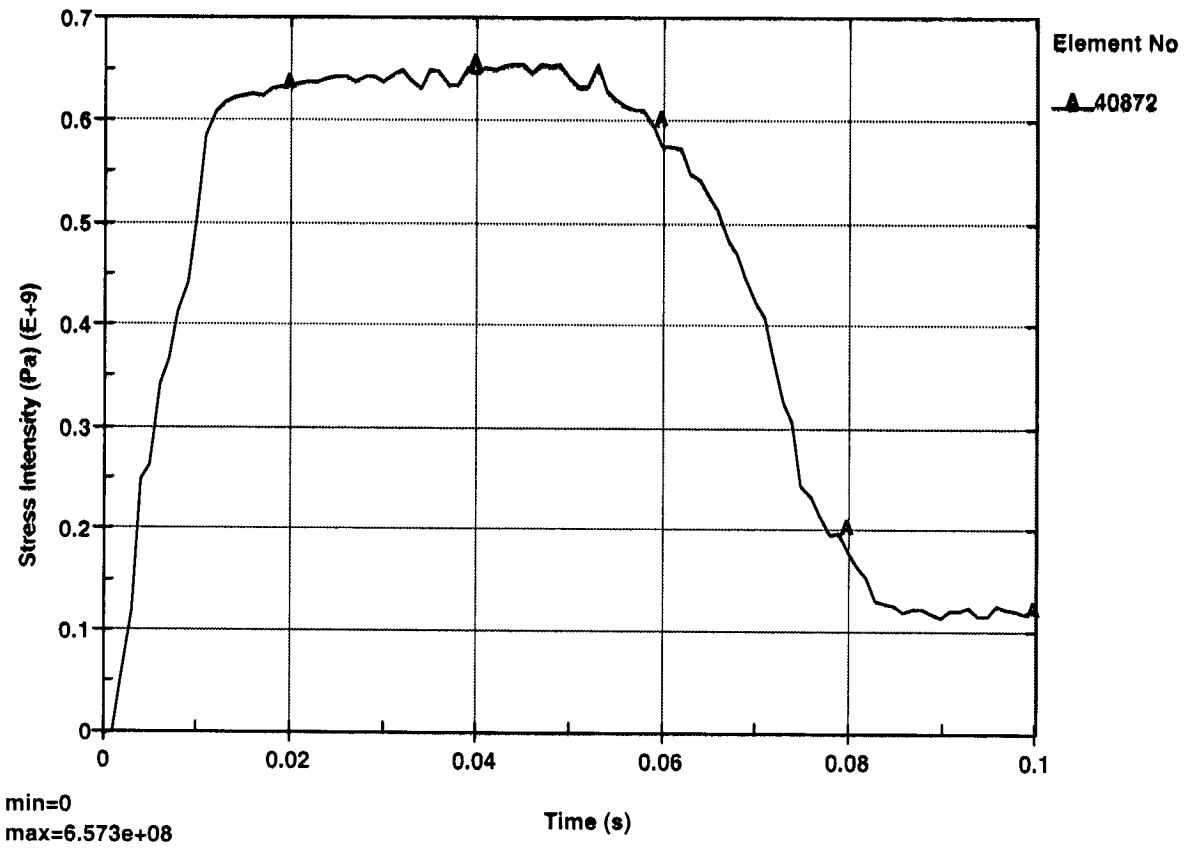


Figure II-39. Maximum Stress Intensity for 36-MT Pointed-edge Rock Fall (Bulkheads)

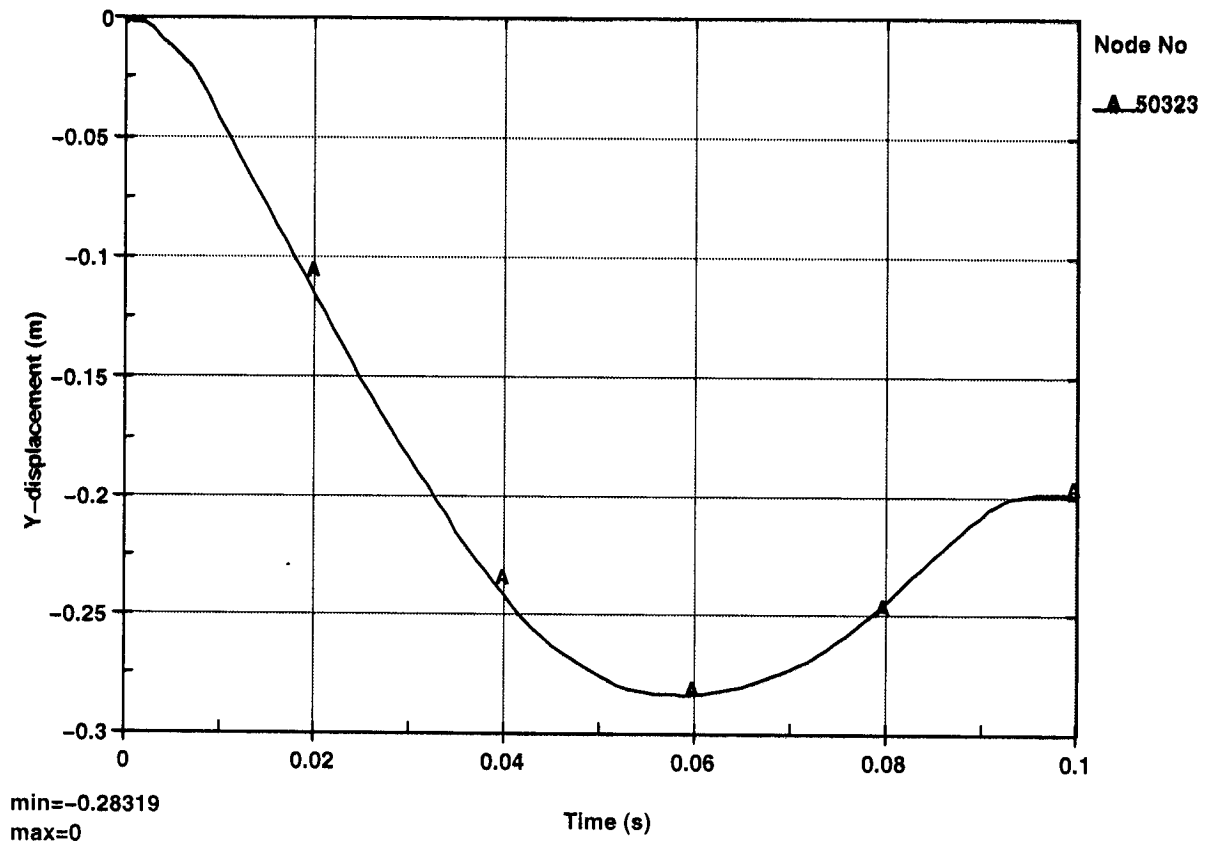


Figure II-40. Maximum Displacement for 52-MT Pointed-edge Rock Fall (Bulkhead stiffeners)

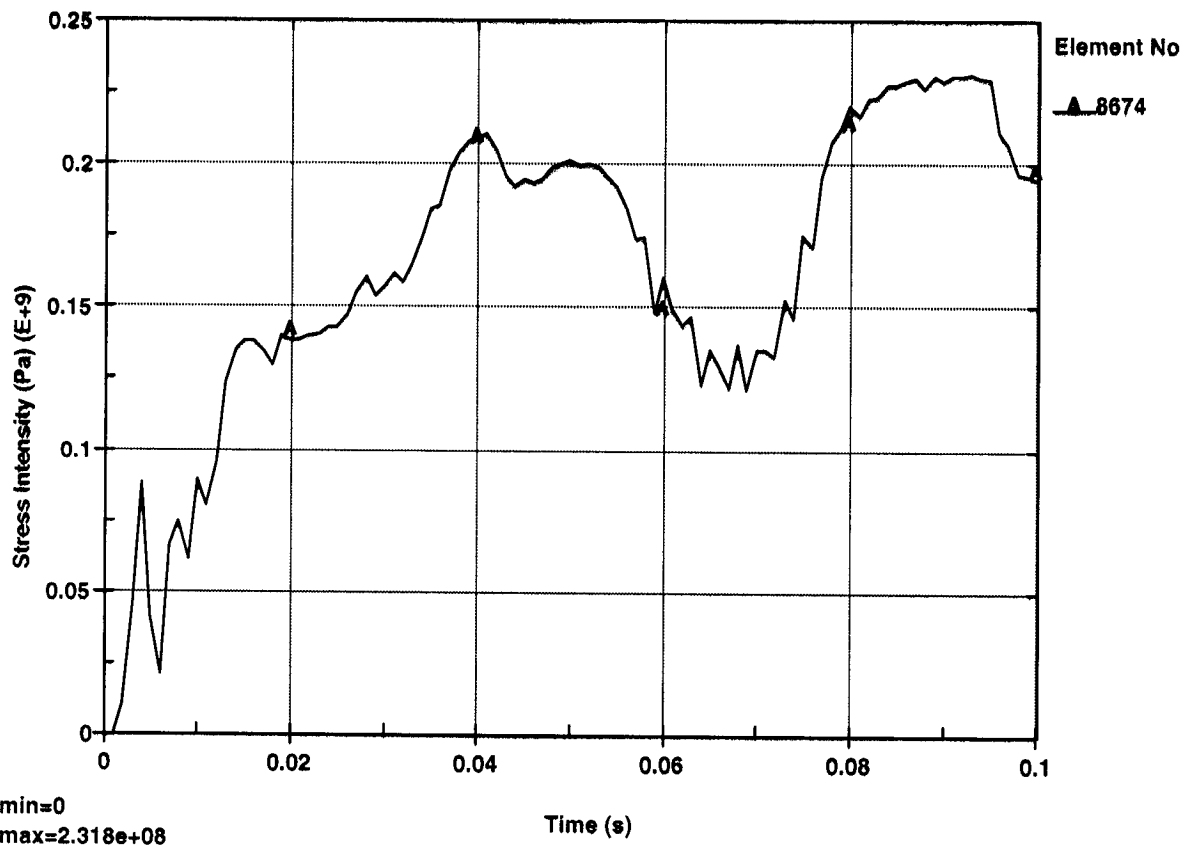


Figure II-41. Maximum Stress Intensity for 52-MT Pointed-edge Rock Fall (Top plate)

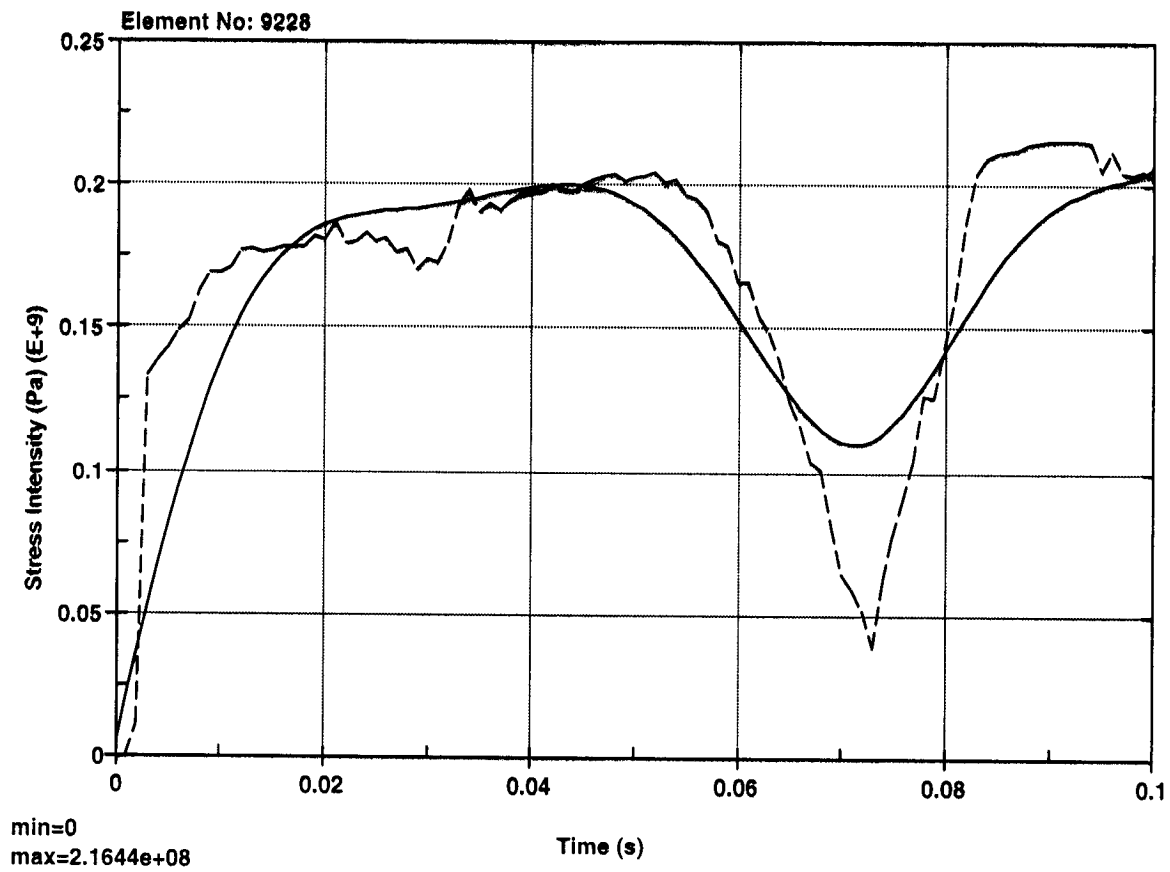


Figure II-42. Maximum Residual Stress for 52-MT Pointed-edge Rock Fall (Top plate)

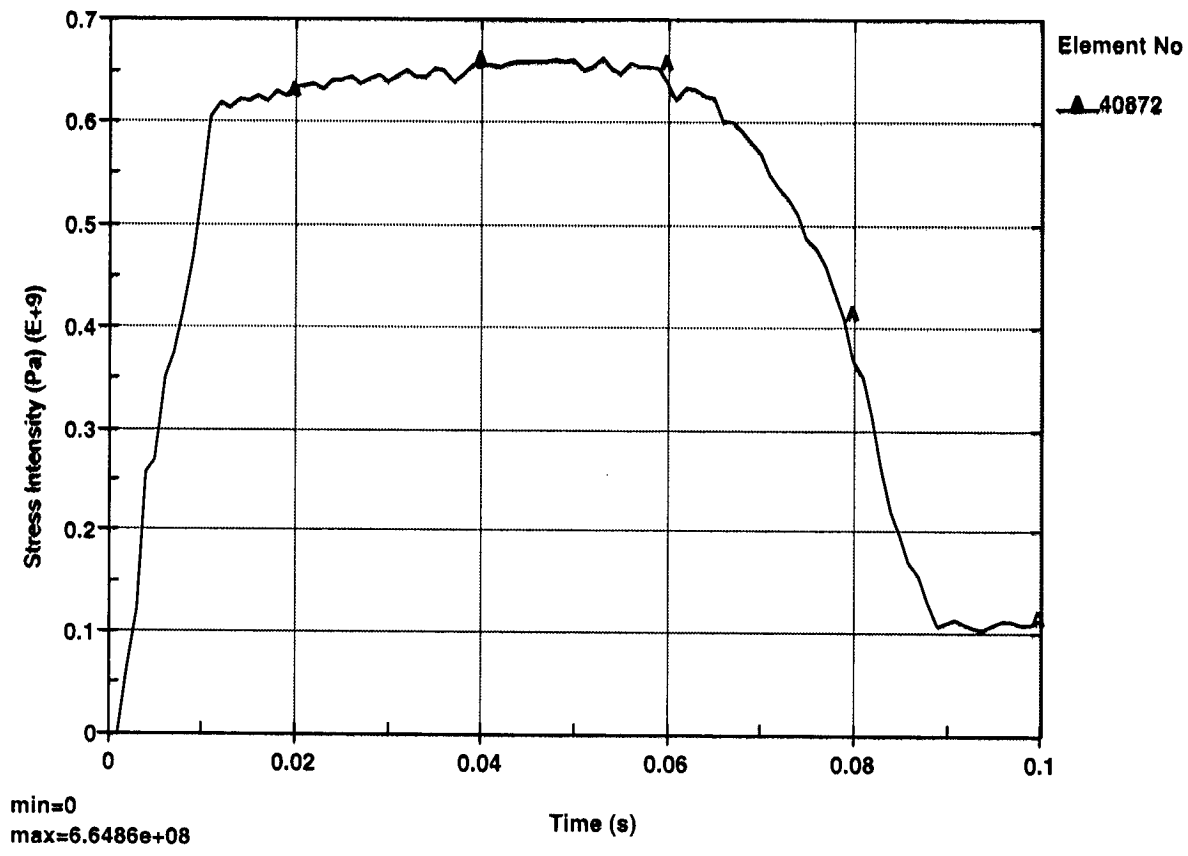


Figure II-43. Maximum Stress Intensity for 52-MT Pointed-edge Rock Fall (Bulkheads)

File Listing 7/13/01 HS

OFFICE OF CIVILIAN RADIOACTIVE WASTE MANAGEMENT  
SPECIAL INSTRUCTION SHEET

1. QA: QA  
Page: 1 of: 1

Complete Only Applicable Items

This is a placeholder page for records that cannot be scanned.

2. Record Date 07/10/2001		3. Accession Number <i>ATT-TO MOL. 20010713.0043</i>	
4. Author Name(s) ZEKAI CEYLAN		5. Author Organization N/A	
6. Title/Description ROCK FALL ON DRIP SHIELD			
7. Document Number(s) CAL-EDS-ME-000001			8. Version Designator REV. 01
9. Document Type DATA		10. Medium CD-ROM	
11. Access Control Code PUB			
12. Traceability Designator DC #28978			
13. Comments THIS IS A SPECIAL PROCESS CD-ROM AND THIS DATA SUBMITTAL TO THE RECORDS PROCESSING CENTER IS FOR ARCHIVE PURPOSES ONLY, AND IS NOT AVAILABLE FOR VIEWING OR REPRODUCTION			